Saskatchewan
Research Council

A REVIEW OF METHODOLOGY FOR MEASURING THE DRIFT AND DEPOSITION OF HERBICIDES AND INSECTICIDES FOR FORESTRY APPLICATIONS

by

S.R. Shewchuk
K. Wallace
J. Maybank

SRC Technical Report No. 220

Publication E-906-21-B-88

April, 1988

A REVIEW OF METHODOLOGY FOR MEASURING THE DRIFT AND DEPOSITION OF HERBICIDES AND INSECTICIDES FOR FORESTRY APPLICATIONS

by

S.R. Shewchuk
K. Wallace
J. Maybank

SRC Technical Report No. 220

SRC Publication No. E-906-21-B-88

April, 1988

SUMMARY

A literature review is provided on methods used to monitor droplet drift and deposition of pesticides in forestry applications. Several prototype methods for monitoring were considered for practical use in British Columbia. Current techniques of monitoring droplet drift with Kromekote cards are thought to be adequate for large droplet measurements.

The Rotorod sampler is considered to be a general sampler that could be easily applied to the forest situation. However, some research effort on types of dye tracers and counting techniques are required before the sampler can be useful to the forest pest management industry.

TABLE OF CONTENTS

	Page
SUMMARY	i
1 INTRODUCTION	1
2 SUGGESTED METHODS FOR ANALYSIS OF DROPLET DRIFT	4
2.1 Kromekote Cards	4
2.2 Rotorod and Rotoslide Samplers	6
3 CONCLUSIONS AND RECOMMENDATIONS	11
4 ACKNOWLEDGEMENTS	13
5 BIBLIOGRAPHY (For Report and Appendices)	15
6 APPENDICES	19
APPENDIX A - OTHER METHODS OF ANALYSIS	20
APPENDIX B - PAPERS RELATED TO USE OF ROTOROD SAMPLERS IN FORESTRY	31
APPENDIX C - THE ROTOROD SAMPLER OPERATIONS MANUAL	78

1 INTRODUCTION

Pesticide spray droplets are customarily released in the atmosphere in such a manner that they move from the release point to the desired deposition surface. In the course of this process some droplets inevitably leave the target area and move downwind.

In this report we will focus primarily on the techniques to measure off-target droplet drift. It is important to keep in mind that there are many completely different aspects of off-target drift. Pesticides can drift in either the droplet or the vapour phase from the application source. Direct droplet loss through off-swath drift has been studied by many authors (Goering et al. 1977; Maybank et al. 1977). There is a wealth of knowledge in the literature about sampling and analytical methodologies. However, there is little information in the literature dealing with the vapour component of drift. In this report only the droplet phase will be considered.

All spray drift droplets in the atmosphere have a settling velocity and residence time which for most size ranges have been satisfactorily described by Mason (1957). For droplets larger than approximately 100 microns settling velocities work well to predict the deposition patterns. However, droplets smaller than this value are significantly affected by atmospheric turbulence and often can remain suspended in the air for significantly long periods of time. This will result in these droplets being deposited several kilometres or more from the release point.

Instrumentation is available to sample two aspects of the drifting material. The airborne fraction and the depositing fraction of the drifting clouds can be quantified with different sampling collectors.

Generally, the airborne factions are measured with active sampling systems and depositing fractions are measured with passive sampling systems. Active sampling involves moving air with pesticide through a filter or absorbing medium. Passive sampling involves the deposition of pesticide particles onto the collector.

Yates et al. (1985) have studied the emitted nozzle droplet spectra in high speed air streams. Droplet size measurements were made directly with a laser probe. Drift amounts were measured as the fraction of droplets less than a specified diameter. Although droplets as large as 400 microns may pose drift hazards, it was generally considered that droplets in the range of 30 to 150 microns in diameter would pose the most significant drift hazard. During spraying in British Columbia, Henigman (1988) has suggested that the herbicide spray size range is up to 600 microns, with droplets in the size range of 50 to 150 microns providing the drift fraction. For insecticide sprays the droplets are in sizes up to 200 microns, with the droplets in the size range of 10 to 80 microns providing the drift fraction. It is clear that there is a wide range of droplet diameters to consider. In addition, the farther one moves off-swath in the downwind direction the smaller will be the droplet sizes encountered. Thus a variety of techniques may have to be applied to measure droplet drift at various downwind distances.

We are searching for a field method to be employed by operational staff to monitor the off-target droplet drift for aircraft (both helicopter and fixed wing) and groundrig applications. The method should allow easy determination of compliance with permit regulations governing pesticide-free and buffer zones as defined by the province of British Columbia. Buffer zones may be up to 200 m wide and are located between

the spray area and the pesticide-free zones. The pesticide-free zone normally surrounds sensitive areas such as water bodies and is usually 10 m wide.

In this report an assessment will be made of off-target drift measurement techniques. Various devices that have been used in forestry and agriculture applications will be considered and their levels of accuracy and convenience of use in a field situation will be addressed. A prototype method to monitor spray drift will be recommended for use in British Columbia forestry operational spraying activity. This method is to provide evidence of compliance with provincial permit regulations governing buffer zones (including pesticide-free zones).

2 SUGGESTED METHODS FOR ANALYSIS OF DROPLET DRIFT

All devices considered from the literature are listed in Table 1 with an assessment of their usefulness to an operational program. The reference source of the information is given along with various comments (see Appendix A for details). Operational programs require field assessment and quick turnaround times for results. Quality analysis techniques, as listed in Appendix A, cannot be applied. However, two of the eight techniques do qualify for field assessment. This is because they can be field assessed with standard procedures.

2.1 Kromekote Cards

Kromekote cards can be analyzed directly by optical means. They are accurate for measurement of large droplets when drifting but less so for smaller drops. Simulated deposition surfaces are listed because droplets on such surfaces can be directly counted as well.

Kromekote paper is a white glossy paper frequently used in conjunction with a visible dye. It is, perhaps, the most common form of collector for water based spraying and has been widely used for many years. Sundaram and Nott (1985) used Kromekote cards and glass slides in looking at Mexacarbate residues on selected components of a conifer forest. They found good agreement between ground deposit variation levels from these devices and those found in litter and soil samples. The cards work very well for large drops. Dorais (1988) has used Kromekote cards to monitor insecticide spray deposition within forests in Quebec. Kromekote cards were not considered a reliable ground deposit collector for insecticide sprays applied by air. Irving (1988) used Kromekote cards. They were ruled out as an indicator of deposit and instead small strips

Table 1. Instruments for Drift Measurement Under Field Operation Conditions.

Characteristics	Kromekote[1] Cards	Petri Dishes or[2] Glass Plates or Mylar Sheets	Simulated[3] Deposition Surfaces (Foliage)	Air[4] Samplers	Cascade[5] Impactors	Impingers[6]	Special[7] Devices (Spheres, Curlers, Other)	Rotorods[8] and Rotoslides
Ease of use in operation setting	Yes	Yes	Yes	No	No	No	Yes	Yes
Optimize monitoring of adjacent areas	Fair	Yes	Yes	Yes	Yes	Yes	Yes	Yes
Employable at the time of spraying	Yes	Yes	Yes	Yes	Yes	Yes	Yes	Yes
Reliability of estimates of actual residue deposit or drift (accuracy)	Fair	Fair	Fair	Yes	Yes	Yes	Fair	Fair
Costly chemical analysis	No	Yes	Yes	Yes	Yes	Yes	Yes	Possibly
Storage for one year	Yes	Yes	Yes	Yes	Yes	Yes	Yes	Yes
Active ingredient*	No	Possibly	Possibly	Yes	Yes	Yes	No	Yes
Fluorimetry	No	Yes	Possibly	Yes	Yes	Yes	Yes	Yes
Visual assessment (eyepiece)	Yes	No	Possibly	No	Possibly	No	No	Possibly
Field analysis	Yes	No	Yes	No	No	No	Possibly	Yes
Useful in an operational program	Yes	No	No	No	No	No	No	Yes

[1]Dorais (1988); [2]Goering et al. (1977); [3]Uk (1977); [4]Maybank (1977); [5]May (1945); [6]Ware et al. (1969); [7]Bury (1987); [8]Murray and Vaughan (1970), Parkin (1975).

*Active ingredient is the direct analysis for the pesticide of interest.

of the cards cut to the same dimensions as a conifer needle were used.

In a recent study the U.S. Forest Service (Reardon 1988) observed deposits of insecticide using Kromekote cards on the forest floor. It was difficult relating the deposit found on the cards to that on the foliage. The technique employed now is to set out Kromekote cards and simply to say "yes the area received some spray because we see a deposit on the cards."

Wallace and Jahren (1988) considered eight sets of Kromekote deposit cards and one set of water sensitive paper. They were analyzed for volume median diameter (VMD), number median diameter (NMD), and coverage in the British Columbia forestry situation. The addition of a fluorescent dye to the tank mix allowed determination of deposit densities from petri dishes. These authors found poor contrast with an image analyzer system of spot counting on these cards.

2.2 Rotorod and Rotoslide Samplers

The Rotorod and Rotoslide samplers can be used in an operational setting because the droplets on the device can be directly counted using fluorescent or optical particle counting procedures (see Appendix A). These samplers are impaction type instruments. The principle of these samplers is that of moving a rapidly rotating collecting surface through the air. The surface can either be a glass slide (as in the Rotoslide sampler) or a specifically designed rod (as in the Rotorod sampler). The exposed and rotating surface makes this device an omni-directional sprayer, independent of wind direction. The device can be reproducibly calibrated. These samplers provide a simple and accurate method for quantitatively measuring pesticide mass and droplet size.

a) The Rotoslide Sampler

The particulate dispersion into and within a 10 to 13 m tall pine forest was studied experimentally at the Brookhaven National Laboratory by Raynor et al. (1974) (see Appendix B). Stained ragweed pollen ranging in size from 14 to 54 microns in diameter was used. The device consisted of Rotoslide samplers mounted at various heights to 21 m and extending 100 m into the canopy. The Rotoslide sampler is described by Ogden and Raynor (1967). The deposit was sampled by grease slides at various points. Particles collected were counted under a microscope. The primary purpose of this research was to study forest canopy dispersion characteristics. The authors were able to adequately sample the movement of a drift cloud into the forest canopy with these instruments.

The droplet numbers and volumes crossing a unit vertical area has been measured recently by Johnstone et al. (1987) with a rotary slide sampler (see Appendix B). The slides were coated with magnesium oxide (MgO). The measurements were converted to estimates of the dose received by the target (tsetse fly) and by the samplers. Droplet impressions on the MgO slides were sized by microscope. This sampler worked well for droplets in the insecticide driftable range.

b) The Rotorod Sampler

The Rotorod is an efficient sampling instrument which can be used to collect airborne particulates in the 1 to 100 microns range. Basic components are a sampler unit, consisting of a constant speed DC motor with associated circuitry and case, and an aerodynamically designed collector rod which is rotated by the sampler unit. Excellent test results are obtainable through proper use of the Rotorod sampler and by careful

evaluation techniques (see Appendix C for operating instructions). The basic Rotorod sampler model is seen in Figure 1. It should be mounted securely to any convenient upright support at its sampling station before operation. The samplers are mounted on a stake at any desired height. The Rotorod sampler collector rods are usually rotated at a nominal 2400 rpm ± 2%. Normal portable operation of the Rotorod utilizes a standard 12 volt lantern battery. This type of battery is standard equipment in the Rotorod sampler kit and provides a minimum of 50 hours continuous operation or 70 hours intermittent operation. The Rotorod sampler has two different rod shapes. The "H" shaped rods are used for studies of particulates in the size range of 1 to 10 microns and the "U" shaped rods are used for studies of particulates in the size range of 10 to 100 microns.

There is available a rod coating material specifically designed to be used with the fluorescent particle material often used to tag particles of drifting material. This coating material, which has a dull nonreflective black surface, provides maximum contrast between the brightly fluorescent particles and the collecting substrate. These particles are assayed under ultraviolet light, which causes them to fluoresce, and as they are usually in the 1 to 5 micron range, all possible interference by background light must be eliminated. They are ideal samplers for forest pesticide applications.

Murray and Vaughan (1970) described a simple tracer technique using fluorescent particles to measure various characteristics of spray drift (see Appendix B for details). This consisted of adding a known number of insoluble (micron sized fluorescent) particles to the liquid pesticide prior to the spray operation. After spraying, samples of natural

Figure 1. The Rotorod Sampler.

and artificial surfaces were assessed. The number of fluorescent particles grouped with a droplet pattern determines the droplet volume, and the total number of fluorescent particles determines the total mass of pesticide in the sample. Droplets with VMD of 10 microns were obtained at distances up to 6.5 km. Mickle et al. (1984) compared Rotorod samplers, which had Kromekote strips of width 0.16 cm placed on the rod face, with air samplers in a forestry environment. They found generally good agreement between these two instruments.

3 CONCLUSIONS AND RECOMMENDATIONS

Considering the potential damage that could be caused by drifting sprays remarkably little research has been performed on drift from sprayers. Drift is gaining in importance as a topic for research, but at present we are left with some fairly primitive methods for measuring drift. Many of the methods discussed for operations in this report fall into this category.

Because of the inherent difficulties with flat surface collectors it is not surprising that often there is little positive correlation between spray volume deposited on the Kromekote cards and drift target measurements. Collectors which are mechanically aspirated are usually rejected in practical operations for reasons of cost and complexity. This implies that the samplers such as Kromekote cards and Rotorods are the sampling methodologies of choice. Kromekote cards have a long history of use and current procedures are adequate for field operational personnel. The dye tracer and deposition technique onto Kromekote paper does have some part in a monitoring program for the British Columbia Ministry of Forests and Lands. However, current Rhodamine B dye stains on the Kromekote paper are often very difficult to analyze for size distribution due to lack of contrast with the paper. A program to consider several different dye stains would be of some value. Various colour and fluorescent dyes which may be considered are: Erythrosine (Red), water blue, Aerial Acid Red XB, Helio OB, FD40 Red, Uvitex OB, plus many others.

Possibly the most useful field method for monitoring droplet drift concentrations in a field environment for the Ministry is the Rotorod sampler. This sampler has been adapted well in forestry buffer zone

studies. It is recommended by a number of research workers. The drifting droplet size of most concern is in the range of 5 to 100 microns and this is the ideal size range for most efficient operation of the sampler. In addition the sampling efficiency is independent of wind direction, which is an important benefit while working within or near an often always turbulent forestry canopy. Some development work and care in handling will be required to make this unit of use to the Ministry because the sampler requires some laboratory and field calibration. The use of either Kromekote strips or MgO coatings on the rods should work quite effectively in a forestry environment.

Since the amount of pesticide drifting at any point downwind of a spray operation is strongly dependent on drop size, it is recommended that several different approaches to drift may be taken. A combination of Kromekote cards and Rotorods should work very well for forestry operational applications.

Finally it is recommended that the Ministry consider a series of field trials to test the efficiency of the Rotorod sampler in a forestry situation. This sampler should be compared against standard high quality samplers such as cascade impactors and air samplers.

4 ACKNOWLEDGEMENTS

Names and affiliations of people who were interviewed for this report are:

R. Crabbe - National Research Council
Ottawa, Ontario

L. Dorais - Ministere des Terres et Forets
Service d'Entomologie et Pathologie
1330 boulevard de l'Entente
Quebec City, Quebec

B. Elliot - Agriculture Canada
Research Station
Saskatoon, Saskatchewan

R. Grover - Agriculture Canada
Research Station
Regina, Saskatchewan

H.J. Irving - Managing Director
Forest Protection Ltd.
P.O. Box 1030
Fredericton, New Brunswick

R. Mickle - Atmospheric Environment Service
Downsview, Ontario

R. Reardon - U.S. Forest Service
Morgantown, West Virginia

C. Weisner - New Brunswick Productivity and Research Council
Fredericton, New Brunswick

W. Yates - University of California
Davis, California

Special acknowledgement should go to Mr. John Henigman of the British Columbia Ministry of Forests and Lands for initiating and providing guidance during the completion of this work. His comments and encouragement were most sincerely appreciated.

Within the Saskatchewan Research Council (SRC) several individuals deserve special thanks for their vital contributions. James Ross assisted in collecting and organizing the papers and Darlene Diduck

worked carefully and quickly to produce the report in a very short period of time. We would like to thank all of these individuals for their contribution.

5 BIBLIOGRAPHY (For Report and Appendices)

Barry, J.W., W.M. Ciesla, M. Tysowsky and R.B. Ekblad. 1977. J. of Economic Entomology Vol. 70, pp. 387-388.

Bryant, J.E. and R.J. Courshee. 1985. The effect of volume of application from hydraulic nozzles on the partioning of a pesticide spray in a cereal canopy. BCPC Monogram No. 28, Symposium on application and biology, Reading University. pp. 201-210.

Bury, C.J.G. 1987. A comparative study of the drift hazard presented by contrasting ground-spraying systems. Cranfield Institute of Technology.

Dorais, L. 1988. Quebec Ministry of Energy and Resources, personal communication.

Farlow, N.H. and F.A. French. 1956. Calibration of liquid aerosol collectors by droplets containing uniform size particles. J. Celloid Sci. 11, pp. 177.

Goering, C.E. and B.J. Butler. 1974. Analysis of paired microresidues using filter fluorimetry. Weed Science 22, pp. 512-515.

Goering, C.E., D.B. Smith, M.L. Huhman, A.R. Kliethermes and M.W. Storm. 1977. Targets for spray drift measurement. Trans. of the ASAE, Vol. 20, pp. 35-37.

Henigman, J. 1988. British Columbia Ministry of Forests and Lands, personal communication.

Himel, C.M. and R. McDaniel. 1975. Standardization of field methods of determination of insecticide spray droplet size. Office of Naval Research Contract N00014-70-A-0309-0003, Annual Report No. 1.

Irving, H.J. 1988. Forest Protection Limited, New Brunswick, personal communication.

Johnstone, D.R., J.F. Cooper and H.M. Dobson. 1987. The availability and fallout of an insecticide aerosol dispersed from aircraft. Atmospheric Environment Vol. 21, pp. 2311-2321.

Johnstone, D.R. 1977. A twin tracer technique permitting the simultaneous evaluation of the field performance of two spraying machines or spraying techniques. J. Agric. Eng. Res. 22, pp. 439-443.

Johnstone, D.R. and K.A. Huntingdon. 1970. A comparison of visual microscope methods of spray droplet size measurement using eyepieces employing the image shearing principle and ... J. Agric. Eng. Res. 15, 1, pp. 1-10.

Joyce, R.J.V., G.W. Schaefer and K. Allsopp. 1981. Distribution of spray and assessments of larval mortality at Annabuglish. In Aerial Application of Insecticide Against Pine Beauty Moth. Ed. by A.V. Holden and D. Bevan.

Last, A.J. and C.S. Parkin. 1987. The measurement of spray deposits on natural surfaces by image analysis. Aspects of Applied Biology, Vol. 14, pp. 85-96.

Last, A.J. 1987. Methods for spray deposit analysis. Cranfield College of Aeronautics. Pesticide application course.

MacCollum, D., B. Johnstone and B.L. Parker. 1968. Determination and measurement of insecticide dust particles in the atmosphere adjacent to orchards. Bulletin of Environmental Contamination and Toxicology, Vol. 3, pp. 368-374.

Mason, B.J. 1957. The Physics of Clouds. Cambridge Press.

May, K.R. 1945. The cascade impactor, an instrument for sampling coarse aerosols. J. Scientific Instruments, Vol. 22, pp. 187-195.

May, K.R. 1950. The measurement of airborne droplets by the magnesium oxide method. J. Sci. Instr. 27, pp. 128-130.

Maybank, J., K. Yoshida and R. Grover. 1977. The magnitude and importance of spray drift from agricultural applications. 70th Ann. Meeting of the Air Pollution Control Association, Toronto.

Mickle, R.E., R. Crabbe, L. Elias, D. Kristmanson, J. Picot, J.D. Reid, B. Steeves, N.B.A. Trivett and C. Weisner. 1984. Assessment of the 1983 spray fate experiment at the Dunphy test site. N.B. Research and Productivity Control, Fredericton, Report No. NB SER G/84/1.

Murray, J.A. and L.M. Vaughan. 1970. Measuring pesticide drift at distances of four miles. J. of Applied Met. Vol. 9, pp. 79-85.

Newton, M., K.M. Howard, B.R. Kelpsas, R. Danhaus, C.M. Lottman and S. Dubelman. 1984. Fate of glyphosate in an Oregon forest ecosystem. J. of Agri. and Food Chemistry, Vol. 32, pp. 1144-1151.

Ogden, E.C. and G.S. Raynor. 1967. A New Sampler for Air-Borne Pollen: The Rotoslide. J. Allergy 40, pp. 1-11.

Parkin, C.S. 1975. Rotorods as a field method for assessing small droplet concentrations in public hygiene spraying. CIBA-GEIGY AARU Research Report 32/75.

Raynor, G.S., J.V. Hayes and E. Ogden. 1974. Particulate dispersion into and within a forest. Boundary-Layer Meteorology, Vol. 7, pp. 429-456.

Reardon, R. 1988. U.S. Forest Service, Morgantown, WV, personal communication.

Richardson, R.G. 1984. Fluorescent tracer technique for measuring total herbicide deposits on plants. Australian Weeds, 3, 4, pp. 123-124.

Riley, C.M. 1985. Deposit assessment of aerially applied sprays of Bacillus Thuringiensis on balsam fir foliage. Internal report. N.B. Research and Productivity Council, Fredericton.

Sharp, R.B. 1974. Spray deposit measurement by fluorescence. Pestic. Sci. 5:197-209.

Sundaram, K.M.S. and R. Nott. 1985. Mexacarbate residues in selected components of a conifer forest following aerial applications of oil-based and aqueous spray formulation. J. Environ. Sci. Health, Vol. B20, pp. 425-444.

Sundaram, K.M.S., A. Sundaram and R. Nott. 1986. Mexacarbate deposits on simulated and live fir needles during aerial spray trials. Trans. of the ASAE, Vol. 29, pp. 382-392.

Teixeira de Almeida, M.E.F. 1983. Measurements of downwind ULV droplet profiles under various meteorological conditions. EPPO Bull. Vol. 13(3):433-437.

Turner, L.R. and K.A. Huntingdon. 1970. The use of water sensitive dye for the detection and assessment of small spray droplets. J. Agric. Eng. Res. 15(4):385-387.

Uk, S. 1977. Tracing insecticide spray droplets by sizes on natural surfaces. The state of the art and its value. Pestic. Sci. 8:501-509.

Wallace, K. and R. Jahren. 1988. An assessment of ground deposits from aerial spray operations in the Kamloops forest region of British Columbia. SRC Publication No. E-906-1-B-88, SRC Technical Report No. 200.

Ware, G.W., B.J. Estesen, W.P. Cahill, P.D. Gerhardt and K.R. Frost. 1969. High-clearance vs. aerial application of sprays. J. of Economic Entomology, Vol. 62, pp. 840-843.

Weisner, C.J. 1988. N.B. Productivity Research Council, Fredericton, personal communication.

Weisner, C.J. 1984. Bacillus Thuringiensis foliar deposition and efficacy against eastern spruce budworm - deposit analysis. N.B. Research and Productivity Council, Report No. C/83/221.

Yates, W.E., R.E. Cowden and N.B. Akesson. 1985. Drop size spectra from nozzles in high-speed air streams. Transactions of the ASAE, 0001-2351/85/2802-0405.

6 APPENDICES

A - OTHER METHODS OF ANALYSIS

B - PAPERS RELATED TO USE OF ROTOROD SAMPLER IN FORESTRY

C - THE ROTOROD SAMPLER OPERATIONS MANUAL

APPENDIX A

OTHER METHODS OF ANALYSIS

A.1 Laboratory Analysis

A.2 Droplet Stain Analysis

A.3 Deposition Surfaces (artificial)

A.4 Deposition Surfaces (natural)

A.5 Air Samplers

A.6 Innovative Samplers

A.1 Laboratory Analysis

There are three basic methods of laboratory analysis. They are: fluorescence, colorimetry, and direct analysis. All procedures are high quality droplet drift measurement techniques not recommended for operational programs.

Fluorescent material is one which, when excited by light of a particular wavelength, instantly emits light of a longer wavelength in a noncollimated form. It is the emitted light which is detected and measured using a photomultiplier tube and thus the reading is direct. The technique for fluorimetric analysis is fundamentally the same as for colorimetric analysis. However, in this instance the tracers used are fluorescent and because the instrumentation and chemicals used are far more sensitive, typical spray tracer concentrations are in the range of 0.01% to 0.05% w/v. With modern equipment it is possible to detect the presence of tracers at levels as low as 0.01 parts per billion (ppb). There is also a high level of linearity between the quantity of fluorescent material present in the solution and the readings obtained from the fluorimeter, thus further improving the accuracy. Rhodamine B, a compound which fluoresces in the red has also been used extensively. The use of fluorescein and Helios OB is well documented in the literature (Goering and Butler 1974; Richardson 1984; and Bryant and Courshee 1985). It is important to recover sprayed samples as quickly as possible due to photodegradation. Account must also be taken of the recovery of the compound from the surface of the target as the compound may be absorbed or adsorbed. Fluorimetry provides a high level of sensitivity but requires a greater need for experienced trained personnel and the equipment is expensive.

Another technique which has been used to varying degrees is the principle of surface fluorimetry. This involves making measurements of fluorescence of a traced spray directly from the surface of the leaf. For this technique it is usual to use intensely fluorescent pigment particles of 2 to 5 microns diameter and make a suspension in the spray. A short accurate pulse of initiating light is directed over a fixed area of the leaf and a photomultiplier tube detects and quantifies the amount of longer wavelength emitted light. Difficulties with the technique are, however, apparent, particularly with calibration, although some workers report its successful use (Sharp 1974).

Colorimetry involves tracing the spray formulation with a soluble coloured dye. Typical dyes include: Erythrosine (red) and water blue at concentrations from about 0.5% w/v up to 5% w/v for ultra low volume rates of application. The concentration of dye in any solution is measured using a colorimeter which measures the attenuation of light of a specific wavelength passing through a sample of the liquid. The absolute minimum detection limit under ideal circumstances is about 0.1 parts per million (ppm), although in practice this may be far from achievable (Last 1987). The spray can be traced on either natural or artificial targets. However, it is preferable to measure directly from the natural surface as artificial target deposits do not fully represent the amount caught by a plant (Uk 1977). Samples should be collected soon after spraying to minimize fading of the dye and should be stored in cool dark conditions. If two dyes with distinct wavelength absorption peaks are used it is possible to make simultaneous spray applications from different equipment and then determine the amount of spray caught on the collecting surface from each spray operation. A detailed

account of the methodology involved can be found in Johnstone (1977).

An alternative option to the use of artificially tracing the spray liquid is to analyze for the presence of the active pesticide ingredient directly. This may involve analysis for the presence of the active ingredient on the foliage, insects or artificial targets. Such analysis is complex and involves the use of expensive gas liquid chromatography equipment and highly trained personnel. The technique is sensitive to the presence of minute quantities of pesticide in the order of 0.1 ppm. This is not a commonly used technique and is restricted to laboratory conditions and usually undertaken only at larger institutions.

A.2 Droplet Stain Analysis

Droplet counting is the simplest form of droplet analysis and involves making counts of droplet numbers in a given area, usually with a hand-held magnifying lens in an operational setting. Generally this is conducted on artificial targets which are sensitive to the spray liquid or to a dye additive. Visual assessment is a purely subjective approach and involves observing the relative coverage or droplet density of a sample and then placing it into an appropriate class, usually on a sliding scale of ten classes. Assessments of this kind can be made for both artificial and natural targets if a fluorescent tracer is included in the spray. The technique is surprisingly accurate and comparisons with chemical analysis have indicated that with practice approximately 80% of subjective assessments are within a 15% error margin of the chemical analysis standard (Last 1987). By sizing droplets and making number counts at the same time it is also possible to calculate the volume of liquid which has been deposited. This is reliable only if the droplet

stains are close to circular and the relationship between stain size and initial droplet size is well established (i.e. spread factor). On natural surfaces this becomes very unreliable and large errors can be introduced.

There are two options when it comes to automated measurement of droplet sizes on natural or artificial targets: the use of a particle sizing instrument based on the principle of image shearing, or the more recent and expanding field of image analysis. The principle of image shearing for the sizing of particles is well documented by Johnstone and Huntingdon (1970) who make a comparison of this technique with standard microscope methods. The technique involves a vibrating mirror which causes the image of the droplets to oscillate and the degree of oscillation is varied by a small knob until the droplet image in question appears as two images just touching each other like billiard balls. The voltage applied to the mirror to cause the oscillation is linearly related to the amount of shearing, hence simple calibration allows a direct readout of the droplet size in microns on a display. Accuracy depends upon magnification and operator experience.

Of all the techniques identified, image analysis is probably the most versatile tool currently available. In simple terms image analysis consists of converting a standard raster scan video image into a digital equivalent and then making use of software application programs to make detailed measurements of the elements contained within the image. Any image which provides suitable contrast between the objects of interest and the background can be used to make the necessary measurements. System accuracy is a product of many factors but the most important ones usually considered are the pixel resolution of the digital image and the

magnification of the lens system used. The quality of the image being used is also an important factor, as lack of contrast and shading can induce significant errors. Aerially applied pesticide spray deposits have been successfully evaluated with a low-cost microcomputer-based image analysis system (Last and Parkin 1987). Uses have demonstrated the rapid characterization of aircraft spray deposit patterns both by measuring droplet numbers per unit area and by percentage cover.

A.3 Deposition Surfaces (Artificial)

In addition to Kromekote cards, many other surfaces have been used to collect pesticides. Barry et al. (1977) have reported the results from an experiment in western Montana in 1972 to study the impaction of particles on the western spruce budworm larvae as a function of particle size. They used glass slides measuring 2.5 x 7.6 cm and coated with Dow Corning silicon grease. The insecticide was applied by helicopter at an air speed of 48 km/h and a release height of 15 m above the canopy. Branch samples were taken to study particle impaction on foliage. All samples were analyzed with a microscope equipped with ultraviolet (UV) light for the presence of particle fluorescence.

MacCollum et al. (1968) measured the insecticide dust particles drifting adjacent to orchards. The depositing material was analyzed by observing the fallout of pesticide dust particles on exposed glass fibre filters in petri dishes at or close to ground level. The technique gave accurate drift residue amounts for the sampling area. Air sampling was also conducted for the pesticides and this gave a clear picture of the relation between concentration and deposition. In addition, fluorescent particles were added to the spray solution and counted by visual techni-

ques. This technique is a rapid visual indicator of the presence of pesticide.

Goering et al. (1977) compared different types of targets for spray drift measurements. Mylar sheets were selected as targets because they were inexpensive and convenient to use. Brilliant Sulfo Flavine was used as a dye tracer with a concentration of 0.5 g/L. The size of the target did not affect the drift deposited spray per unit area.

Newton et al. (1984) used mylar sheets to assess the deposition of herbicides within a forest. These sheets were found to be poor indicators of aerial deposits. When compared to foliage deposits no relationship could be found. Because there was no consistent relationship between deposits on mylar sheets and foliar concentration the mylar sheets were not recommended for quantitative evaluations of aerially applied herbicide.

Turner and Huntingdon (1970) describe a water sensitive paper using bromophenol blue which is a pH sensitive indicator. The paper can detect droplets down to 10 microns, but because of its high sensitivity it is susceptible to marking by fingerprints, etc. and is difficult to use under high humidity conditions. A magnesium oxide coated slide can be used as well for smaller droplets (May 1950). Water sensitive film based on 35 mm photographic film was used by Farlow and French (1956) for cloud physics studies. The solvent dissolves the top layer of the cellulose acetate paint and if the paint is bleached with acetone, then a measurable impression remains.

A.4 Deposition Surfaces (Natural)

Many workers have shown that two well replicated spray applications

can result in very different deposits on target foliage. Water based spray droplets when dyed with a suitable water soluble dye could be discerned, counted and sized on conifer foliage (Dorais 1988). The technique of counting individual droplets on needles is very laborious and time consuming. However, there is a strong relationship between spray deposit measured as droplets per needle and the drift deposit. Riley (1985) counted the total number of droplets on both sides of balsam fir needles that had been sprayed with Bt (Bacillus thuringiensis). Both sides of the needles were scanned and the individual droplets counted. An excellent correlation with drift deposit was found.

In a paper on Bt deposition to a forest canopy in New Brunswick, Weisner (1984) tried to relate the foliar deposit of Bt to field efficiency at a single concentration and application rate on balsam fir and red spruce. A study was undertaken to ensure maximum delivery in the range of 30 to 50 microns after evaporation. A number of water soluble dyes were used in this case including Erio Acid Red, Amaranth and Red 3. These dye stains showed up on the fir and spruce foliage even after prolonged freezer storage. All deposits were counted by a microscope procedure.

Last and Parkin (1987) have used a small microcomputer-based image analysis system to make automated measurements of spray deposits directly from natural surfaces. A fluorescent tracer (Tinopul CBS-X), good optics and sensitive camera are all important to provide good contrast suitable for analysis. The authors concluded that this technique has some difficulty for high flow rate sprays (about 200 L/ha), because the deposit does not necessarily consist of discrete droplet stains. Image analysis can provide a practical useful tool to measure deposits direct-

ly applied to the plant surface but it is not an operation procedure.

A report on the 1978 aerial spraying for the pine beauty moth (Joyce et al. 1981) described a target set at 20 droplets/cm^2. Fluorescent particles were added to the spray mixture. The spray droplets were allowed to deposit on Bristol cards and droplet stain diameters were measured. In addition, branch tip samples were taken from the tops and bottoms of the trees. The deposit cards were placed under the tree canopy. Five needles were taken from each branch and the number of visible droplets counted. The authors found that drift was difficult to assess accurately with this method. They accounted for drift by assessing the difference between emitted dosage and measured tree dosage which was averaged over six trees.

A.5 Air Samplers

Several types of air samplers are simple enough and robust enough to be considered as target droplet spectrum samplers. They are usually used for assessing drift droplets. A suction sampler draws in a volume of air and by directing it against some obstacle, can provide an efficient collection of droplets. The most useful form of a suction device is the cascade impactor (May 1945). This is basically an instrument with several impaction stages. At each stage an air nozzle causes droplets to impact onto a glass slide. The nozzle width reduces progressively at each stage, causing an increase in air speed and hence reduction in mean particle size collected at each stage. The main disadvantage of cascade impactors is their pumping requirement. They require a large vacuum pump and this can make it difficult for field use. They are, however, suitable instruments to measure droplet concentrations in

the range of 1 to 100 microns.

An alternative to moving the air towards an obstacle to provide increased impaction is to rotate the impaction surface. This technique is utilized by Rotorods which are discussed in the main text.

Ware et al. (1969) collected aerial drift using glass plates, cascade impactors and air samplers (impingers). The cascade impactor and air sampler data were in complete agreement with the glass plate collectors. These authors were particularly impressed by the cascade impactor as a tool for monitoring drift. The air samplers were similar to a scrubber system filled with ethylene glycol and scrubbed air at 28 L/ minute.

A.6 Innovative Samplers

Mexacarbate deposits on simulated and live balsam fir needles were measured at different crown heights using aluminum coils as the simulated foliar surface (Sundaram et al. 1986). The aluminum coil can provide a comparative picture of the deposits that can be obtained on a live fir foliage since the deposits on the two surfaces showed a linear relationship.

Teixeira (1983) measured the downwind drift with thin collector cylinders. Vertical profiles of droplets impacting onto the cylinder (3 mm diameter) were measured at distances up to 160 m downwind. Thin cylinders are very attractive in droplet drift studies because they are a much smaller collecting surface than the flat plates. Fluorescent particles were added to the carrier mineral oil to trace the spray droplets on the collectors. All experiments were carried out over a wheat canopy. The spray deposit collectors were analyzed in terms of stain

size and number of fluorescent particles. The spray analysis required only the sizing of the stains under a microscope.

A novel new collector has recently been proposed for pesticide drift by Bury (1987). The collector, a hair curler, was nearly five times as efficient as 2 mm diameter plastic tubing. Tests were conducted with this device for the drift from three separate nozzles. The sampler successfully identified the quantitative differences in the driftable fraction from each of the nozzles separately. The hair curler satisfies criteria such as: broad spectrum of capture efficiency, ease of handling, ease of dye wash off, compactness and cost. The curler is a complex shape similar to a cylindrical structure with many, very fine, spikes on the surface. Even though its overall diameter is about 2 cm, the lattice structure and surface projections provide a network of subcollectors which should allow the unit to collect both large and small droplets. According to Bury (1987) the curler appears to be an improvement upon traditional plastic tubing collectors.

For the capture of droplets smaller than 50 microns diameter, fibrous media can be employed. A practical form of fibrous collecting medium is the droplet harp developed by Himel and McDaniel (1975). This consists of a harp shaped frame on which fibers of 10 microns wire can be wound. It is difficult to collect small droplets under high humidities.

APPENDIX B

PAPERS RELATED TO USE OF ROTOROD SAMPLERS IN FORESTRY

PARTICULATE DISPERSION INTO AND WITHIN A FOREST*

GILBERT S. RAYNOR
Brookhaven National Laboratory, Upton, N.Y. U.S.A.

and

JANET V. HAYES and EUGENE C. OGDEN
New York State Museum and Science Service, Albany, N.Y., U.S.A.

(Received in final form 14 March, 1974)

Abstract. Particulate dispersion into and within a 10- to 13-m tall pine forest was studied experimentally at Brookhaven National Laboratory using stained ragweed pollen and other tracers ranging from 14 to 54 μm in diam. Seventy-two continuous point source releases lasting 20 to 40 min were made at various distances from within the forest edge to 60 m upwind and at heights of 1.75 to 14.0 m. In most experiments, differently colored ragweed pollen was released simultaneously from three locations. Thirty-six longer tests were made using pollen from area sources of ragweed and three with pollen from distant sources. All tests were made during the day with steady winds and unstable lapse rates outside the forest. The sampling network consisted of 119 rotoslide samplers mounted at heights from 0.5 to 21.0 m at 57 positions extending 100 m into the forest. Deposition was sampled by greased microscope slides at each sampling position. Meteorological measurements were taken in and near the forest.

Data were classified by particle characteristics; by source type, distance and height; and by meteorological parameters. Isopleths were drawn on scale diagrams of the sampling grid to illustrate concentration patterns. Changes in centerline concentration, crosswind integrated concentration, mass flux, plume width, plume height, deposition, and deposition velocity were related to distance within the forest and other variables. Results were compared to those of similar releases over open terrain and those of previous forest dispersion studies elsewhere.

The plume approaching the forest is broadened both vertically and horizontally by increased turbulence at the forest edge and flows mainly into the trunk space and above the forest. Lateral spread is slow within the forest, but vertical spreading beyond the entrance region is greater than in the open. Particles become mixed uniformly below the canopy while appreciable interchange takes place through this layer. Concentration within the forest decreases at a faster rate than in the open, but change in total mass flux within and above the forest is not significantly different. Loss of material takes place by impaction near the forest edge and in the tree tops and by deposition within the forest. Most loss takes place to the foliage rather than the ground, and larger particles are lost faster than smaller ones.

1. Introduction

Although much of the Earth's surface is still forested, most experimental data on short-range dispersion have been obtained over open terrain, while operational diffusion models are not designed to simulate diffusion in forest conditions. In many regions, however, plumes or clouds of air pollutants are just as likely to traverse forested areas as open fields. A few limited experimental studies as well as the available information on forest micrometeorology indicate that dispersion through a forest may differ significantly from that over open terrain. The experiments reported here

* This research was carried out under the auspices of the New York State Museum and Science Service and the U.S. Atomic Energy Commission and was partially supported by Research Grant No. R-800677 from the Division of Meteorology, U.S. Environmental Protection Agency.

Boundary-Layer Meteorology 7 (1974) 429–456. *All Rights Reserved*
Copyright © 1974 by D. Reidel Publishing Company, Dordrecht-Holland

were designed to study dispersion of particulates into a forest edge and within the forest after release from upwind point and area sources and had the following specific objectives:

(1) to determine the behavior of the plume as it approaches the forest edge,

(2) to determine how the plume divides between that portion which enters the edge and that which rises above the forest,

(3) to determine the rate of vertical particle interchange through the canopy,

(4) to determine dispersion and loss rates within the forest as compared to those over open terrain under similar conditions,

(5) to identify the mechanisms important in removal of particulates from the air within the forest and to evaluate their relative effectiveness,

(6) to relate these findings to source location, particle characteristics and meteorological factors.

In support of these objectives, instrumentation was installed to study the micrometeorology of the forest and its surroundings. The dispersion experiments were designed to be similar in scale and techniques to those conducted earlier over open terrain to facilitate comparison of results. A later report will describe results of additional tests in which tracers were released within and above the forest.

Several earlier experimental studies of forest dispersion have been reported but none involved continuous point or area source releases and all differ significantly from ours, making direct comparison difficult. Studies using aircraft line-source releases of tracer materials were conducted by Bendix Corporation (Hamilton, 1963) and Tourin and Shen (1969). Burnett and Thompson (1956) studied drift and canopy penetration of aircraft-released insecticides. Bowne *et al.* (1969) utilized line sources emitted from a moving vehicle upwind of a large woodlot complex or a smaller wooded area.

Instantaneous or short-period releases inside forests were used in studies by Tourin and Shen (1969), Melpar (1968) and Fritschen *et al.* (1970). Visual observations of smoke releases inside a jungle were described by Clayton *et al.* (1970). Wind tunnel studies of tracer diffusion into model forests were reported by Meroney (1968) and Meroney and Yang (1969). Studies of ragweed pollen penetration into forested areas were conducted by Neuberger *et al.* (1967), while Tauber (1967) discussed various aspects of pollen transport and removal within forests. Many papers on forest meteorology have been published, some of which were discussed earlier (Raynor, 1971).

In recent years, numerous models of wind and turbulence within and above forests have appeared, but only a few models of forest diffusion are known. Several of the authors referenced above related their results to regression equations or modifications of the Gaussian plume model. Two other papers may be mentioned:

(a) Calder (1961) developed a model for the penetration into a forest canopy by aerosols released along an elevated, infinite, crosswind line above an extended, uniform forest canopy. Concentration below the canopy is related to that above through a canopy ventilation rate. He did not consider edge penetration nor releases below the canopy.

(b) Ford and Lomen (1969) presented a model for diffusion from an instantaneous point source release under a forest canopy based on Batchelor's (1949, 1952) model for diffusion in homogeneous turbulence. They assumed perfect reflection at the ground and complete absorption at the canopy, both unrealistic assumptions for our experiments.

Meroney and Yang (1969) briefly reviewed these and other models. None is directly applicable to the conditions of our tests. Thus, only a description of the experiments and their results are included here.

The data on which this paper is based were presented in detail in two informal reports (Raynor *et al.*, 1972a, 1973). Some preliminary results of these experiments were described earlier (Raynor, 1967). A later paper described the wind and temperature structure in and around the experimental forest (Raynor, 1971).

2. Experimental Site

The experimental site was described in detail by Raynor (1971) and by Raynor *et al.* (1972a). Briefly, the forest has a straight edge in a nearly east-west direction with an

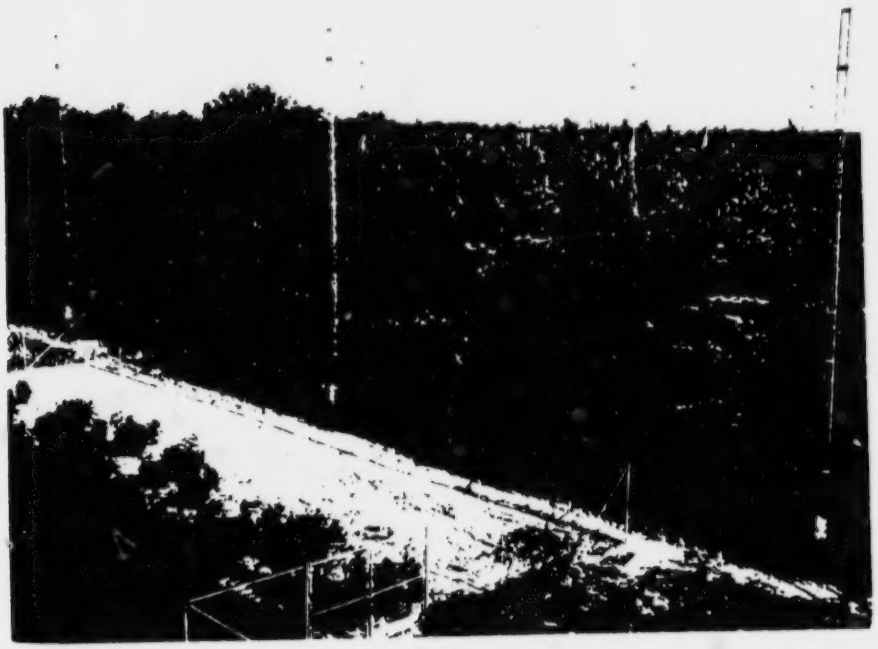

Fig. 1. View of the south edge of the forest in 1966 showing some of the towers and part of the area source ragweed plot.

at six heights from 1.75 to 45.7 m on towers in the nearby field. All thermometers were aspirated. Other recorded data included wind direction, speed and gustiness (Singer and Smith, 1953) at higher levels of the 128-m meteorology tower, pressure, relative humidity, sky condition and the synoptic situation.

Turbulence measurements, which were also made in and above the forest with sensitive bivanes, aided in the interpretation of dispersion results. Air flow and turbulence within the forest were observed visually during several series of smoke puff releases at various heights from ground level to canopy top.

Although the micrometeorology of the forest area was described earlier (Raynor, 1971), a brief review seems desirable to facilitate interpretation of the data presented below. Winds approaching the forest edge decrease only slightly in speed, but increased horizontal and vertical turbulence takes place in this region. Air which penetrates the forest edge flows primarily into the more open trunk space, so that speeds there are greater than those in the crown for a downwind distance of about 60 m. This distance is called the entrance region. Speeds decrease rapidly with distance inside the forest until equilibrium is reached at about 60 to 80 m. Beyond this distance, speeds vary little with height below midcanopy and do not change with distance. They average about 0.5 m s^{-1} under typical daytime conditions or about 20% of speeds outside the forest. Speeds above 1.0 m s^{-1} are rare even with high winds outside.

During the day with unstable lapse rates outside, a temperature inversion is typical below the canopy. However, unequal heating of the treetops and mechanical mixing induced by the rough and uneven surface cause considerable turbulent interchange through the canopy and rather complete mixing below. Visual observations of smoke releases revealed that subsidence was most likely in the open areas, with upward motions in the denser parts of the forest. Burnett and Thompson (1956) reported that natural openings in the canopy assisted penetration of aircraft-released insecticides.

5. Sources

All particles used in point-source dispersion experiments were emitted in a liquid suspension from atomizing nozzles which produced a spray of fine droplets having a mean diameter of about 15 μm. The concentration of particles in the liquid was kept low enough to minimize the probability of agglomeration. After emission, the droplets quickly evaporated, leaving the particles entrained in the ambient air.

In most tests, prestained ragweed (*Ambrosia*) pollen (Raynor *et al.*, 1966) was used as a tracer and, in nearly all tests, simultaneous releases of differently colored pollen were made from three locations. In a few tests, other pollens or spores were used with or in place of ragweed pollen to study the effect of particle size. In several early tests, radioactive copper spheres (Raynor and Smith, 1964) were used.

Source locations were chosen to study the effect of distance from the edge, and of height, on penetration into and diffusion within the forest. Locations ranged from 6 m within the forest to 60 m upwind and heights from 1.75 m to 14.0 m. Characteristics of the tracers are given in Table I.

open field to the south (Figure 1). Over 90% of the trees are pines and the remainder consist of several deciduous species. Stem density is 1474 trees per hectare. Mean tree height increased from about 10.5 to 13 m during the years when experiments were undertaken. At the forest edge, dense foliage extends to ground level, but inside the forest, few living branches remain below 3 m. The canopy is mostly closed, but several small openings are present. Undergrowth is sparse and local.

3. Sampling Network

The sampling network (Figure 2) includes 119 rotoslide samplers (Ogden and Raynor, 1967) mounted on 16 triangular steel towers from 15 to 21 m tall and on low-level

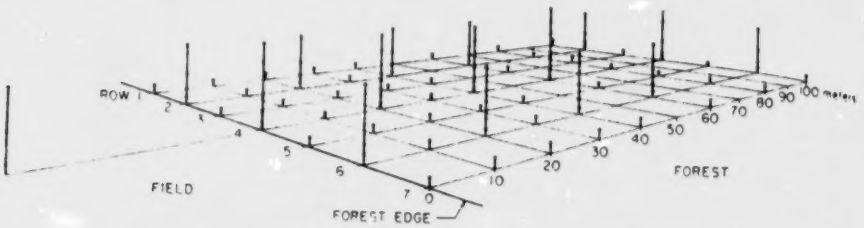

Fig. 2. Perspective diagram of forest sampling grid. Dots represent sampler positions.

sampler supports at 41 other locations. Sampling positions are placed along seven rows, 10 m apart, extending into the forest at right angles to the edge. The first position in each row is 1 m outside the edge, and the others are located at 10, 20, 30, 40, 60, 80 and 100 m inside the forest. The array includes one instrumented tower 30 m upwind of the forest.

Samplers are mounted at a height of 1.75 m at all 57 positions and at heights of 3.5, 7.0 and 14.0 m on all towers. Along the central row, samplers are mounted at 0.5 m at all positions and at 17.5 m on the five towers. An additional sampler is mounted at 21.0 m on the tower 60 m from the edge. All samplers can be started and stopped simultaneously. Since the sampling network was installed gradually over a period of several years, earlier tests do not include data from as many positions as later ones. The installation schedule was given earlier (Raynor *et al.*, 1972a). Deposition to the ground was measured using two greased microscope slides on the ground at each sampling position.

4. Meteorological Data

Meteorological measurements were taken in support of all tests. Wind speeds were recorded by 25 sensitive cup anemometers mounted along the central row of towers at distances from 0 to 100 m from the edge and in the field. Heights ranged from 1.75 to 21.0 m.

Temperatures were measured at four heights from 1.75 to 14.0 m in the forest and

TABLE I

Characteristics of tracer particles

Type	Shape	Surface	Size (μm)
Ragweed (*Ambrosia*) pollen	Spheroidal	Spiny	18-20
Timothy (*Phleum*) pollen	Spheroidal (may collapse)	Smooth	30-35
Paper Mulberry (*Broussonetia*) pollen	Spheroidal (may collapse)	Smooth	14
Club Moss (*Lycopodium*) spores	Modified pyramidal	Slightly rough	32
Fern (*Osmunda*) spores	Spheroidal	Smooth	54
Copper spheres	Spheroidal	Smooth	9.5

Area sources were produced by plots of cultivated ragweed grown in the field upwind of the forest edge. During the first two years of area source tests, the 464-m^2 plot measured 30.5 × 15.2 m with the long axis parallel to the forest edge and the nearest plants about 2 m away. In the last three years, the plot measured 30.5 × 10.1 m or 308 m^2 with the nearest plants about 7 m from the forest. Most pollen was released from the upper half of the plants, which varied from 1–2 m in height in different years.

Several additional tests were made with background ragweed pollen from unknown, distant sources during periods when the cultivated source was absent.

6. Procedure

Point-source test periods were selected for a wind direction blowing into the forest at right angles to the edge and for speeds great enough to ensure a relatively constant mean direction. All tests were made during the day, most with unstable lapse rates and none during precipitation. Most tests lasted from 20 to 40 min; significant changes in meteorological conditions did not occur during these intervals. Particles collected were counted by use of a microscope, and rotoslide counts converted to concentrations (grains m^{-3}). Deposition counts were reduced to units of grains m^{-2}. Wind speeds and other meteorological data were recorded during each test. Procedures for area-source tests were similar except that test-periods normally lasted several hours.

Data from all tests were plotted in three planes on scale diagrams of the sampling grid. Isopleths of concentration were drawn to show the pattern in each dimension.

Analytical procedures were similar to those used in earlier studies of dispersion over open terrain (Raynor *et al.*, 1970, 1972b) and were chosen to describe plume shape, change of concentration with distance and rate of particulate loss. Point source data were normalized by output rate before further analyses, but area source data were used as concentrations since outputs were unknown. Data were classified by source distance, source height and particle type. Means and standard deviations were calculated for groups of similar data. Results presented below are primarily from average values, but complete data with means and standard deviations for each individual test have been presented in the reports by Raynor *et al.* (1972a, 1973).

7. Tests

The data presented here were obtained from 111 releases made in 64 tests conducted from 1964 to 1970. Seventy-two point source releases were made during 27 separate tests. In eight of these tests, simultaneous releases were made at three different distances from the forest edge but at the same height, either 1.75 or 2.0 m. In 10 tests, simultaneous releases were made from three heights at a single distance. Three or four tracers with different physical characteristics were released from one location in three tests. The other six were early tests in which only single releases were made.

Thirty-six tests were obtained using ragweed pollen emitted naturally from upwind area sources, twenty-two from the 308-m^2 source and 14 from the 464-m^2 plot. Ragweed pollen from distant sources was sampled in three tests, two of which were simultaneous with point source releases.

8. Results

8.1. Concentration patterns

Concentration patterns from all tests were orderly and internally consistent, due to the chosen meteorological conditions and emission durations. The patterns show a general resemblance to those resulting from similar tests conducted over open terrain

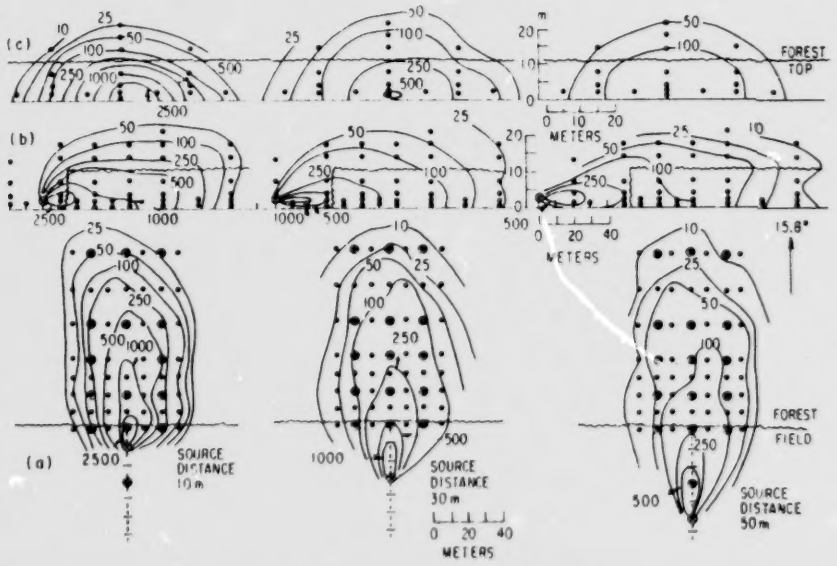

Fig. 3. Concentration isopleth patterns resulting from simultaneous point source releases of ragweed pollen at a height of 1.75 m at 3 distances upwind from the forest edge. (a) horizontal plane at a height of 1.75 m. (b) downwind-vertical plane along grid centerline. (c) crosswind-vertical plane at forest edge.

although they differ in several important details as a result of the flow patterns caused by the presence and characteristics of the forest. Thus, they vary with source location within the local boundary and with meteorological conditions.

Figure 3 illustrates normalized dispersion patterns in three planes resulting from simultaneous release of ragweed pollen at distances of 10, 30, and 50 m from the forest edge at a height of 1.75 m.

Figure 3a shows concentration patterns at source height. The broadening of the plume as it approaches the forest edge is typical and results from increased crosswind turbulence as the air approaches the dense stand of trees. This effect was also noted by Bowne *et al.* (1969). The marked decrease in forest edge concentration with increase in source distance results largely from dispersion, although some loss by deposition also occurs. The isopleth shapes show that lateral dispersion after the plume enters the forest is small and that decrease in concentration accelerates at about 80 m in the forest. In many cases, a rapid rate of loss is also evident just within the edge due to impaction on the foliage since wind speeds here are still relatively high. The loss farther within the forest results largely from deposition since wind speeds are low and movement of the plume slow. Deposition, as used here, includes gravitational settling to the upper sides of foliage and branches as well as to the ground, while impaction implies inertial collision with obstacles during transport in a more or less horizontal direction.

Figure 3b is a downwind-vertical plot of concentration along the grid centerline and shows that the plume widens in the vertical as well as the horizontal. Most particles from the 10-m distant source enter the forest at a low level, although some are carried

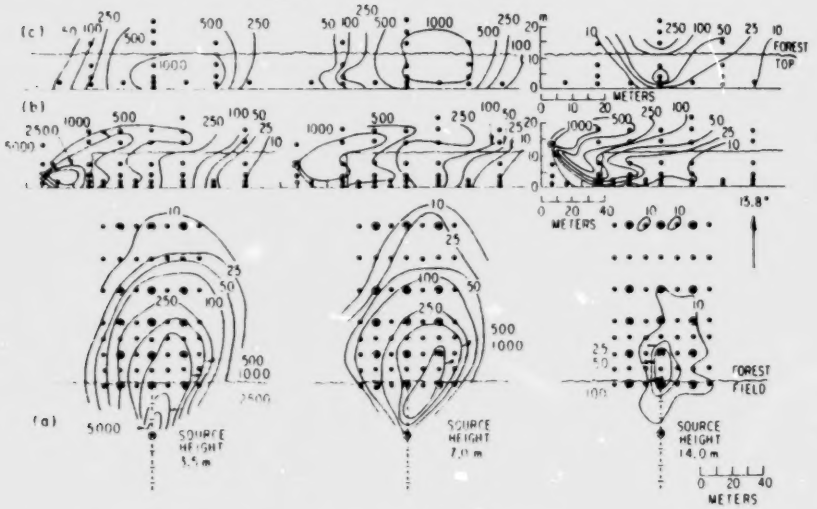

Fig. 4. Concentration isopleth patterns resulting from simultaneous point-source releases of ragweed pollen at a distance of 30 m and 3 heights. (a), (b) and (c) as in Figure 3.

above the treetops before they reach the forest edge. With increasing upwind source distance, an increasing percentage of the particles is entrained in the flow above the forest. The nearly vertical isopleths beyond 60 m result from interchange through the forest crown, with thorough mixing below. Rather similar patterns were found by Meroney and Yang (1969) in a wind-tunnel study of diffusion into a model forest.

Note the change in horizontal scale in Figure 3c which is a crosswind-vertical plot of concentrations at the edge of the forest. The decreases in both maximum concentration and concentration gradient with increasing source distance are evident.

Figure 4 illustrates similar data from releases at the 3.5-, 7.0- and 14.0-m heights, 30 m from the forest edge. Figure 4a shows patterns at 1.75 m. Concentrations at this level decrease with increasing source height while the location of the maximum occurs farther downwind.

Figure 4b, the downwind-vertical plots, shows that most particles penetrate the forest in the trunk space or rise above it and that an increasing percentage rises above with increasing source height. However, appreciable amounts follow both pathways from both high and low sources, while little penetration occurs in the crown. Within the forest, interchange through the canopy is again evident.

Figure 4c illustrates the crosswind-vertical particle distribution at the forest edge. The height of maximum concentration increases with source height, although the pattern for the 14-m release includes a secondary maximum at a low level.

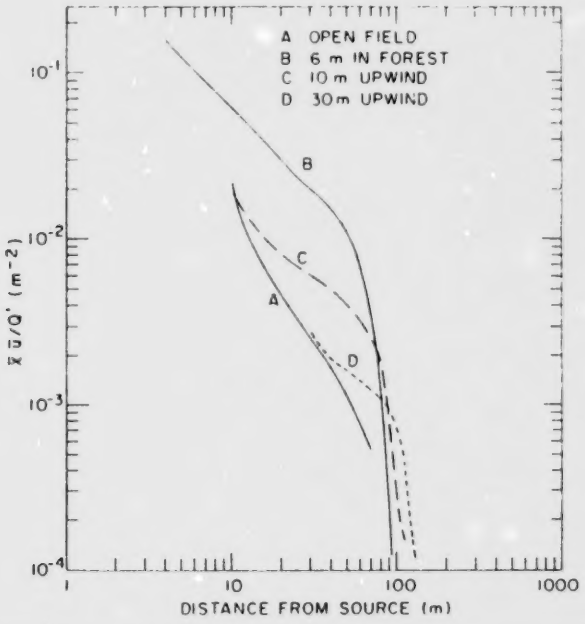

Fig. 5. Mean normalized 1.75-m centerline concentration from point sources of ragweed pollen at 1.75-m height as a function of distance from source.

Three point source releases were made 6 m inside the forest edge. These resulted in rather narrow plumes, particularly near the source since the release point was downwind of the edge effect. The patterns resemble those over open terrain although gradients are even steeper. Appreciable material appears above the forest within a short downwind distance.

Patterns from area-source releases differ somewhat. The width of the source area and the greater wind direction fluctuations associated with the longer duration of the test both contribute to a somewhat wider pattern, but other features are similar to those of point-source releases at similar distances and heights.

8.2. Centerline concentrations

To facilitate comparison with other data, axial concentration measurements ($\bar{\chi}$) are frequently normalized by the source-height wind speed ($\bar{u}$) and the emission rate (Q'). Curves of $\bar{\chi}\bar{u}/Q'$ for the means of all point-source releases from a height of 1.75 m at three selected distances are compared in Figure 5 to the curve from a group of similar releases over open terrain using the wind speed at the release point. Initial rate of decrease is less in the forest than in the open, but final rate is greater.

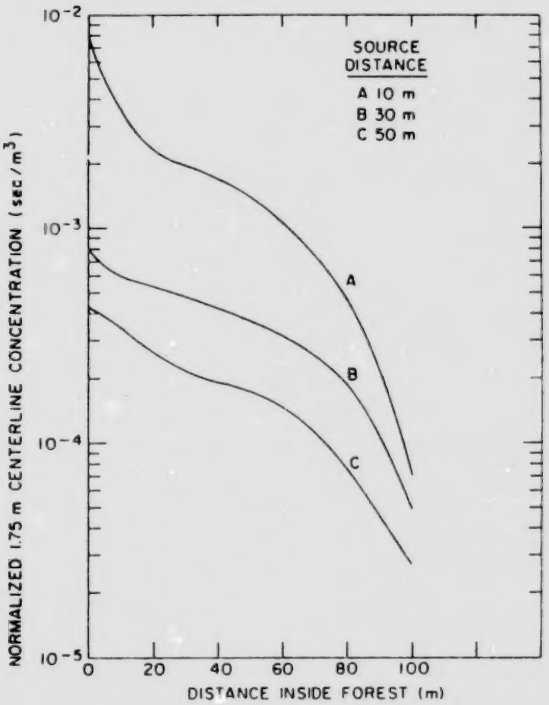

Fig. 6. Normalized 1.75-m centerline concentration as a function of distance in the forest for simultaneous point-source ragweed pollen releases at 1.75-m height and 3 distances.

For other presentations below, point-source data are normalized only by the output rate, and area-source concentration data are not normalized. For most comparisons, concentrations are normalized to 100% at the forest edge since dispersion within the forest is of primary interest.

Figure 6 illustrates change of concentration with distance within the forest for simultaneous releases of ragweed pollen at one height but three distances from the forest edge. Diffusion outside the forest has reduced initial concentrations from the more distant sources by factors of 10 and 20 as compared to the 10-m source. However, concentrations at 100 m differ by less than a factor of 3 indicating faster dispersion of the more concentrated plume. The changes in slope reflect impaction losses in the first 20 m, slow dispersion to 60 m and loss by deposition thereafter.

Similar data for a typical test with releases from a single distance and three heights are shown in Figure 7. Curves from the two lower levels do not differ greatly and show the same features as those of Figure 5, but concentrations from the 14-m source peak at 30 m in the forest and decline at a slower rate. At these distances, much of the material at the 1.75-m level has been transported downward from above the forest where concentrations change more slowly with distance.

Change in axial concentration for all releases from a height of 1.75 m at six selected distances is shown in Figure 8. Data for upwind releases are normalized to 100% at

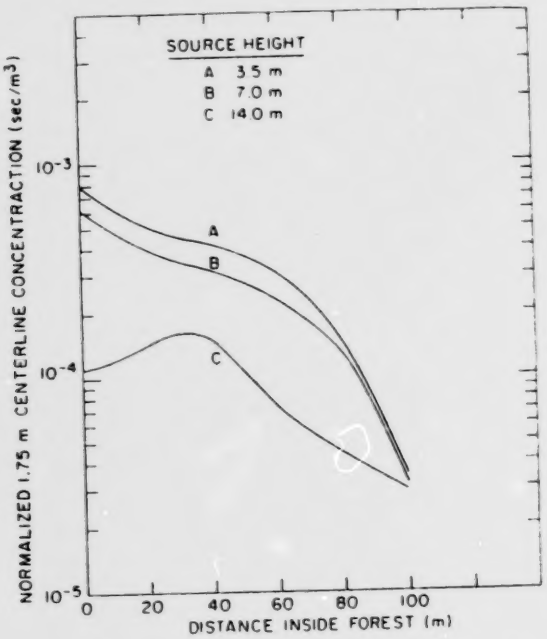

Fig. 7. Normalized 1.75-m centerline concentration as a function of distance in the forest for simultaneous point-source ragweed pollen releases at 3 heights and 30-m distance.

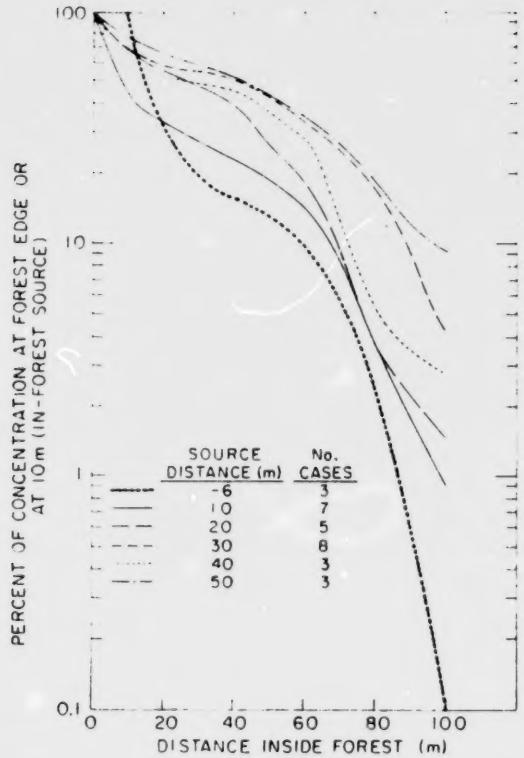

Fig. 8. Mean percent of 1.75-m centerline concentration at the forest edge as a function of distance in the forest for point-source ragweed pollen releases at a height of 1.75 m and 6 distances.

the forest edge and those from the releases 6 m within the forest to 100% at 10 m. With minor exceptions, rate of decrease is inversely related to source distance. Changes in slope are similar to those pointed out earlier. Reduction in axial concentration is 90% or more over the 100-m travel distance.

Similar curves are plotted in Figure 9 for all releases at the four specified heights, 30 m from the forest edge. Rate of loss is inversely related to source height, although curves from the three lower levels are closely grouped. Except for the 14-m release, concentrations at 100 m are again less than 10% of those at the edge.

Centerlines at source height were also examined for the releases above 1.75 m. Those at 3.5 and 7.0 m decreased at about the same rate as the lower releases from the same distances. Those at 14 m had higher values at 10 and 20 m but about the same as the lower sources at greater distances.

Centerline concentrations from area sources decrease at a rate similar to those from more distant low-level point sources in the first 40 m (Figure 10) since plume widths

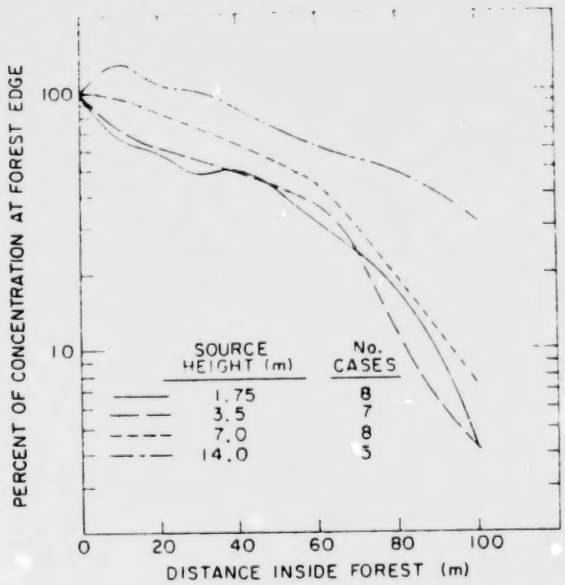

Fig. 9. Mean percent of 1.75-m centerline concentration at the forest edge as a function of distance in the forest for point-source ragweed pollen releases at a distance of 30 m and 4 heights.

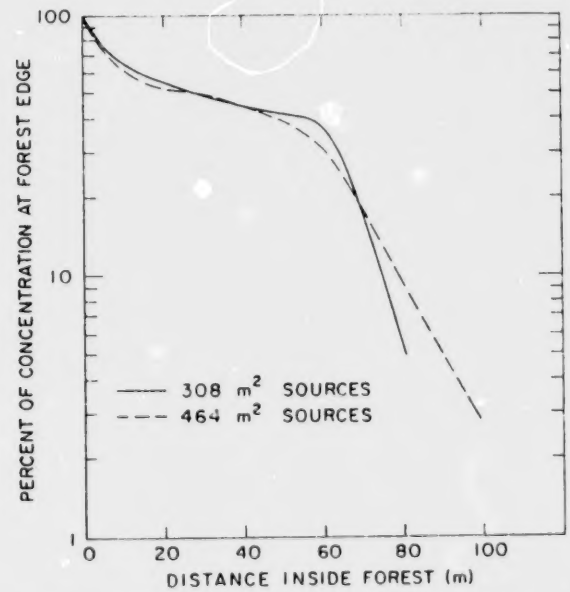

Fig. 10. Mean percent of 1.75-m centerline concentration at the forest edge as a function of distance in the forest for area-source ragweed pollen releases.

at the forest edge are similar. The rate of loss beyond 60 m is somewhat greater because most pollen from area sources enter the forest at a low level and less is available above to replenish particles at the 1.75-m level as they settle. Thus, concentrations at 100 m are only 3% or less of those at the edge.

The role of particle size was investigated by simultaneous releases, in several tests, of two or more particle types from a single location. Differences in rate of loss of four

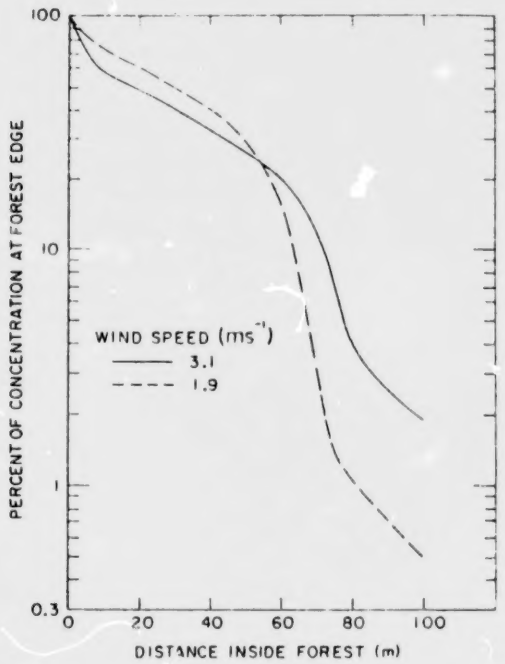

Fig. 11. Percent of 1.75-m centerline concentration at the forest edge as a function of distance in the forest for point-source ragweed pollen releases 20-m distant at a height of 2 m under two mean wind speeds.

pollen and spore species are small, although concentrations at 100 m are inversely related to particle size. Results from these tests indicate that gravitational settling is less important than dispersion processes.

The relationship of centerline concentration to wind speed was also studied, although the range of wind speeds during these tests was not great. Figure 11 shows data from two releases 20 m from the edge at a height of 2 m. Rate of decrease in the first 10 m is greater for the case with the higher wind speed since impaction losses predominate here, but the rate beyond 60 m is greater for the lower speed case showing the importance of deposition within the forest. No consistent relationship with other meteorological variables was found.

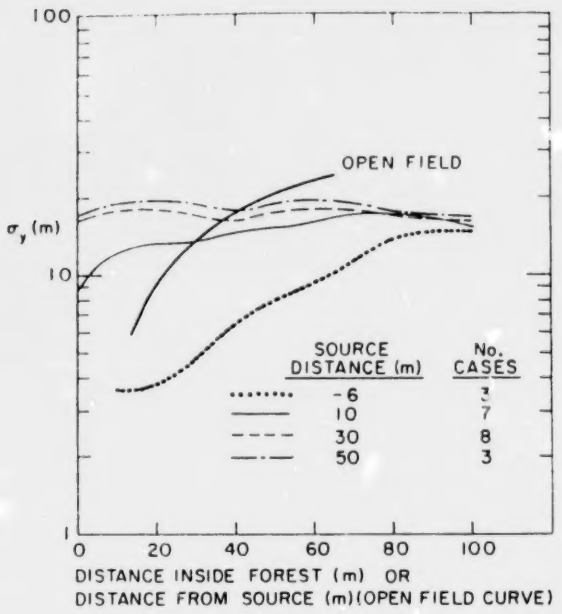

Fig. 12. Plume width (σ_y) as a function of distance for point-source ragweed pollen releases at 1.75-m height at four distances from the forest edge and in an open field.

8.3. Plume width

The standard deviation of the crosswind distribution of particles in the plume (σ_y), was selected as a measure of plume width and computed by conventional techniques. Results confirm the earlier interpretation of isopleth patterns that little lateral dispersion occurs after the plume enters the forest. Thus, σ_y is determined primarily by dispersion outside the forest. As shown in Figure 12, σ_y is slightly larger for the more distant sources but, except for the 10-m source, shows no growth with distance for plumes penetrating the edge. Plumes originating within the forest, however, show a growth to a distance of 80 m. For comparison, a σ_y curve derived from similar releases of ragweed pollen over open terrain (Raynor *et al.*, 1970) is shown. Although initial values in the forest are higher, more distant values are lower, indicating less lateral dispersion.

Results for point-source releases from other elevations and for other particles and for area-source tests were similar. All show essentially no growth in σ_y except for point sources near the edge where growth is evident for 20 to 30 m into the forest.

8.4. Plume height

The standard deviation of the vertical distribution of particles along the plume centerline (σ_z) was chosen as a measure of plume height and computed by methods

similar to those used to determine σ_y. However, σ_z could only be computed for those plumes which remained mostly below the upper samplers. In addition, σ_z could not be calculated for some low-level plumes because the particles became uniformly distributed vertically at the greater distances.

σ_z shows a greater separation by source distance than σ_y and a more continuous, although slow, growth with distance (Figure 13a). Values are much larger than those for open field releases and nearly as large as those of σ_y indicating that the forest enhances vertical dispersion while suppressing lateral spread. Data were also studied from releases of other particles, from releases at other heights and from area sources. All are similar to those presented. Melpar (1968) reported that vertical diffusion within the forest was very much more rapid with distance than it would be in the open but became more alike with time.

The ratio σ_z/σ_y gives a measure of plume shape. Ratios from these tests and from open field ragweed pollen releases are shown in Figure 13b. In contrast to the open field data where the ratio decreases with distance, ratios of forest measurements increase slightly or remain constant with distance, suggesting that dispersion rates in both the vertical and horizontal directions have reached a constant ratio.

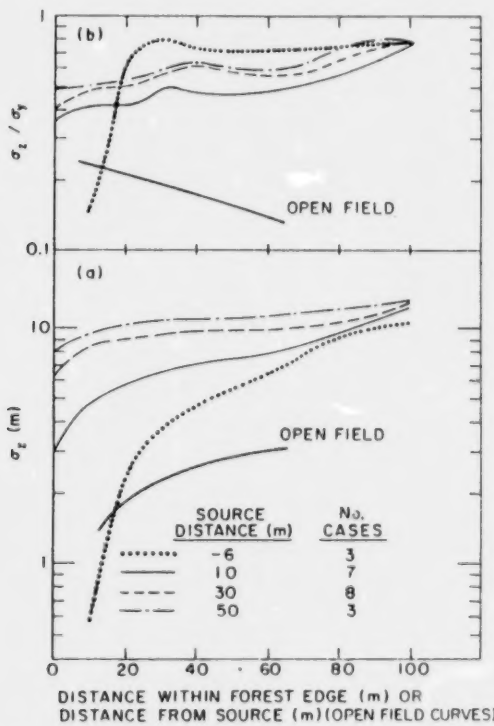

Fig. 13. (a) Plume height (σ_z) and (b) plume shape (σ_z/σ_y) as a function of distance for point-source ragweed pollen releases at 1.75-m height at four distances from the forest edge and in an open field.

8.5. Crosswind integrated concentration

Concentration data for most cases were integrated graphically in the crosswind direction at all sampling distances. Since some extrapolation beyond the sampling grid was always necessary, cases which could not be reliably extrapolated were excluded. Results were examined by distance and height of release. Decrease in 1.75-m crosswind integrated concentration (CIC) (Figure 14) was slower than decrease in centerline concentration (Figure 8) and showed little relationship to distance of release suggesting that the progression in the centerline curves of Figure 8 was due primarily to differential lateral dispersion.

The 1.75-m CIC from higher level releases (Figure 15) also decreased more slowly than the corresponding centerline values (Figure 9) but showed a similar separation by source height.

CIC at source height was also examined for higher level releases and found to be similar to those at 1.75 m except that the percentage of the 14-m release was somewhat higher to a distance of 20 m, similar to the centerline curve.

CIC at 1.75 m was also studied for area sources (Figure 16). They decreased at a rate similar to those from low-level point sources (Figure 14) and somewhat more

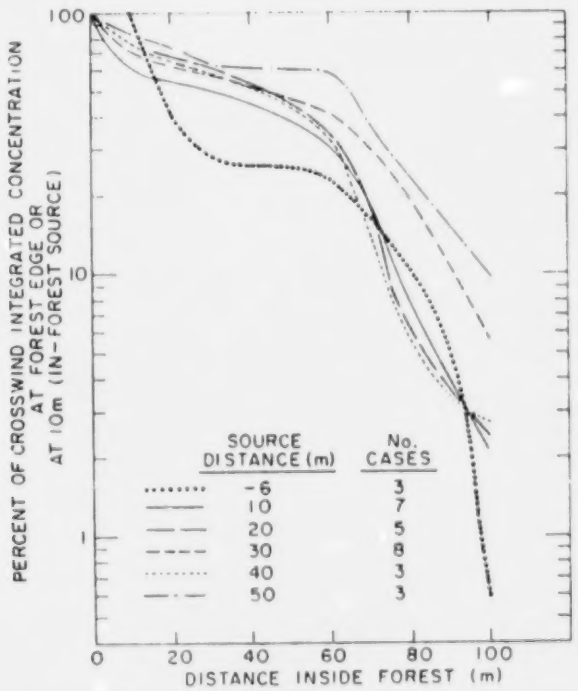

Fig. 14. Mean percent of 1.75-m crosswind integrated concentration at the forest edge as a function of distance in the forest for point-source ragweed pollen releases at a height of 1.75 m and six distances.

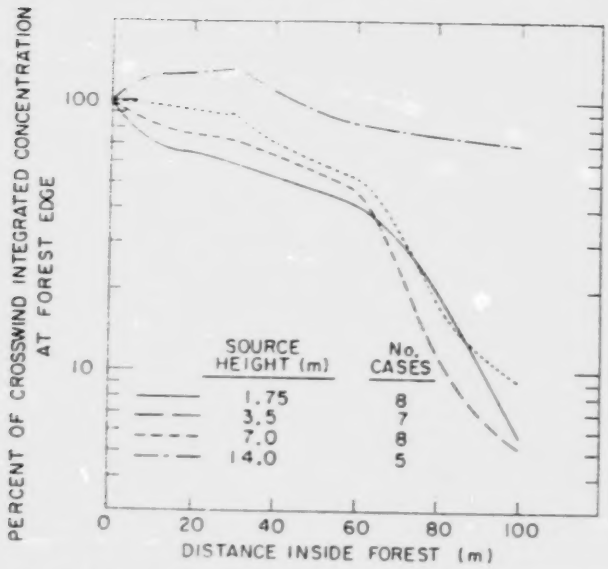

Fig. 15. Mean percent of 1.75-m crosswind integrated concentration at the forest edge as a function of distance in the forest for point-source ragweed pollen releases at 30-m distance and four heights.

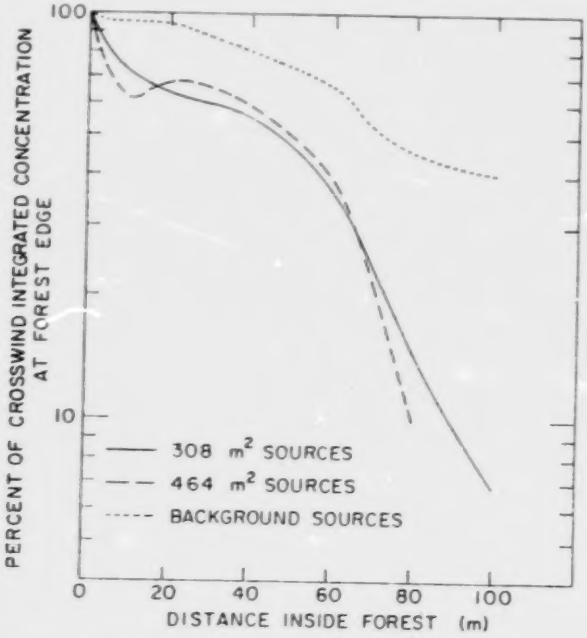

Fig. 16. Mean percent of 1.75-m crosswind integrated concentration at the forest edge as a function of distance in the forest for area-source and background ragweed pollen.

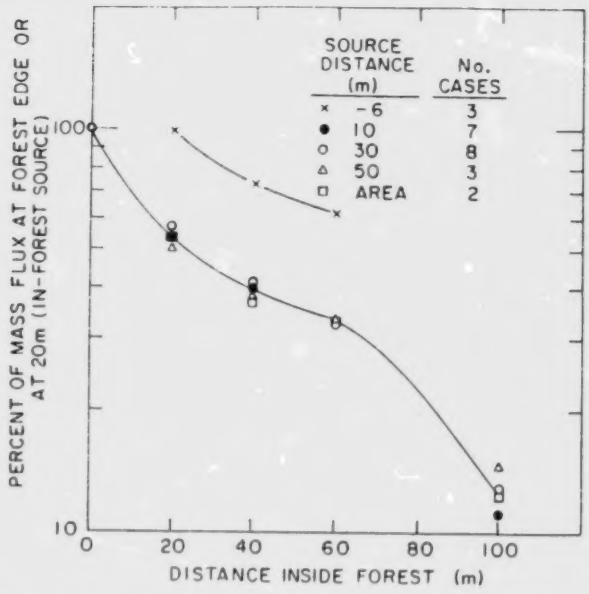

Fig. 17. Mean percent of mass flux at the forest edge as a function of distance in the forest for point-source ragweed pollen releases at a height of 1.75 m and four distances and area source releases.

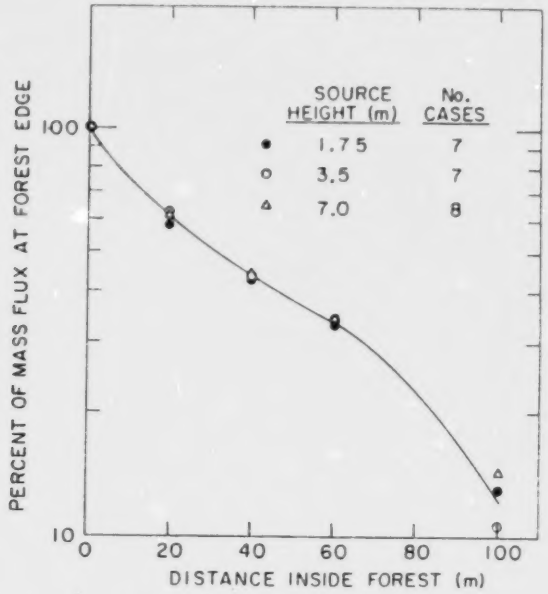

Fig. 18. Mean percent of mass flux at the forest edge as a function of distance in the forest for point-source ragweed pollen releases at 30-m distance and three heights.

slowly than centerline concentrations (Figure 10). A few cases could not be included because of their width beyond the sampling grid or because the plume centerline made too great an angle with the grid.

Data from the three tests sampling background pollen were integrated only across the width of the sampling grid since similar concentrations continued indefinitely in both crosswind directions. As shown in Figure 16, these CIC decreased much more slowly than those from point or area sources. Since initial concentrations vary little in either the horizontal or vertical direction, this decrease may be attributed to actual loss of particles rather than dispersion.

8.6. Mass flux

The total number of particles remaining airborne at each sampling distance was determined by integration. Mass flux was calculated for all point-source releases except (a), a few high-level emissions in which much of the material was transported above the forest; and (b), some early tests taken before the three rows of towers were installed. Some extrapolation in the crosswind and vertical directions was necessary to include all particles. Only two area-source tests could be used since many were taken before the tower array was installed, and plumes in most of the rest were too wide for reliable extrapolation.

Decrease in mass flux with distance within the forest showed little variability with source distance, source height or type of source, as shown in Figures 17 and 18 where the data points are so close together that only single lines are drawn through them. All decreased at essentially the same rate, which did not differ appreciably from the rate found for similar ragweed pollen releases over open terrain (Raynor *et al.*, 1970). Apparently the ascent of part of the plume at the forest edge compensates for the increased loss by impaction and deposition within the forest.

Mass flux for releases at a height of 14 m should decrease at a slower rate with distance since fewer particles are subject to impaction, and deposition would occur farther downwind due to the higher wind speeds above the canopy. On the other hand, particles released beyond the edge effect within the forest should be lost faster.

Study of individual tests shows that decrease in mass flux occurs faster at lower wind speeds. Data from two tests in which particles were emitted at distances of 20 and 40 m and a height of 2 m are shown in Figure 19. For both distances, loss is appreciably greater at the lower wind speed.

Seven tests were made with releases at 3.5-m height and 30-m distance. Although the 1.75-m wind speeds only varied from 2.3 to 3.5 m s^{-1}, the percentage of material remaining airborne at 60 m clearly increased with wind speed (Figure 20). These results reinforce earlier evidence that the major mechanism of particle loss is deposition within the forest due to low wind speeds and slow transport below the canopy rather than impaction to the foliage. If the latter mechanism were predominant, the trend with wind speed should be reversed.

In order to evaluate particle transport and rate of loss through each major vertical layer of the forest, mass flux was computed separately at each sampling distance for

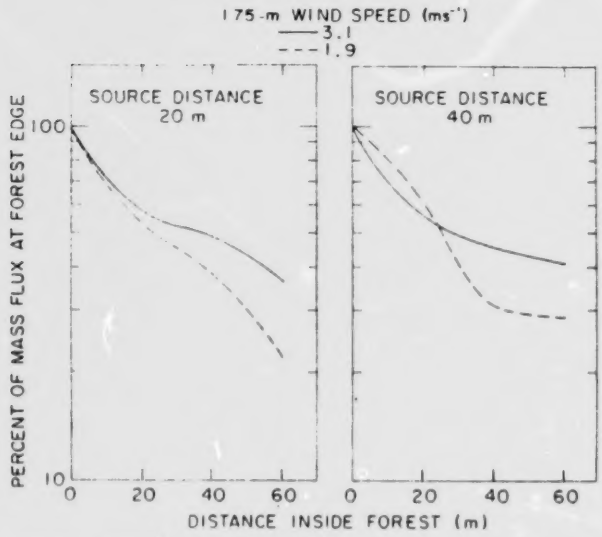

Fig. 19. Mean percent of mass flux at the forest edge as a function of distance in the forest for point-source ragweed pollen releases at two wind speeds and two distances.

the trunk space, canopy and the space above the trees. Results from all releases at a height of 1.75 m and two distances from the edge are shown in Figure 21. For the 10-m distant releases, equal fluxes are present in the canopy and in the trunk space at the edge of the forest and only about a tenth as much above the trees. By 25 m, more material is above the forest than in either lower layer, and by 100 m, the amount above the trees is nearly seven times the amount in both forest layers. Depletion is fastest in the trunk space and slowest in the above-canopy level. Interchange between the layers takes place continuously so individual particles do not necessarily remain in the same layer.

Results for the 30-m distant release are similar except that the total number of particles is lower, more material is initially at a higher level and the amount above the trees predominates nearer the edge. These differences are all due to greater dispersion before the plume reaches the forest edge.

Data from releases at three heights at the 30-m distance are compared in Figure 22. The initial amount above the trees increases somewhat with source height, but other differences are slight. Thus, rate of loss and partition of material between layers are not sensitive to source distance over the range studied or to height, provided that much of the material reaches the forest below treetop height.

The effect of particle size was examined next. Different particles were emitted with ragweed pollen in only four tests, but since several were emitted simultaneously, nine comparisons are possible. In eight, the amount of timothy or paper mulberry pollen or *Lycopodium* spores remaining at 100 m differed by no more than 5% in either

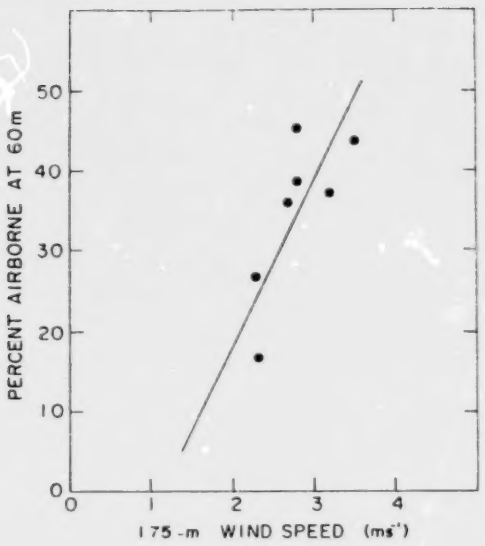

Fig. 20. Percent of mass flux at the forest edge remaining airborne at 60 m in the forest as a function of 1.75-m wind speed in the open.

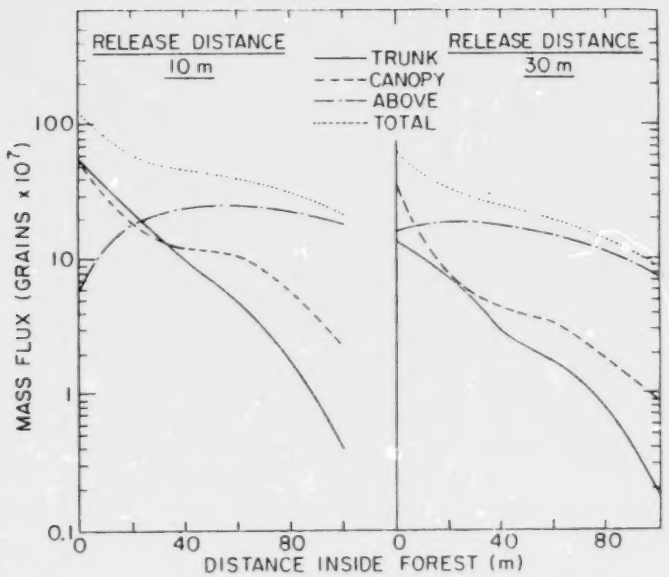

Fig. 21. Total mass flux and mass flux in three layers as a function of distance in the forest for point-source ragweed pollen releases at 1.75-m height and two distances.

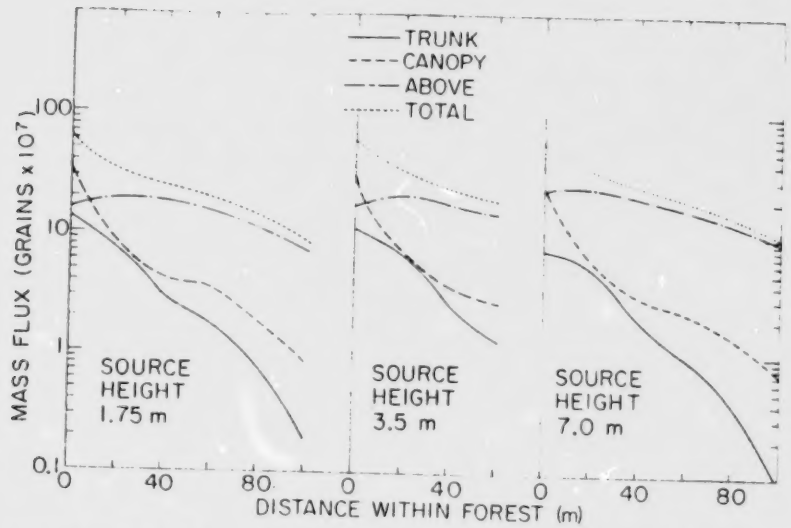

Fig. 22. Total mass flux and mass flux in three layers as a function of distance in the forest for point-source ragweed pollen releases at 30-m distance and three heights.

direction from the amount of ragweed pollen. In a single test, *Osmunda* spores, the largest particle used, were more than 10% less than ragweed pollen at 100 m. However, greater variation occurred between separate ragweed pollen releases. Thus, particle size, over the range tested, does not appear to affect the rate of particle loss in the forest significantly.

8.7. Deposition

In earlier sections, the predominant role of deposition over impaction in removing particles from the air in the forest was shown. No attempt was made to obtain quantitative measurements of particle attachment to foliage by either process but some observations were made. After one of the tests using radioactive particles as a tracer, foliage samples were taken at several distances from the source and assayed. Appreciable counts were obtained, generally decreasing with distance, from both pine needles and leaves of deciduous trees. Pine needles were later examined under a microscope and numerous colored pollen grains were found lodged in the hollows on the rougher side of the needle. In another examination, large quantities of various pollens were recovered from a small group of pine needles. Thus, the ability of foliage to capture and retain particles is amply demonstrated although the two methods of capture could not be evaluated separately. Neuberger *et al.* (1967) and Tauber (1967) also documented the effectiveness of foliage in capturing airborne particles.

Deposition to the ground was measured during all tests, but only a small proportion of the particles lost from the air was found on the ground. A comparison between

changes in mass flux and deposition of ragweed pollen over the same distances showed that only about 1% reached the forest floor from most releases at the 1.75-m height, although about 4% was found from the releases at 10 and 15 m from the forest edge. Between 2 and 3% of the loss from the 3.5- and 7.0-m sources at 30-m distance was found on the ground. The three larger particle sizes deposited somewhat more heavily and ranged from 3 to 9% for 1.75-m sources at various distances while the small paper mulberry pollen grains deposited least.

Deposition tended to be spotty or irregular, and the change with distance along the centerline was not smooth even for the mean of several tests. However, a general decrease with distance was usually found except for higher level sources where maximum deposition was often found at some distance in the forest.

Centerline deposition decreased at roughly the same rate as centerline concentration for sources outside the forest, and crosswind integrated deposition (CID) changed at the same rate as CIC. Deposition from the sources 6-m inside the forest, however, showed a different pattern with a double maximum at 20 to 40 m in both centerline and CID measurements with a decrease of two orders of magnitude in the next 40 m.

Deposition from area sources was heavier than that from point sources since a larger percent of the grains entered the forest at a low level and many were clumped. During the two runs for which mass flux was computed, the amount measured on the ground averaged 12% of that lost from the air.

Centerline deposition measurements were more orderly from area than from point sources. Decrease in centerline deposition with distance was considerably greater than decrease in centerline concentration. At 60 m, measurements were 8% of those at the edge and at 100 m, about 1%. CID decreased at a somewhat slower rate. Measurements at 60 m were from 8–12% and at 100 m about 2% of those at the edge.

8.8. Deposition velocity

Deposition velocity (V_d) was determined from measurements of deposition and of concentration at the 0.5-m height and was computed for all tests at each sampling location, unless measurements were too low to be reliable. Measurements are summarized in Table II.

V_d within the forest was generally low and less than those measured over open terrain (Raynor *et al.*, 1970, 1972b). This is believed due to the low level of turbulence within the forest. Ragweed frequently deposited at less than its gravitational settling rate of 1.56 cm s^{-1} except from the area source where V_d beyond 20 m exceeded this rate somewhat. V_d was even higher close to the area source but this is due largely to clumped grains. Deposition rates for other pollens and spores were usually close to their gravitational rate.

Thus, deposition rate to the forest floor is orderly, independent of distance from the edge, proportional to particle size and gravitational settling rate and frequently less than that over open, grass-covered terrain. No information was obtained on deposition rate to elevated forest surfaces.

TABLE II

Mean velocities of deposition (cm s^{-1})

Source distance (m)	Source ht. (m)	No. tests	Particle type	Distance from edge (m)					
				0	20	40	60	80	100
6	1.75	3	Ragweed pollen	–	0.9	0.7	0.8	0.3	–
10	1.75	6	Ragweed pollen	2.9	1.9	2.1	2.0	2.3	5.9
20	1.75	3	Ragweed pollen	0.6	0.7	1.2	1.1	–	–
30	1.75	7	Ragweed pollen	0.7	0.9	0.7	0.9	2.7	2.0
50	1.75	3	Ragweed pollen	0.6	0.6	0.8	0.7	–	–
30	3.5	6	Ragweed pollen	1.0	0.5	0.4	0.9	–	–
30	7.0	7	Ragweed pollen	0.7	0.9	1.3	1.9	1.3	–
30	14.0	3	Ragweed pollen	1.8	1.1	–	–	–	–
10	1.75	1	Timothy pollen	2.2	3.9	3.5	2.6	1.4	13.6
30	1.75	1	Timothy pollen	4.2	8.8	2.1	3.6	1.1	9.2
50	1.75	1	Timothy pollen	2.2	6.3	1.9	3.9	3.8	–
10	1.75	1	*Lycopodium* spores	2.3	2.9	2.3	2.0	2.5	2.0
50	1.75	1	*Lycopodium* spores	1.4	1.1	2.1	2.5	1.4	5.7
10	1.75	1	Paper Mulberry pollen	0.1	0.2	0.3	0.5	0.3	1.1
50	1.75	1	Paper Mulberry pollen	0.3	0.4	0.5	0.5	0.6	1.0
15	1.75	1	*Osmunda* spores	7.7	12.2	10.6	5.6	–	–
308-m^2	Area	18	Ragweed pollen	8.4	3.2	2.2	1.7	2.0	1.9

9. Discussion and Conclusions

Our results show that the forest modifies dispersion primarily by changing local meteorological conditions and flow patterns and secondarily by direct removal of particles. Under the conditions of our tests, dispersion is orderly and dispersion patterns internally consistent. Results are reproducible from one test to another under similar conditions and therefore predictable, even though an operational prediction model is not yet available.

Dispersion into the forest differs in several important aspects from that over open terrain. The most important is the pronounced broadening of the plume both vertically and horizontally before the forest edge. The magnitude of the broadening is undoubtedly a function of foliage density at the edge. Very dense foliage would obstruct the wind almost as a solid body and cause most of the air to rise while a forest with an open trunk space to the edge would allow maximum penetration and minimum broadening of the plume while channeling much of the air into the subcanopy level. The Brookhaven forest is intermediate between these two extremes.

Within the forest, lateral spreading takes place mainly in the entrance region. Here, wind speeds are still strong enough so that lateral dispersion is greater than vertical dispersion as over open terrain. This effect is aided by the denser foliage at the edge. Farther in the forest, vertical motions are enhanced and crosswind expansion becomes slow.

Within the flow approaching the edge, organized vertical motions produced by the

forest barrier govern vertical flow patterns. These tend to split the flow into two pathways, above the forest and into the trunk zone. Beyond the entrance region inside the forest, vertical motion increases and material quickly becomes uniformly mixed below the canopy.

Turbulence measurements show that the intensity of turbulence within the forest reaches a maximum at midcanopy level. Here, the vertical component equals the lateral and is about three times as great as in the free air above the forest and eight times as great as in the trunk space. The mechanisms producing this condition are both mechanical and convective. At the canopy level, mechanical turbulence is enhanced by protruding treetops of different heights and densities. Downward motions are particularly noticeable in the wake of these obstacles. Convective turbulence is generated by unequal heating between the sunlit and shaded sides of each tree and by holes and openings in the canopy. These combine to convert much of the horizontal motion above the forest into vertical motion which penetrates the canopy. These motions are vigorous enough to modify the effects of the subcanopy inversion and produce thorough mixing below plus much interchange through the canopy.

Rate of change in low-level concentration within the forest is not greatly different from that over open terrain in the entrance region but is appreciably greater thereafter. Total mass flux appears to decrease at about the same rate as in the open over the distance studied. The greater average height of the plume apparently compensates for particle losses. When partitioned by layers, it is seen that rate of loss in both the trunk space and canopy is much greater than above the forest or in the open.

It should be pointed out that concentration measurements give only one picture of vertical particle distribution in a forested region. Another view is obtained by use of dosage which gives a measure of the number of particles passing a given point. Since wind speeds are much greater above than in a forest, computation of dosage reveals that a much larger percentage of the material flows above the forest than is apparent from measures of concentration. The same principle holds over open terrain if wind speed increases with height but there both wind speed and dosage differences are normally less. However, concentration was used in these analyses to facilitate comparison with other studies.

Mechanisms of particle removal within the forest include impaction and deposition. The former predominates in the entrance zone where speeds are still comparable to those in the open and in the upper portions of the canopy. Deposition becomes more important within the forest where wind speeds are light and plume movement slow. However, more deposition takes place to foliage than to the ground, a process enhanced by the relatively greater vertical transport beyond the entrance region.

Since all tests were taken in the daytime with reasonably steady winds and unstable lapse rates in the open, the effects of varying meteorological conditions were not documented fully. Both concentration and mass flux decrease more rapidly at lower than at higher wind speeds. No relationship was found with other meteorological variables.

The effect of particle size was studied in several tests. Differences between the 20- and the 32- to 35-μm diameter particles were slight. However, loss of the 14-μm diameter paper mulberry pollen was appreciably less, and that of the 54-μm diameter *Osmunda* spores was considerably greater. These differences are related to both gravitational settling rate and impaction efficiency.

Thus, a reasonably clear picture has been obtained of forest dispersion and the relevant physical processes governing this phenomenon under the conditions of this study. Tests at night or with light and variable winds, use of a gas or very small particles as a tracer or tests in a forest of different composition, height or density would undoubtedly reveal important differences, some of which can be inferred from results of other studies.

Acknowledgements

The help of many individuals made this study possible. The late Anna Kokinelis gave continuous assistance in pollen counting, data reduction and analysis. John McNeil and former assistants, Lester Cohen and Thomas Dowlearn, constructed, maintained and operated equipment and helped in field tests. Robert M. Brown was helpful in the acquisition of meteorological data. The support of Maynard E. Smith, former Meteorology Group Leader, facilitated the entire project.

References

Batchelor, G. K.: 1949, 'Diffusion in a Field of Homogeneous Turbulence. I. Eulerian analysis', *Australian J. Sci. Res.* **2**, 437–450.

Batchelor, G. K.: 1952, 'Diffusion in a Field of Homogeneous Turbulence. II. The Relative Motion of Particles', *Proc. Camb. Phil. Soc.* **48**, 345–362.

Bowne, N. E., Entrekin, H. D., Smith, K. W., and Hilst G. R.: 1969, 'Aerosol Diffusion over Woodlot Complexes', Vol. 1, Summary and Results, Report TRC 343, Travelers Research Corp., Hartford, Conn. 295 pp.

Burnett, G. F. and Thompson, B. W.: 1956, 'An Investigation of the Behaviour of Coarse Aerosol Clouds in Woodland', *Bull. Ent. Res.* **47**, 495–524.

Calder, K. L.: 1961, 'A Simple Mathematical Model for the Penetration of Forest Canopy by Aerosols', BL Tech. Study 37, U.S. Army Chem. Corps, Fort Detrick, Md. AD262228, Armed Services Tech. Inf. Agency, Arlington, Va. 30 pp.

Clayton, W. H., Sanford, T. E., and Ackerman, B.: 1970, 'Evaluation of Atmospheric Transport and Diffusion', Third Semiannual Report. Res. and Dev. Tech. Rept. ECOM-0381-3, U.S. Army Electronics Command, Fort Monmouth, N.J. 68 pp.

Ford, E. F. and Lomen, D. O.: 1969, 'Diffusion Under a Jungle Canopy', Final Report, Volume III – Mathematical Model. Melpar, Inc., Falls Church, Va. 124 pp.

Fritschen, L. J., Driver, C. H., Avery, C., Buffo, J., Edmonds, R., Kinerson, R., and Schiess, P.: 1970, 'Dispersion of Air Tracers into and Within a Forested Area: 3', Res. and Devel. Tech. Rept. ECOM-68-G8-3, U.S. Army Electronics Command, Fort Huachuca, Ariz. 53 pp.

Hamilton, H. L., Jr.: 1963, 'Jungle Canopy Penetration', Final Report. Volume I, Diffusion Measurements. Report BSC 36174, The Bendix Corp., Bendix Systems Division. 125 pp.

Melpar, Inc.: 1968, 'Diffusion Under a Jungle Canopy', Vol. 1, Main report. Melpar, Inc., Falls Church, Va. 176 pp.

Meroney, R. N.: 1968, 'Characteristics of Wind and Turbulence in and Above Model Forests', *J. Appl. Meteorol.* **7**, 780–788.

Meroney, R. N. and Yang, B. T.: 1969, 'Wind Tunnel Studies of the Air Flow and Gaseous Plume

Diffusion in the Leading Edge and Downstream Regions of a Model Forest', Tech. Rept. ECOM C-0423-6, Colorado State Univ., Ft. Collins, Colo. 63 pp.

Neuberger, H., Hosler, C. L., and Kocmond, W. C.: 1967, 'Vegetation as Aerosol Filter', *Biometeorol* **2**, 693–702.

Ogden, E. C. and Raynor, G. S.: 1967, 'A New Sampler for Air-Borne Pollen: The Rotoslide', *J Allergy* **40**, 1–11.

Raynor, G. S.: 1967, 'Effects of a Forest on Particulate Dispersion', In Proc. USAEC Meteorol Information, Chalk River, Ontario, Sept. 1967. Report AECL-2787, C. A. Mawson (ed.), Atomic Energy of Canada Ltd., Chalk River, Ontario, p. 581–588.

Raynor, G. S.: 1971, 'Wind and Temperature Structure in a Coniferous Forest and a Contiguous Field', *Forest Sci.* **17**, 351–363.

Raynor, G. S. and Smith, M. E.: 1964, 'A Diffusion-Deposition Tracer System', Report BNL 859 (T-343), Brookhaven National Laboratory, Upton, N.Y. 17 pp.

Raynor, G. S., Cohen, L. A., Hayes, J. V., and Ogden, E. C.: 1966, 'Dyed Pollen Grains and Spores as Tracers in Dispersion and Deposition Studies', *J. Appl. Meteorol.* **5**, 728–729.

Raynor, G. S., Hayes, J. V., and Ogden, E. C.: 1972a, 'Experimental Data on Particulate Dispersion into and Within a Forest. Part I. Dispersion from Upwind Point Sources', Informal report BNL 17750, Brookhaven National Laboratory, Upton, N.Y., 95 pp.

Raynor, G. S., Ogden, E. C., and Hayes, J. V.: 1972b, 'Dispersion and Deposition of Timothy Pollen from Experimental Sources', *Agric. Meteorol.* **9**, 347–366.

Raynor, G. S., Hayes, J. V., and Ogden, E. C.: 1973, 'Experimental Data on Particulate Dispersion into and Within a Forest. Part II. Dispersion from Upwind Area Sources', Informal report BNL 18064, Brookhaven National Laboratory, Upton, N.Y. 39 pp.

Raynor, G. S., Ogden, E. C., and Hayes, J. V.: 1970, 'Dispersion and Deposition of Ragweed Pollen from Experimental Sources', *J. Appl. Meteorol.* **6**, 885–895.

Singer, I. A. and Smith, M. E.: 1953, 'Relation of Gustiness to Other Meteorological Parameters', *J. Meteorol.* **10**, 121–126.

Tauber, H.: 1967, 'Investigations of the Mode of Pollen Transfer in Forested Areas', *Rev. Palaeobotan. Palynol.* **3**, 277–286.

Tourin, M. H. and Shen, W. C.: 1969, 'Deciduous Forest Diffusion Study. Final Report, Volume I, Diffusion Studies in a Deciduous Forest', Report No. 3004, Litton Systems, Inc., Minneapolis, Minn. 325 pp.

Atmospheric Environment Vol. 21, No. 11, pp. 2311–2321, 1987
Printed in Great Britain

0004-6981/87 $3.00 + 0.00
Pergamon Journals Ltd

THE AVAILABILITY AND FALL-OUT OF AN INSECTICIDAL AEROSOL DISPERSED FROM AIRCRAFT DURING OPERATIONS FOR CONTROL OF TSETSE FLY IN ZIMBABWE

D. R. JOHNSTONE, J. F. COOPER and H. M. DOBSON

Department of Pesticide Application and Management, Tropical Development and Research Institute, Porton Down, Salisbury, Wilts. SP4 OJQ, U.K.

(*First received 28 December 1986 and received for publication 14 April 1987*)

Abstract—Droplet availability (numbers and volume crossing unit vertical area) has been measured by means of rotary slide samplers and the measurements have been converted to estimates of the most likely dose received by a tsetse fly using collection efficiency data for samplers and flies derived from laboratory wind tunnel study. The resulting dosage levels indicate high probability of effective fly control, except that in the centre of the block the parting effect of change of wind direction between sorties which occurred during the first two cycles of application has left a narrow band uncovered by spray. Deposition to the ground at points within the block and up to 4 km beyond the downwind margin has been measured to provide data for correlation with environmental effects to be observed by an independent biological study team.

Key word index: Insecticide, aircraft spraying, deposition, dispersion, aerosols.

INTRODUCTION AND OBJECTIVES

The application of low dosages of an insecticide dispersed as an aerosol from fixed-wing aircraft between dusk and dawn has provided, in recent years, a means to control tsetse fly in central southern Africa (Allsopp, 1984). The target is the adult fly present within the canopy of the savannah woodland habitat. The flies normally rest at night on the twigs or branches of preferred trees. An early qualitative laboratory wind tunnel study (Hadaway and Barlow, 1965) indicated that the optimum drop size range for deposition on flies resting on cylindrical obstacles appeared to be from 10 to 30 μm. Droplets in this size range are sufficiently small to remain suspended for some time and to be carried on the prevailing light air currents through the canopy, diverging around larger obstacles, while depositing effectively on the resting flies.

One objective of the trial of which this study formed a part was to monitor both the efficacy and associated environmental effects of a series of applications of the insecticide deltamethrin. Measurements were required to assess both the availability of drifting droplets (for impaction on resting flies) and the drift and subsequent sedimentation of the aerosol drops in relation to their likely environmental effects.

The physiochemical measurements described below were undertaken with the object of obtaining a broad picture of the distribution of aerial drift and of sedimentation to the ground within and just downwind of the sprayblock, both to forecast the efficacy of the treatments and to provide data to relate to the ongoing biological appraisal of efficacy and other environmental effects.

Location

A trial sprayblock of some 300 km^2 lying between Kotwa and Nyamapanda along Zimbabwe's NE border with Mozambique. The sprayblock was rectangular measuring approximately 20 × 15 km, and aligned with the principal axis inclined in an approximately NNW–SSE direction.

MATERIALS AND METHOD

A single marker line was set up with pegs along the main A2 highway running E–W across the northern half of the block (see Fig. 1). Pegs were numbered from 1 to 67, corresponding to swath increments of 250 m per peg, but only the first 60/64 pegs were utilized on cycles I/II.

The block was flown in two sorties per cycle. The morning sorties (flown on the navigation equipment only) were intended to cover pegs 1–36, but that of cycle I finished short after 12 passes (of three aircraft) at peg 31. The second sorties (flown on the evening of the same day) were commenced by three aircraft (first five passes, cycle I; first four passes, cycle II), but were completed by two aircraft (final eight passes), individual swath width again nominally 250 m. These sorties were flown on a combination of the navigation equipment and mobile marker beacon and commenced on peg 31 and terminated on peg 60, cycle I (pegs 37 and 64 respectively, cycle II).

The aircraft, two Cessna 401 and one Beechcroft Baron, each equipped with a single rotary atomizer (Micronair AU4000), flew in formation with 250 m lateral separation (combined swath 750 m) at a nominal 240–260 km h^{-1} on alternate 150–330°M

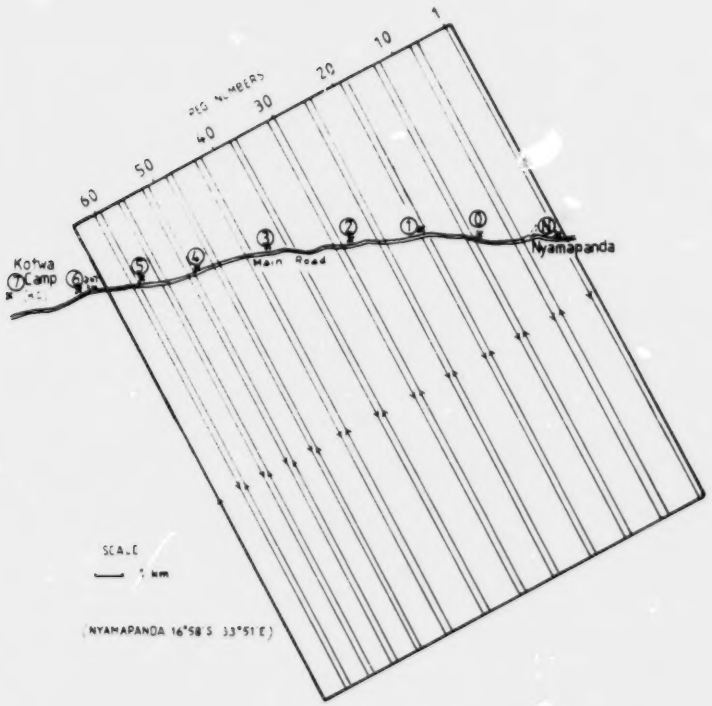

Fig. 1. Disposition of samplers across the sprayblock and intended flight paths of lead aircraft.

headings. The formulation (as sprayed) contained deltamethrin at 0.4 % concentration, plus a fluorescent tracer, Uvitex OB, at 0.2 % concentration (for both visual and fluorimetric examination of the sampled droplets).

The flow rate was intended to provide a volume application of 6.4 ℓ km^{-2} and a mass application of 0.25 g ha^{-1} of deltamethrin. Atomizers were set to 35° blade angle for sortie I of cycle I and to 30° blade angle thereafter to provide the requisite droplet spectra.

The same linear sampling layout was adopted for both sorties of cycle I, with eight rotary MgO-coated and plain glass vertical slide samples (0.63 cm wide slides; Andrews *et al.*, 1983) at approximately 2 km intervals, commencing in the E from a point between pegs 11 and 12 and extending beyond the western boundary of the block to km posts 218 and 216, the latter sampler being located within the Kotwa camp site. This sampling layout was modified slightly for the second cycle to extend to peg 1 for the morning sortie. The basic sampling was augmented by horizontal static ground slide samplers at selected sites. Four wind-run anemometers, sited at every other sampling station, provided data on windspeed during the sampling period. Samplers were switched on approximately 1–2 h before spraying commenced and were run for 2–3 h after termination, before collection. The droplets sampled on the MgO slides were subsequently counted and sized with the aid of a microscope and u.v. illumination, while the deposits on the plain glass slides were analysed by fluorimetry (Perkin–Elmer LS2).

RESULTS

The disposition of the samplers is sketched in Fig. 1. Tables 1 and 2 record details of the timings of the morning and evening sorties for cycles I and II, respectively.

Table 3 sets out, for cycles I and II, fluorimetric measurements of tracer deposits on the slides, the derived volume/unit area, and, by comparison with the measurements on the MgO slides, the percentage evaporation.

Tables 4 and 5 set out, for cycles I and II, the measured droplet parameters, $nmd(d_n)$, $vmd(d_v)$ and the volume/unit vertical area (V/A), together with the average windspeed recorded over the extended sampling period (or an interpolated estimate where no adjacent anemometer was present). Tables 4 and 5 also display an analysis to estimate the most likely deltamethrin dose (in ng) received by a resting fly. For this purpose the raw droplet number and size counts are corrected for the predetermined collection efficiency of the sampler for each specific size class to allow a truer

Table 1. Log of operation, cycle I (25/7/86)

Spray run No	Intended peg No./ X-block distance (km)		Aircraft: Time of passage (h)	Aircraft: No	Aircraft: Heading (° M)	Aircraft: Position error E or W of intended peg (m)	Doppler windspeed/ direction (kts/° M)		Ground windspeed at 2 m/direction (kts/° M)	
Sortie 1										
1	1	0	0543	3	150	Overhead beacon				
2	6	1.25	0552	3	330	Overhead				
3	7	1.5	0558	3	150	250W				
4	12	2.75	0610	3	330	250E				
5	13	3.0	0616	3	150	400E				
6	18	4.25	0625	3	330	400E			< 1	315
7	19	4.5	0633	3	150	400E				
8	24	5.75	0642	3	330	750E				
9	25	6.0	0648	3	150	600E				
10	30	7.25	0658	3	330	1000E				
11	31	7.5	0704	3	150	1000E				
12	36	8.75	0714	3	330	1250E				
Sortie 2										
1	31	7.5	1743	3	150	—				
2	36	8.75	1754	3	330	—				
3	37	9.0	1800	3	150	—	6	044		
4	42	10.25	1810	3	330	—				
5	43	10.5	1815	3	150	—				
6	47	11.5	1826	2	330	—	5	088	1	045
7	48	11.75	1830	2	150	—				
8	51	12.5	1842	2	330	—				
9	52	12.75	1848	2	150	—				
10	55	13.5	1900	2	330	—	7	094		
11	56	13.75	1904	2	150	—				
12	59	14.5	1915	2	330	—	7	105		
13	60	14.75	1921	2	150	—				

estimate of the spray parameters (d_w^*, d_v^*) and the volume passing unit vertical area (V'/A). A further correction is made for the departure from isokinetic sampling due to variation of windspeed to give $(V'/A)_u$. Since there has been loss of volatile solvent from the spray droplets between atomization and collection, the mass of insecticide passing unit area can only be determined if the amount of this loss is known. The percentage evaporation has been determined by comparison of the measured volumes/unit area derived from the MgO slides with those volumes (v) per unit area estimated from the mass (m) of tracer per unit area determined on the corresponding plain glass slides (where $v = m/c$ and the initial concentration (c) of the tracer is known). The relation between evaporation and the sampler *vmd* is shown in Fig. 2. If the measured evaporation is designated as E_m(%), then the correction factor is $(100/100 - E_m)$ and this furnishes the volume/unit area had no evaporation occurred $(V'/A)_{u\&E}$. The mass of insecticide per unit area (M/A) is obtained by multiplying this figure by the initial insecticide concentration.

If a resting fly has a cross-sectional area of say 0.25 cm^2, the mass/fly, $m_{(CE=100)}$, at a collection efficiency (CE) of 100%, is obtained as 0.25 × mass/unit vertical area (Johnstone and Cooper, 1986). However, the collection efficiency of the fly will depend on windspeed and droplet size in a manner which has been the subject of laboratory determination (Johnstone *et al.*, in preparation), see Fig. 3, so that, identifying the droplet diameter with the corrected *vmd* and the windspeed with the average measured windspeed (u), a correction for the graphically derived value of CE can be made, giving the most likely mass of deltamethrin/fly, presented in the final column as $m_{(CE\,at\,u\&d_v)}$. This dose has been plotted against peg number (and distance across the sprayblock) in Figs 4 and 5 (cycles I and II, respectively).

Deposition to the ground (mass deltamethrin/unit area) has been shown in Figs 6 and 7 along with the variation in droplet size (*vmd*) (Fig. 8).

DISCUSSION AND CONCLUSIONS

A similar pattern of spray distribution is evident for both cycles I and II.

The prevailing wind at aircraft height was from between E and S, more or less along the direction of the spray runs, but near the ground (at a height of under 10 m) the airflow was observed to be somewhat different. In the morning, light NW air movement was

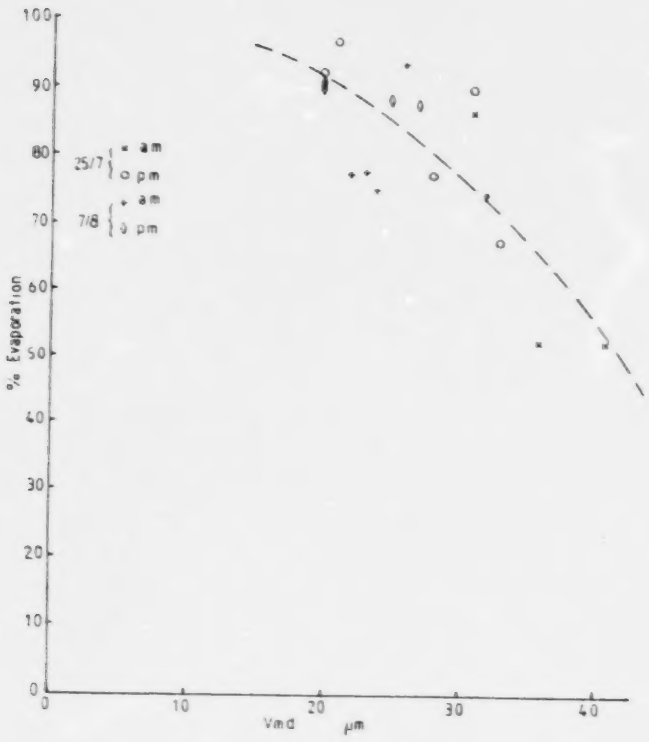

Fig 2 Relation between droplet evaporation (difference between volumes determined by fluorimetry and by droplet size measurement) and sample *vmd* (as measured).

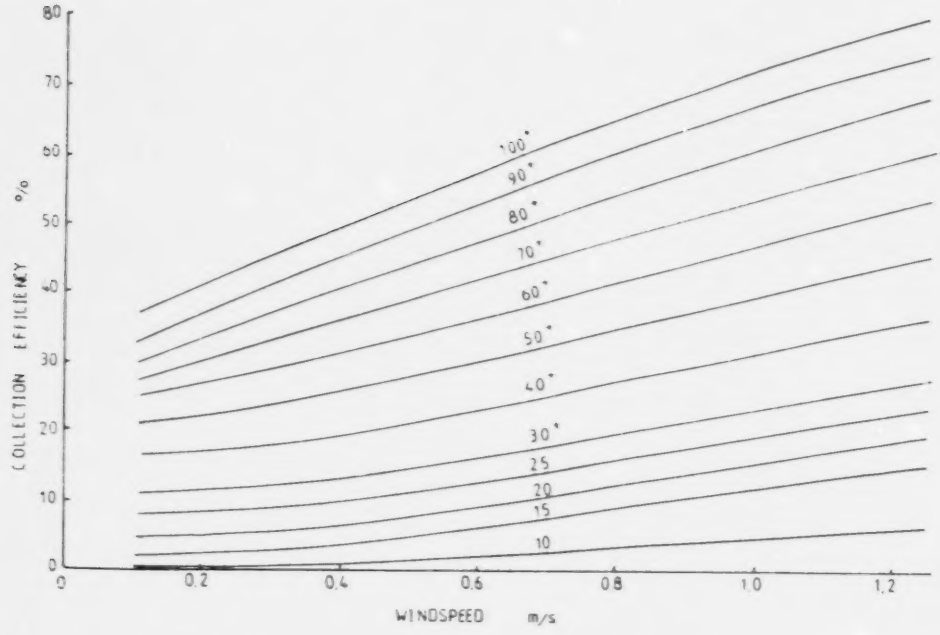

Fig 3 Variation of droplet collection efficiency of tsetse flies with windspeed at stated droplet sizes (based on wind tunnel measurements, with extrapolation + to larger sizes).

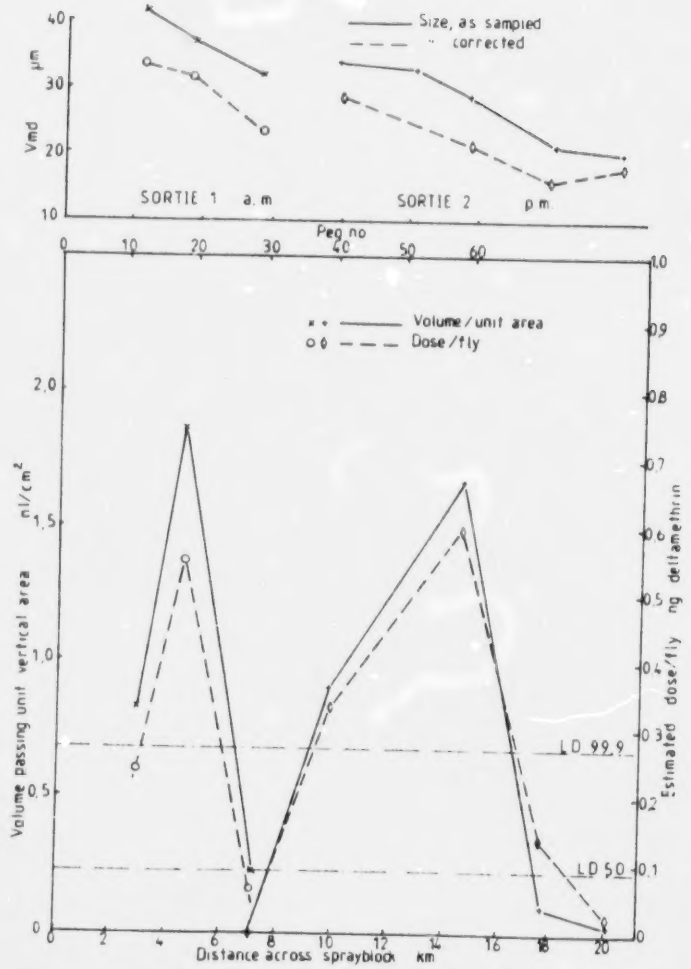

Fig 4 Variation of droplet size and flux of airborne drift over a transect of the block, with an estimate of the most likely insecticide dose received by a tsetse fly
Cycle I, 27/7/86

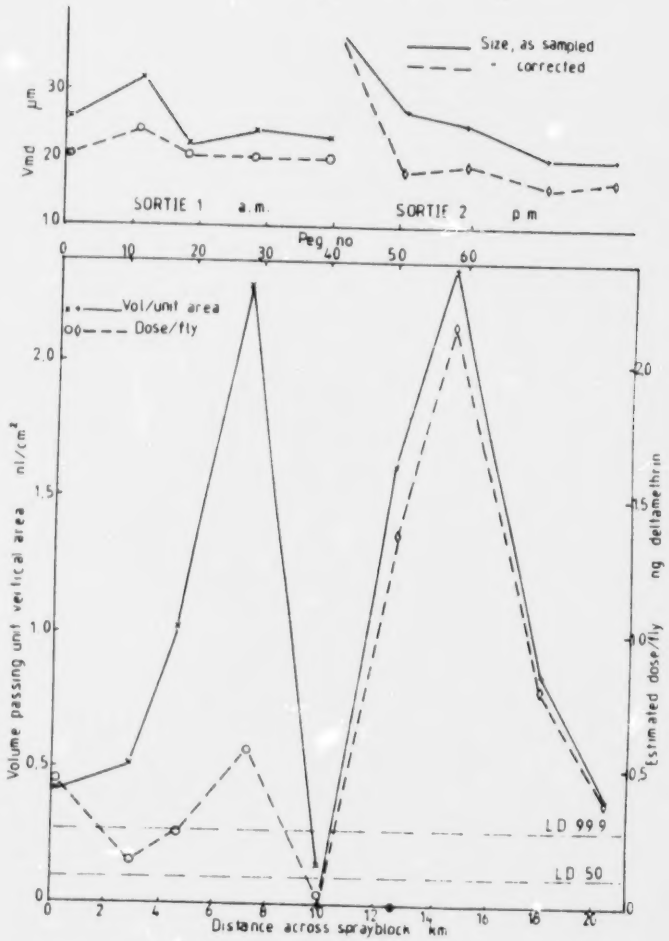

Fig 5 Variation of droplet size and flux of airborne drift over a transect of the block, with an estimate of the most likely insecticide dose received by a tsetse fly
Cycle II, 7/8/86

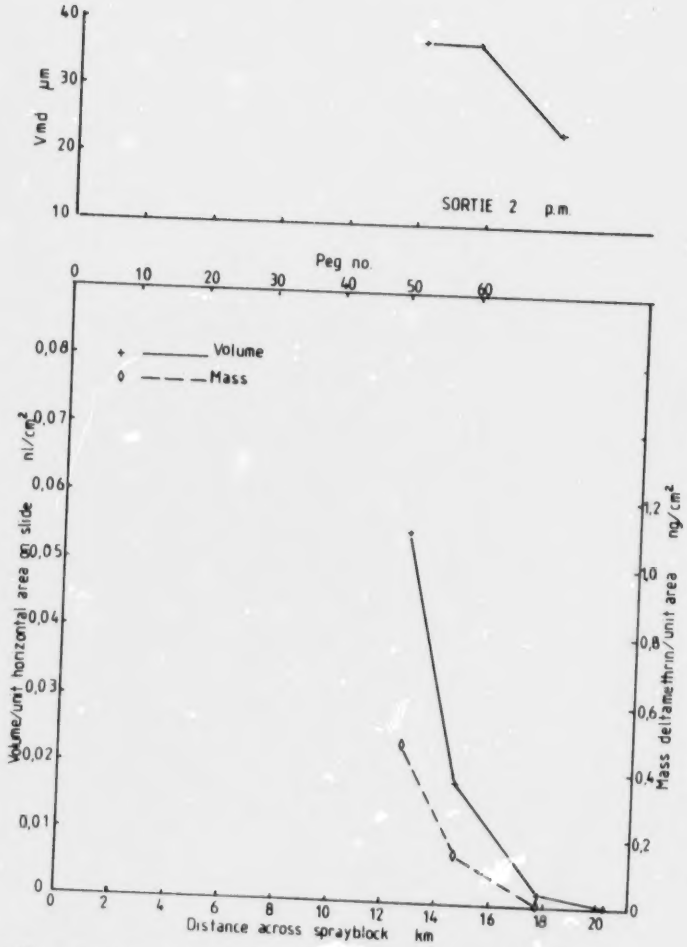

Fig. 6. Variation of droplet fall-out to the ground (size, mass and volume) over a transect of the block. Cycle I, 27/7/86.

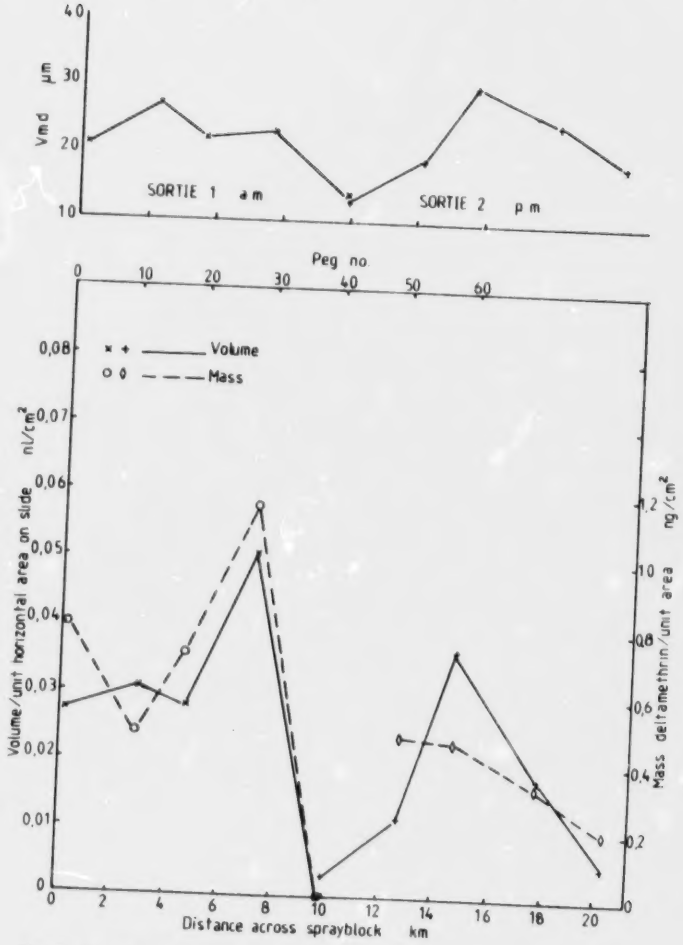

Fig. 7. Variation of droplet fall-out to the ground (size, mass and volume) over a transect of the block. Cycle II, 7/8/86.

Table 2. Log of operation, cycle II (7/8/86)

Spray run No	Intended peg No./ X-block distance (km)		Time of passage (h)	Aircraft No	Heading (° M)	Position error E or W of intended peg (m)	Doppler windspeed/ direction (kts/° M)		Ground windspeed at 2 m/ direction (kts/° M)	
Sortie 1										
1	1	0	0539	3	150	Overhead beacon				
2	6	1·25	0547	3	330	100W	6	130		
3	7	1·5	0555	3	150	250E				
4	12	2·75	0605	3	330	50W	5	150		
5	13	3·0	0612	3	150	100W				
6	18	4·25	0622	3	330	150W	5	160	< 1	260
7	19	4·5	0628	3	150	200W				
8	24	5·75	0638	3	330	250W	5	165		
9	25	6·0	0644	3	150	250W				
10	30	7·25	0654	3	330	150W	5	150		
11	31	7·5	0700	3	150	150W				
12	36	8·75	0710	3	330	100W	5	155	< 1	250
Sortie 2										
1	37	9·0	1743	3	150	—			< 1	045
2	42	10·25	1754	3	330	—	5	110	< 1	000
3	43	10·5	1759	3	150	—				
4	48	11·75	1812	3	330	—	6	117	< 1	025
5	49	12·0	1818	2	150	—				
6	52	12·75	1831	2	330	—	8	129	1–2	025
7	53	13·0	1837	2	150	—			1–2	030
8	56	13·75	1849	2	330	—	8	129		
9	57	14·0	1855	2	150	—				
10	60	14·75	1908	2	330	—	8	134		
11	61	15·0	1914	2	150	—				
12	64	15·75	1927	2	330	—	7	136		

evident throughout the period of spraying so that the spraycloud appeared to drift against the prevailing overhead SE wind and move obliquely across the E–W sampling line, thus no spray was sampled to the W of the third sampling point (between pegs 28 and 29) in sortie 1, cycle I, or beyond pegs 39/40 in sortie 1, cycle II. In the evening the low level air movement was initially from the NE, but veering over the period of sortie 2, cycle I, to ESE, so that no spray was sampled at, and to the east of, the sampling point between pegs 28 and 29 for this sortie, or to the east of pegs 39/40 during sortie 2, cycle II, but some spray drifted beyond the ultimate peg number 60 (64, cycle II) and was sampled at the 218 and 216 km posts about 2 and 4 km downwind from the final spray run, respectively. The amounts found were very small for cycle I, corresponding to 33 and 8% of the LD_{50} dose of deltamethrin for a tsetse fly, respectively (Hadaway *et al*., 1976), but were considerably larger for cycle II (378 and 172% of the LD_{50} dose, respectively).

Within the block, a combination of the morning and evening sorties indicates the likelihood of good control of fly over the first 20–25 pegs and again from peg 35 onwards, but provokes some doubt as to effective control in the region between pegs 25 and 35 where the parting effect of the switch in wind direction between sorties has resulted in an avenue of 1–3 km more or less devoid of spray in both the first and second cycles of a five cycle control operation.

Ground deposits outside the block and to the W were insignificant for cycle I, but amounted to 0.2 ng cm^{-2} at the site 4 km beyond the nearest boundary in cycle II. Peak deposition to the ground within the block was 0.5 ng cm^{-2} for the evening sorties, but 1.2 ng cm^{-2} for sortie 1 of cycle II and these levels may be sufficient to allow correlation with complementary biological observations of the environmental study team.

Acknowledgements—The authors are indebted to the Wellcome Research team, Drs Bob Martin and Denise Potter, for carrying out the fluorimetric analyses and to Mr Harry Waters of Coopers (Zimbabwe) and Mr Reg Allsopp of ASRDP for more general support.

Table 3 Fluorimetric determination of tracer deposits, derived volume unit area and evaporation

	Sample position No.	Mass of tracer (ng/slide)	Volume/unit area* (n/cm^{-2})	Evaporation† (%)
Cycle I				
Sortie 1	0	95.1	12.2	51.6
	1	146.6	18.8	51.8
	2	28.9	3.70	85.4
	3	0	0	—
	4	0	0	—
	5	0	0	—
	6	0.05	0.064	—
	7	0.65	0.083	—
Sortie 2	0	0	0	—
	1	0.3	0.038	—
	2	0	0	—
	3	60.7	7.78	66.6
	4	14.7	1.88	—‡
	5	80.2	10.3	76.3
	6	4.1	0.53	96.2
	7	1.9	0.24	91.7
Cycle II				
Sortie 1	N	61.1	7.82	92.6
	0	72.3	9.25	73.4
	1	75.3	9.64	76.6
	2	115	14.7	74.1
	3	10.2	1.30	76.9
	4	1.0	0.13	—
	5	1.0	0.13	—
	6	1.0	0.13	—
Sortie 2	1	0.35	0.04	—
	2	0.30	0.04	—
	3	44.6	5.71	—
	4	75.8	9.70	86.9
	5	115	14.7	87.4
	6	28.9	3.7	89.8
	7	15.2	1.95	89.2

*Volume equivalent to that present on emission. Area of slide = $0.65 \times 6.0 = 3.9\ cm^2$; concentration of tracer = 0.2%, therefore multiply ng by 0.128 to convert to n/cm^{-2}.

†Percentage evaporation = $100\ (V_F - V_C)/V_F$, where V_F = volume/unit area determined by fluorimetry and V_C volume/unit area determined by droplet size/count (see Tables 4 and 5).

‡MgO slide interferred with and did not sample whole period.

Table 4. Deltamethrin droplet study, cycle 1 (25/7/86)

Pn	s (km)	d_n (μm)	d_v (μm)	V/A (nl cm^{-2})	u (m s^{-1})	d'_n (μm)	d'_v (μm)	V'/A (nl cm^{-2})	$(V'/A)_u$ (nl cm^{-2})	E (%)	$(V'/A)_{u\&E}$ (nl cm^{-2})	M/A (ng cm^{-2})	m ($CE = 100$) (ng)	CE (%)	m (CE @ u & d'_v) (ng)
Sortie 1															
11/12	2.6	25	41	5.90	0.19	14	33	10.0	0.834	51.6	1.72	6.92	1.72	14	0.241
18/19	4.4	27	36	9.06	(0.28)	20	31	14.9	1.85	51.8	3.84	15.3	3.84	13	0.500
28/29	7.0	22	31	0.54	0.37	13	23	1.45	0.238	85.4	1.63	6.52	1.63	8.5	0.138
39/40	9.6	—	—	0	—	—	—	0							
50/51	12.5	—	—	0	1.0	—	—	0							
58/59	14.5	—	—	0	—	—	—	0							
>67	18.0	—	—	0	1.7	—	—	0							
KC	20.0	—	—	0	—	—	—	0							
Σ	Σ	27	38	5.35	(0.28)	15	27	7.23	0.891	(52)	1.85	7.42	1.85	10	0.186
Sortie 2															
11/12	2.6	—	—	0	0.11	—	—	0							
18/19	4.4	—	—	0	—	—	—	0							
28/29	7.0	—	—	0	0.34	—	—	0							
39/40	9.6	25	33	2.60	(0.43)	19	28	4.76	0.900	66.6	2.69	10.7	2.69	12.5	0.336
50/51	12.5	27	32	0.20	0.52	—	—	—							
58/59	14.5	21	28	2.44	(0.52)	14	21	7.32	1.67	76.3	7.04	28.1	7.04	8.5	0.599
>67	18.0	18	21	0.02	0.53	13	16	0.42	0.097	96.2	2.55	10.2	2.55	5.5	0.140
KC	20.0	19	20	0.02	(0.53)	16	18	0.11	0.025	91.7	0.301	1.20	0.301	7.0	0.021
Σ	Σ	22	30	1.28	(0.50)	16	23	3.02	0.670	(68)	2.09	8.37	2.09	10	0.209

Table 5. Deltamethrin droplet study, cycle II (7/8/86)

Pn	s (km)	d_n (μm)	d_v (μm)	V/A (nℓ cm^{-2})	$\bar{u}$ (m s^{-1})	d'_n (μm)	d'_v (μm)	V'/A (nℓ cm^{-2})	$(V'/A)_u$ (nℓ cm^{-2})	E (%)	$(V'/A)_{u\&E}$ (nℓ cm^{-2})	M/A (ng cm^{-2})	m ($CE = 100$) (ng)	CE (%)	m (CE (ω u & d'_v) (ng)
Sortie 1															
1	0.3	20	26	0.581	0.52	16	20	1.83	0.419	92.6	5.66	22.6	5.66	8.0	0.453
11/12	2.6	23	32	2.46	0.21	13	24	5.42	0.505	73.4	1.89	7.59	1.89	8.0	0.152
18/19	4.4	20	22	2.26	(0.31)	17	20	7.86	1.08	76.6	4.62	18.4	4.62	6.0	0.277
28/29	7.0	21	24	3.81	0.41	16	20	12.5	2.27	74.1	8.78	35.1	8.78	6.5	0.571
39/40	9.6	20	23	0.30	(0.30)	17	20	1.03	0.137	76.9	0.593	2.37	0.593	6.0	0.036
50/51	12.5	–	–	0	0.22	–	–	0							
58/59	14.5	–	–	0	–	–	–	0							
>67	18.0	–	–	0	–	–	–	0							
Σ	Σ	20	24	2.14	(0.34)	16	20	6.7	1.02	(80)	5.10	20.40	5.10	6.5	0.332
Sortie 2															
18/19	4.4	–	–	0	–	–	–	0							
28/29	7.0	–	–	0	0.24	–	–	0							
39/40	9.6	40	40	0.015	0.33	40	40	0.018	0.003	(48)	0.006	0.024	0.006	19	0.001
50/51	12.5	19	27	1.273	0.81	14	18	4.51	1.62	86.9	12.4	49.5	12.4	11	1.36
58/59	14.5	20	25	1.859	(0.80)	13	19	6.59	2.34	87.4	18.5	74.3	18.5	11.5	2.13
>67	18.0	17	20	0.377	(0.80)	13	16	2.39	0.850	89.8	8.33	33.3	8.33	9.5	0.792
KC	20.0	19	20	0.211	0.77	14	17	1.15	0.396	89.2	3.80	15.2	3.80	10	0.380
Σ	Σ	19	23	0.851	(0.80)	13	18	3.55	1.19	(82)	6.62	26.4	6.62	11	0.728

REFERENCES

Allsopp R. (1984) Control of tsetse flies (Diptera: *Glossinidae*) using insecticides; a review and future prospects. *Bull. ent. Res.* **74**, 1–23.

Andrews M., Flower L. S., Johnstone D. R. and Turner C. R. (1983) Spray droplet assessment and insecticide drift studies during large scale aerial application of endosulfan to control *Glossina morsitans* in Botswana. *Trop. Pest Mgmt* **29**, 239–248.

Hadaway A. B. and Barlow F. (1965) Studies on the deposition of oil drops. *Ann. appl. Biol.* **55**, 267–274.

Hadaway A. B., Barlow F. and Turner C. R. (1976) The susceptibility of different species of tsetse flies to some insecticides. Miscellaneous Report No. 23. Centre for Overseas Pest Research, College House, London.

Johnstone D. R. and Cooper J. F. (1986) Forecasting the efficiency of the sequential aerosol technique for tsetse fly control. *Pestic. Sci.* **17**, 675–685.

Johnstone D. R., Cooper J. F., Dobson H. M. and Turner C. R. The droplet collection efficiency of resting tsetse flies. (In preparation.)

ight up to 150 m
s at Brookhaven
90.
ds of time. *Meteor*
t. J. Roy. Meteor
of wind over leve
lem., No. 54, 45–9
ange to standard
Rev., 91, 83–87.
Properties of spec
ters. *Quart. J. Roy*
e relation between
Roy. Meteor. Soc
London, Van Nos
wind shear in the
Dept. of Transport
1955: Estimates of
e gust velocity of
gust load data by
Note 3362, 47 pp.
random noise. *Bell*
ver Great Britain
57–265.
C. for periods ending
ty and gusts with
463–488.
York, McGraw-Hill
e. *Proc. Roy. Soc*
al theory of turbu
gy spectra of atmo
of Meteor. Phys
ts in Australia. Bull
ralia, 133 pp.

Measuring Pesticide Drift at Distances to Four Miles

JAMES A. MURRAY AND LELAND M. VAUGHAN

Metronics Associates, Inc., Palo Alto, Calif.

(Manuscript received 1 October 1969, in revised form 3 November 1969)

ABSTRACT

Drift resulting from pesticide spray operations is an environmental contaminant and potential hazard. In order to quantitatively evaluate the relationship between a source and the extent of its contamination, it is necessary to measure the downwind amounts of pesticide that are still airborne as well as the deposition on the ground and foliage. Furthermore, it is also necessary to quantitatively characterize the droplet size parameters of these airborne and deposited amounts in order that the results of any given field test be extended for use in a general evaluation of the drift problem. A simple tracer technique to measure the required characteristics of the spray drift is described.

The fluorescent particle (FP) spray tracing technique essentially consists of adding a known number of insoluble, micron-sized FP to the pesticide liquid prior to the spray operation. After spraying, the samples of artificial or natural surfaces are assessed. The number of FP grouped within an individual droplet pattern determines the droplet volume, and the total number of FP present represents the total mass of pesticide present in the sample. Also given are the results of field tests in which collections of droplets with volume median diameters $< 10\mu$ were obtained at distances up to 4 mi downwind. Airborne dosages as low as 10^{-10} (gm-min liter^{-1}) were also measured by the FP spray technique.

1. Introduction

During recent years there has been an increasing public awareness of the environmental contamination and potential hazard resulting from the application of pesticides, and for many years the agricultural industry has also been aware of the problem as well as that of controlling the target pests. In both problems, the importance of meteorology is recognized, but, in general, the mechanisms by which meteorology influences either the control operation or the subsequent drift are not widely understood. One of the prime causes for this situation has been the lack of adequate techniques with which to quantitatively measure the behavior of the full size spectrum of spray droplets as they travel through the atmosphere or are deposited. Such a spray tracing technique alone is not a panacea for the pest control and contamination problems, but it is a research tool that can provide a basic understanding which will eventually lead to a sound technical solution of these problems.

The fluorescent particle (FP) tracer technique was first developed in the late 1940's by Metronics personnel, then with the predecessor group, the Stanford Aerosol Laboratory (Grinnell *et al.*, 1946; Leighton *et al.*, 1947) and publicly reported in 1951 (Perkins *et al.*). A description of the current FP tracer technique was published in 1965 (Leighton *et al.*). In the early days it was used as an atmospheric air tracer for use in both the U. S. Army Chemical Corps and air pollution investigations. In 1965, the FP technique was adapted to tagging spray droplets (Vaughan *et al.*) to be used in forest pest control studies by the U. S. Forest Service (Himel and Moore, 1967). The FP spray technique was subsequently used by the University of Georgia (Himel and Moore, 1969) in tests to determine droplet size of insecticide impacting on cotton pests.

The drift from a U. S. Navy developed droplet aerosol generator (Stains *et al.*, 1969) has been demonstrated to be effective for the control of disease vector insects at distances to 2 mi. The present concern for control of disease bearing mosquitoes and other pests, as well as for any potential hazards related to drift, requires a quantitative knowledge on amounts of insecticide in the aerosol cloud and its deposition. This paper will summarize the current status of the latest extensions of the FP spray technique related to drift measurements.

2. The fluorescent particle spray tracing technique

The tracer particles are micron-size, insoluble crystals which fluoresce brightly when illuminated by 366 nm UV light and viewed through a microscope. The FP are readily distinguishable from almost all naturally occurring particulates by means of their color, size and intensity. There are three readily distinguishable colors of fluorescent particles available: yellow, green and red. Also, different characteristic densities, such as the ZnCdS at 4 gm cm^{-3} and the special plastic VYAC® material made by American Cyanimid at 1.5 gm cm^{-3}, have been used. This option of densities is useful in controlling the settling rates of the FP in unagitated liquid reservoirs. The fluorescent properties of the FP are physically stable under exposure to sunlight, and the FP are chemically stable to corrosive pesticides.

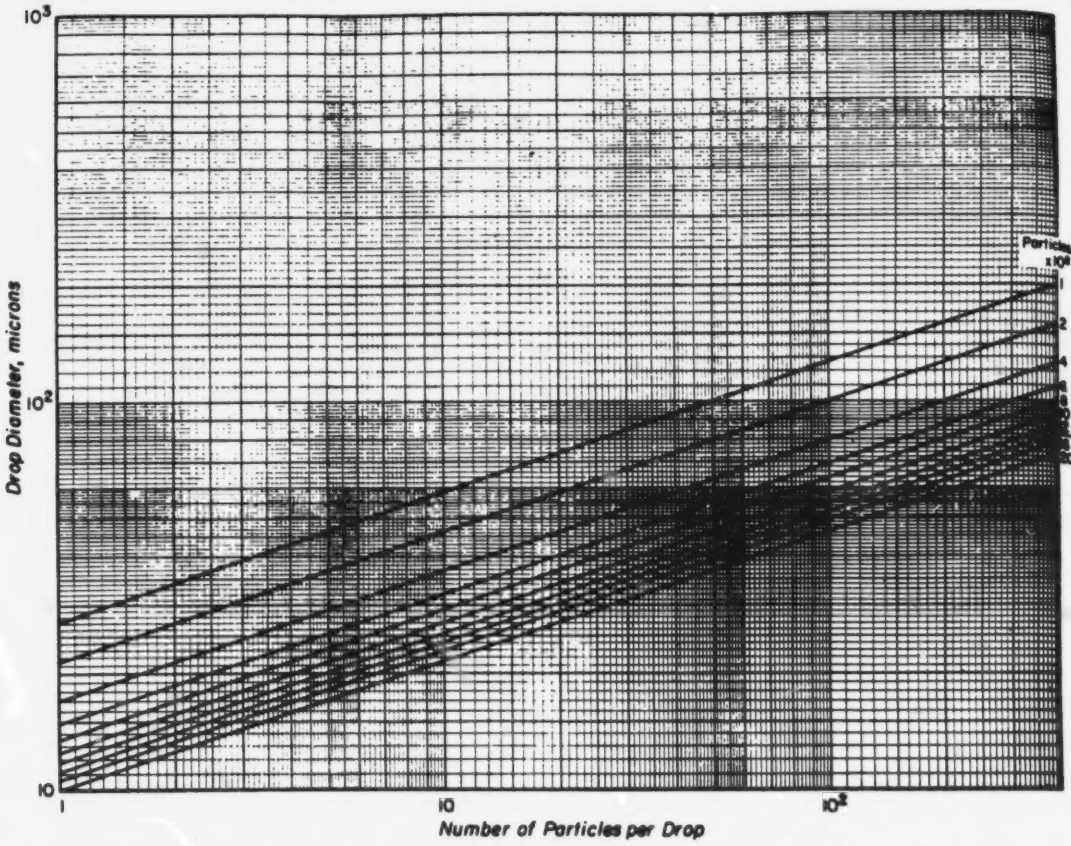

FIG. 1. Average number of particles per drop as a function of drop size and number of particles cm^{-3} of bulk liquid.

The essence of this FP spray tracing technique is to add a known number of FP to a known volume of liquid in the spray tank. The number of FP are then distributed throughout the volume of liquid such that each sub-volume of liquid contains its own representative number of FP. This proportionality between the number of FP and volume is maintained when the liquid is sprayed. Thus, each droplet, depending on its volume, has its proportional number of FP. On a sampling surface, the presence of the droplet is only detected by the presence of the FP, and the number of FP associated with that droplet determines its size. Also, the total number of FP on a sampling surface determines the total volume of insecticide present without having to sum the vloume contributed by each droplet on the surface.

Since the assessment of the FP spray technique is on a number basis, it is essential that the original FP concentration in the spray liquid be known. Concentrations as high as 2×10^{9} FP cm^{-3} can be measured for source strength determinations by serially diluting the initial concentration to a lower concentration when a measured volume of the final concentration is drawn through a membrane filter depositing a countable number of FP. The FP will remain on the surface of the membrane filter where they can be counted under the microscope. The relationship between source strength concentration (FP cm^{-3}), drop size, and mean number of FP per drop is given in Fig. 1.

3. Proportionality of FP number to insecticide mass

The primary assumption underlying the FP spray technique is that the proportionality of FP to liquid volume remains constant throughout the spraying operation both while stored in the spray tank and while undergoing droplet formation. A series of tests were performed which verify the latter portion of this assumption. Summarized in Table 1 is a comparison of the recoveries of FP, dieldrin, and fluorescent dye. In this test a known number of FP, a known mass of dieldrin and a known mass of soluble fluorescent dye were added to a liter of No. 2 cycle oil. The liquid was then sprayed and the droplets were collected on fallout plates. The FP was microscopically assayed; the dieldrin was

TABLE 1. Recovery of fluorescent particles (FP), soluble fluorescent dye (SFD) and dieldrin (D), giving the amount of each constituent recovered from spray droplets collected on a glass microscope slide per unit of constituent in the bulk liquid. Bulk liquid was a 1 liter solution-suspension containing 24.5×10^{10} FP (25.016 gm), 3.6371 gm of SFD and 10.0389 gm of D.

	Recovery								
	FP		SFD		D		Recovery ratios		
Trial	Number	$\left(\frac{\text{Number}}{24.5\times10^{10}}\right)10^6$	(μg)	$\left(\frac{\mu g}{3.6371}\right)$	(μg)	$\left(\frac{\mu g}{10.0389}\right)$	FP:D	SFD:D	FP:SFD
A-1	661,000	2.68	10.8	2.97	26.0	2.59	1.03	1.15	0.90
A-2	525,000	2.13	7.57	2.08	18.4	1.83	1.16	1.14	1.02
B-1	1,776,000	7.21	25.6	7.04	71.6	7.13	1.01	0.99	1.02
B-2	1,943,000	7.89	22.0	6.05	69.4	6.91	1.14	0.88	1.30
C-1	1,117,000	4.54	16.7	4.59	44.0	4.38	1.04	1.05	0.99
C-2	1,159,000	4.71	15.2	4.18	41.0	4.08	1.15	1.02	1.13

soluble dye was fluorimetrically assayed. For each sample, the recovery (the ratio of material collected to the total material in the initial liquid) was computed. The recoveries are expected to be the same for each material, provided there is no change in the proportionality of the tracer to liquid or active material to liquid during the spray operation. As seen in Table 1, the recoveries for the three different materials are about the same. That is, the ratios of the different recoveries average about unity. In other words, the FP tracer is a quantitative measure of the total mass of active ingredient present in a sampling of the droplet deposition. The above is strictly true only for nonvolatile liquids, and if evaporation is considered, the FP tag of the initial volume is required to yield the deposited volume.

4. Proportionality of FP number to droplet size

Another test was performed to determine if the proportionality between the number of FP and the individual droplet volume was maintained and could, in fact, be used to establish the size of the individual droplets. Fig. 2 shows the summary of results relating the number of FP and the droplet diameter. Kromekote cards prestained with oil red dye were calibrated to determine the stain diameter indicated on the card resulting from

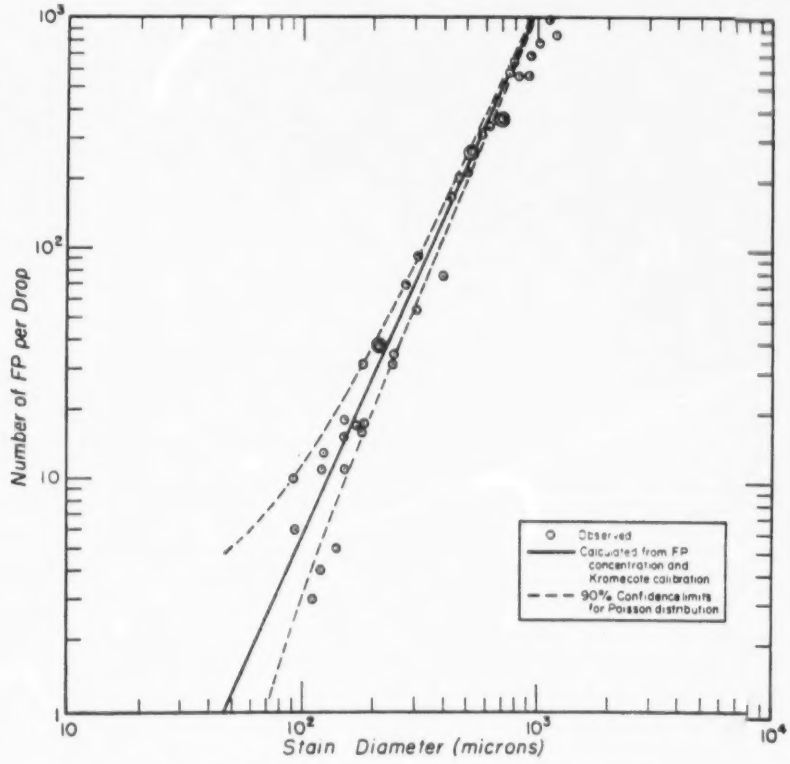
Number of FP per Drop
Stain Diameter (microns)
Observed
Calculated from FP concentration and Kromekote calibration
90% Confidence limits for Poisson distribution

FIG. 2. Number of FP per drop as a function of stain diameter on Kromekote cards dyed with duPont oil red dye.

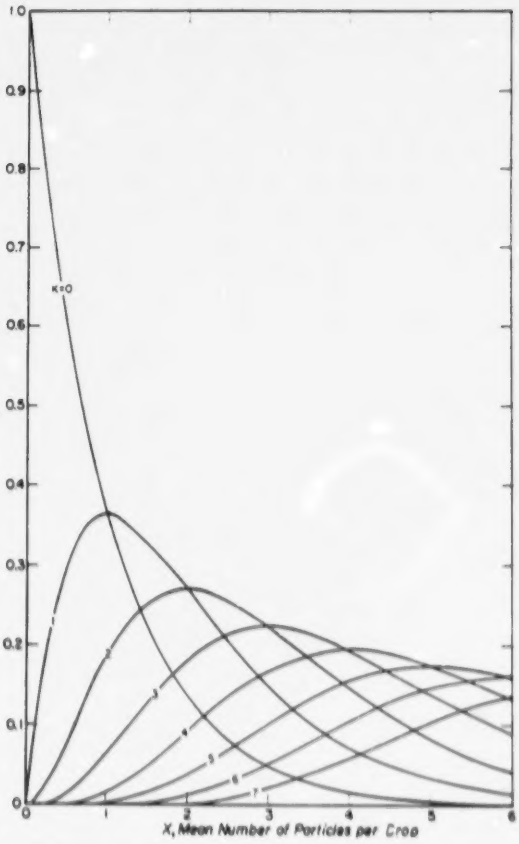

FIG. 3. Probability of observing exactly k particles in a drop as a function of the mean number of particles per drop.

the deposition of known size droplets of oil. Other cards taken from the same batch from which the calibration was performed were sprayed with the same type oil which now contained a known concentration of FP. The data points in Fig. 2 show the number of FP actually counted within the measured stain diameter. The solid line is computed from a droplet volume which corresponds both to a given number of FP and also to a given stain diameter. Notice that for the larger droplets, the number of FP counted for the given droplet is less than the number which was expected for that volume. This was attributable to the difficulty in recognizing a single FP among the hundreds within the droplet pattern. This, in effect, provides an upper limit of the droplet size that can be measured when this initial FP concentration is used, and if the interest is in this size range, a lower concentration could be used.

It is recognized that the droplet size distribution does not consist of a series of quantum steps precisely proportional to the discrete number of FP contained in that droplet. The 90% confidence limit of this statistical uncertainty is shown by the dashed curves. As the observed number of FP in a droplet becomes lower, the uncertainty interval becomes greater. This is expected from the behavior of a Poisson distribution. For the case in which all the droplets are exactly the same size and in which the mean number of FP per droplet is small the probability of seeing exactly k particles per droplet is given in Fig. 3. For example, if the mean number of FP per drop is unity, then about 36.8% of the droplets will contain no FP (i.e., they cannot be observed), 36.8% of the droplets will contain 1 FP, and the balance of the droplets will contain more than 1 FP.

It can be demonstrated that there is an unique relationship between the number of droplets that are occupied with a single FP and the total number of occupied droplets. For example, if 58.2% of the occupied droplets were singly occupied, the mean number of FP per droplet would be unity. In this instance 368 droplets out of 1000 would be unoccupied, and of the 632 occupied droplets, 368 would be singly occupied. This yields a ratio of singly occupied to total occupied of 368/632 or 58.2%. The problem becomes more complicated when a distribution of droplet sizes is present, but this unique property still exists for the known size distributions.

5. Measuring drift

Once aerosolized the insecticide is carried by atmospheric motions. A portion of the droplets deposit on the ground and on the foliage, while a portion is diffused horizontally and vertically. The amount and size of the droplets that deposit can be measured by observing the FP material on fallout cards (e.g., Kromekote) or on natural surfaces. The total number of FP on the sample yields the total mass of pesticide, and the numbers of FP within the individual droplet patterns yield the droplet size distribution. This procedure measures the residue deposited by drift.

As the airborne droplet concentrations become less and the droplet size becomes smaller during the downwind travel of the aerosol cloud, the deposition sampling requires an ever increasing sensitivity because there are fewer droplets to deposit and the smaller droplets are less likely to deposit. The amount of pesticide that is expected to deposit farther downwind can be estimated by determining the amount remaining airborne.

One method to measure the amount of material still airborne is to compute a mass balance. The total mass released can be measured directly. The total pesticide deposited within the deposition sampling grid can be approximated, determining an average deposition density for the overall area. This type of measurement generally is not very accurate, and if the drift cloud still airborne is only a small percentage of either the amount released or the amount deposited, this approach is inadequate.

A superior approach for measuring the longer range drift is to sample the airborne cloud directly. The aerosol cloud can be sampled by the Rotorod, a small, dry-cell powered device. The principle of the Rotorod is that

TABLE 2. FP spray test technology involving measurements of insecticide dosage at 1 m above ground and of ground level deposition on 24 September 1968. The test site was a freshly mown oat field adjacent to San Francisco Bay and the insecticide density 1 gm cm^{-3}.

Distance (ft)	FP dosage $\left(\frac{\text{FP-min}}{\text{liter}}\right)$	Insecticide dosage at 1 m above ground $\left(\frac{\text{cm}^2\text{-min}}{\text{liter}}\right)10^{-9}$	$\left(\frac{\text{drops-min}}{\text{liter}}\right)$	Kromecote card measurements of ground deposition $\left(\frac{\text{FP}}{\text{m}^2}\right)10^4$	$\left(\frac{\text{cm}^2}{\text{m}^2}\right)10^{-6}$	$\left(\frac{\text{drops}}{\text{inch}^2}\right)$	$\left(\frac{\text{gallons}}{\text{acre}}\right)10^{-6}$
500	310	150	470	16	77	150	82
1000	280	140	430	7.8	37	74	40
1500	710	340	1100	5.2	25	50	27
2000	550	270	840	3.9	19	38	20
2500	440	210	650	3.6	17	34	18
3000	370	180	560	2.4	12	24	13
3500	200	100	310	1.7	8.2	16	8.8
4000	130	64	200	1.2	5.8	12	6.2
4500	130	64	200	1.1	5.3	11	5.7
5000	48	24	74	0.7	3.4	6.8	3.6

of driving a rapidly rotating collection surface through the air, rather than pumping an air jet past a stationary collection surface. The exposed and rotating collection surface makes the Rotorod an omnidirectional sampler which is independent of wind speeds < 25 mph. Therefore, the Rotorod is insensitive to problems associated with aspirated samplers due to fluctuations in wind speed and direction. The chief disadvantage of the Rotorod is that its sampling efficiency is < 100%. However, for droplets in the size range encountered in the longer distance drift studies, the collection efficiency can be reproducibly calibrated. Furthermore, it was found that the collection efficiency was nearly constant for the range of aerosol sizes encountered (Murray *et al.*, 1968). Thus, the areosol samples collected with the Rotorod are representative of both the droplet size distribution and total mass in the ambient cloud.

The results described thus far have used laboratory or small-scale tests to calibrate individual aspects of the FP spray technique. The validity of the mass measurements, of the droplet size distribution, and of the aerosol sampler have been covered. How all these individual calibration tests are integrated can be illustrated by examples from several field tests. Given in Table 2 are the results of one field test measuring drift to distances of 5000 ft. The aerosol dosage and the ground deposition were measured at 500-ft intervals. The test objective was to measure the output of a U. S. Navy spray device and its performance in the control of adult mosquito populations.

The FP dosage is computed by dividing the total number of FP on the collection surface by the air sampling rate (52 liters min^{-1}) per H-shaped collector rod and the collection efficiency (70%). If the FP count is high, statistical methods can be used to estimate the total count without sacrifice to overall accuracy. Since the FP concentration is known, the liquid volume dosage can be computed by dividing the FP dosage by the FP concentration. The FP and liquid volumes deposited on the Kromekote cards can be determined in a similar manner.

The ultimate sampling sensitivity of the Rotorod is one FP. However, the statistical significance and reliability obtained with one FP is small. If 10 FP are observed on a sampling surface, the confidence, based on Poisson statistics, of that sample is ±25%, 56% of the time. From the practical standpoint, samples containing fewer than 10 FP are considered insignificant. This corresponds to a dosage of 0.7×10^{-10} cm^3 min liter^{-1} if the initial concentration is 2×10^9 FP cm^{-3}.

In order to compute the drop dosage, the volume mean diameter of the droplet size distribution must first be determined. Given in Table 3 is the droplet size distribution for the test. This size distribution is based on the FP observed in the droplets collected by the Rotorods. Also, these represent the average for the entire sampling line because no significant change in size can be found.

Since the small droplets produced by the Navy spray device contain only small numbers of FP, statistical methods must be used to compute the drop size distribution, while for larger drops the number of FP per drop is directly proportional to drop volume. The number of FP per drop is assumed to have a Poisson distribution, i.e.,

$$P_k = \frac{(cx)^k}{k!}e^{-cx}, \qquad (1)$$

where P_k is the probability of seeing k particles in a drop, x the drop volume (cm^3), and c the bulk concentration of FP (number cm^{-3}).

TABLE 3. Measured droplet size distributions resulting from the Navy insecticide low volume aerosol generator measured on Rotorod sampler 1 m above ground on 24 September 1968. The test site was a freshly mown oat field adjacent to San Francisco Bay.

Drop diameter (μ)	Drop size distributions: Number per cent	Number cumulative per cent	Mass per cent	Mass cumulative per cent
<5	2.7	2.7	0.3	0.3
5–10	67.3	70.0	37.7	38.0
10–15	27.5	97.5	48.8	86.8
15–20	2.4	99.9	11.6	98.4
>20	0.1	100.0	1.6	100.0

Since the total volume of all droplets, including the unoccupied droplets, is tagged by the FP, the moments of the volume distribution may be computed from the observed droplet patterns. The equation for the nth moment is

$$\bar{x}^n = \frac{1}{c^n} \sum_{k=1}^{\infty} \left[\frac{(k+n+1)!}{k!} \right] N_{k-n-1} \Big/ \left[\sum_{k=1}^{\infty} (k+1) N_{k-1} \right], \tag{2}$$

where N_{k-n-1} is the number of drops containing $k+n+1$ particles, and N_{k-1} the number of drops containing $k+1$ particles.

From (2) the first two moments were computed from the droplet patterns on the Rotorod and the equivalent parameters for a log-normal drop size distribution were determined. The resulting size distribution is given in Table 3 for the test. In addition to volume mean diameter, the volume median diameter (VMD) and mean surface area diameter can be computed.

It should be noted that the computation of the moments is valid even if the observed droplet distribution represents only a portion of the original size distribution produced by the spray device. In this case, however, the collected samples are representative of the original size distribution. Because of their very small size, losses by deposition or differences in diffusion were negligible.

From the dosage and deposition data there exists a method independent of the FP size information for estimating the droplet diameter. A deposition velocity can be computed by dividing the deposition density by the airborne dosage. The deposition velocity is equal to or greater than the quiescent air settling velocity. The deposition velocities measured at each of the sampling sites are given in Table 4. In addition to the deposition velocities measured in the field are the fall velocities computed from Stoke's law using the mean surface area diameter determined from the FP droplet sizing data.

TABLE 4. FP-spray test technology, Test 1. Measurement of fall velocity has been made by comparison of ground deposition and 1 m dosage.

Distance (ft)	Dosage at 1 m $\left(\frac{\text{drops-min}}{\text{liter}}\right)$	Ground deposition* $\left(\frac{\text{drops}}{\text{m}^3}\right)10^4$	Deposition velocity (cm sec^{-1})
500	470	23	0.81
1000	430	11	0.43
1500	1100	7.8	0.12
2000	840	5.9	0.12
2500	650	5.3	0.14
3000	560	3.7	0.11
3500	310	2.5	0.13
4000	200	1.9	0.16
4500	200	1.7	0.14
5000	74	1.1	0.25

Note: For Test 1 Stoke's law fall velocity for 7.7 μ mean surface area diameter, density 1 gm cm^{-3}, is calculated to be 0.17 cm sec^{-1}.

* On Kromekote cards.

The agreement between the velocities measured by two independent methods is remarkably close. The 500- and 1000-ft stations show a somewhat higher than expected deposition velocity, but this can be explained by spray rig equipment failure due to a parting of the pressure hose causing a discontinuity of the operation near the base of the sampling line. Except for the two sampling stations mentioned, the generally good agreement of the independently computed fall and deposition velocities can be taken as field demonstrations verifying the assumptions underlying the FP spray technique.

Given in Table 5 are results of a field test in which a drift cloud was measured at distances to 21,000 ft downwind of a 1.2 mi line source in which the total liquid released was 1.07 gallon. This test was to determine the area of mosquito control and the drift remaining airborne beyond the area. In addition to the single north-south sampling line perpendicular to the release line, Rotorod samplers were placed at 30 and 60 ft above ground level and at selected sites east and west of the 5000-ft sampling stations.

The line source was shorter than the sampling line and as a result the edge effects of the aerosol cloud can be seen in the data given in Table 5. The cloud was on center line at about 4000 ft, but it appeared to have meandered back at the greater distances. The influence of meteorological stability on the diffusive properties of the area can be measured directly from the changes in the dosage intensity. The peak values of dosage intensity are in agreement with values calculated from Pasquill's (1962) diffusion parameters for stability class B which is characteristic of the light winds and moderate insolation prevailing during the test.

From the FP results the VMD of the droplets was determined to be 4.2 μ. There was no apparent change in VMD with downwind distance, and none is expected for droplets of this size. The drift deposit can be estimated from the aerosol dosage and the fall velocity of the VMD droplet (i.e., 0.04 cm sec^{-1}). Thus, from Table 5 at 4 mi we have 2.2×10^{-9} cm^3-min liter$^{-1}\times0.04$ cm sec$^{-1}\times$liters (1000 cm^3)$^{-1}\times$60 sec (min^{-1}) $= 5.3\times10^{-6}$ cm^3 cm^{-2} or 5.6×10^{-3} gallon per acre. As stated earlier, since the deposition velocity may be greater than the fall velocity, the 5.6×10^{-3} gallon per acre figure is probably a conservative estimate of the deposition. However, the deposition velocity is not expected to exceed the fall velocity by a factor of 5. Therefore, the above calculation provides a realistic order of magnitude estimate of the deposition density.

6. Summary

The FP spray technique provides a simple and accurate method for quantitatively measuring insecticide mass and droplet size. The entire spectrum of droplet sizes is tagged, and with a practical field concentration of 2×10^9 FP cm^{-3} of insecticide all droplets >10 μ have a high probability of containing one or more FP. Ac-

TABLE 5. Downwind aerosol exposures for FP spray test resulting from Navy insecticide low volume aerosol generator with Dursban on 31 October 1968

Distance (ft)	Dosage $\left(\frac{\text{FP}-\text{min}}{\text{liter}}\right)$	Dosage intensity $\left(\frac{\text{min}}{\text{liter}}\right)10^{-12}$	Insecticide dosage at 1 m above ground $\left(\frac{\text{cm}^3\text{-min}}{\text{liter}}\right)10^{-9}$	$\left(\frac{\text{gm-min}}{\text{liter}}\right)10^{-9}$	$\left(\frac{\text{drops-min}}{\text{liter}}\right)$
1500	95.8	16	64	46	780
3000	56.0	8.9	37	27	450
4000	6.5	1.1	4	3	48
(center)					
5000	24.6	4.1	17	12	210
(center)					
5000	22.6	3.7	15	11	180
(30 ft up)					
5000	19.8	3.3	13	9	160
(60 ft up)					
5000	13.2	2.2	9	6	110
(¼ mi west)					
5000	69.8	12	47	34	570
(¼ mi east)					
5000	6.8	1.1	4	3	50
(1 mi west)					
5000	1.1	0.18	0.81	0.58	10
(1 mi east)					
6500	65.8	11	44	32	530
8000	48.0	7.9	32	23	390
10,000	33.4	5.5	22	16	270
21,000	3.3	0.54	2.2	1.6	27

sol dosage sensitivity is about 10^{-10} cm³-min liter^{-1}. The aerosol dosage may be used as an indicator of deposition. Drift at distances to 4 mi downwind of the sprayer has been quantitatively measured.

Acknowledgments. The research reported in this article forms part of a program for increasing the effectiveness of disease vector control measures supported by Department of the Navy, Office of Naval Research, under Contract N000014-69-C-0230 (NR 306-007), and part of a program for control of spruce budworms supported by U. S. Forest Service, Pacific Southwest Forest and Range Experiment Station, under Contract 21-24.

REFERENCES

Grinnell, S. W., W. A. Perkins, F. X. Webster and P. A. Leighton, 1946: Bimonthly Rept. No. 2, Contract W-18-035-CWS-1256, Stanford University, 24 pp.

Himel, C. E., and A. D. Moore, 1967: Spruce budworm mortality as a function of aerial spray droplet size. *Science*, **156**, 1250–1251.

——, and ——, 1969: Spray droplet size in the control of spruce budworm, boll weevil, bollworm and cabbage looper. *J. Econ. Entomol.*, **62**, 916–918.

Leighton, P. A., W. A. Perkins, S. W. Grinnell and F. X. Webster, 1947: Bimonthly Rept. No. 11, Contract W-18-035-CWS-1256, Stanford University, 74 pp.

——, ——, ——, and ——, 1965: The fluorescent particle atmospheric tracer. *J. Appl. Meteor.*, **4**, 334–348.

Murray, J. A., T. S. Brown and F. X. Webster, 1968: FP tracer co-dispersal and sampling studies. Tech. Rept. No. 135, Metronics Associates, Inc. (Defense Documentation Center AD 682 012), 176 pp.

Pasquill, F., 1962: *Atmospheric Diffusion*. London, Van Nostrand, 207–214.

Perkins, W. A., P. A. Leighton, S. W. Grinnell and F. X. Webster, 1951: *Proc. Second Natl. Air Pollution Symp.*, Pasadena, Calif. p. 42.

Stains, G. S., E. M. Fussell, J. P. Keathley, L. M. Vaughan and J. A. Murray, 1969: Caged insect kills of up to two miles utilizing a new low volume aerosol generator. *Mosquito News* (in press).

Vaughan, L. M., P. L. Magill and R. W. McMullen, 1965: Application of the fluorescent particle tracer technique to forest spray research. Memo. Rept. 278-1, Metronics Associates, Inc., Palo Alto, Calif., 20 pp.

APPENDIX C

THE ROTOROD SAMPLER OPERATIONS MANUAL

Technical Manual No 417-6

OPERATING INSTRUCTIONS FOR THE ROTOROD® SAMPLER

Metronics Associates, Inc.
3201 Porter Drive
Stanford Industrial Park
Palo Alto, California 94304
Phone: 415/326-5632

ROTOROD SAMPLER INSTRUCTION MANUAL

		Page
I	Introduction	4
II.	Sampler Unit Preparation	4
	A. Model 60 A	4
	B. Model 60 A-T	4
	C. Model 60 A-B	6
III.	Sampler Unit Operation	6
	A. Model 60 A and 60 A-T	6
	B. Model 60 A-B	8
IV.	Collector Rod Handling	8
V.	Collector Rod Coating	8
	A. Coating Materials and Procedures	8
	1. Rubber Cement	10
	2. Silicone Grease	12
	3. Blackened Silicone Adhesive	15
	B. Removal of Rod Coatings	15
VI.	Aerobiology Sampling	16
	A. Fixed Collector Sampling Head	16
	B. Retracting Collector Sampling Head	16
VII.	Evaluation of Samples	18
	A. Air Sampling Rates for Type-H, U, U-CP and Fixed Type-I Rods	18
	B. Air Sampling Rates for Retracting Type-I Rods	20
VIII.	Rotorod Sampler Specifications	22
	A. General Specifications	22
	B. Battery Specifications	22
	C. Collector Rod Specifications	22

List of Figures

Figure		Page
1.	Basic Rotorod Sampler	Frontispiece
2.	Field Mounted Rotorod Sampler-Conduit	5
3.	Field Mounted Rotorod Sampler-Taped	5
4.	Tripod Mounted Rotorod Sampler	5
5.	Battery Connections for Balloon Mounted Rotorod	7
6.	Balloon Mounted Rotorod Sampler	7
7.	Collector Rods, Type-H, U and I	9
8.	Collector Rod Tag in Place	11
9	Dipping Collector Rod in Rubber Cement	11
10.	Mounting Collector Rod on Rotorod Sampler Hub	11
11.	Collector Rod Transit and Storage Case (H and U)	14
12.	"I" Rods in Transit and Storage Vials	14
13	Retracting Collector Sampling Head	17
14.	Electro-Mechanical Performance Form	19

Rotorod Sampler Instruction Manual

I. Introduction

The Metronics Rotorod Sampler is an efficient sampling instrument which can be used to quantitatively collect airborne particulates in the 1-100 micron range. Basic components are a sampler unit, consisting of a constant speed DC motor with associated circuitry and case, and an aerodynamically designed collector rod which is rotated by the sampler unit. Excellent test results are obtainable through proper use of the Rotorod Sampler and by careful evaluation techniques. The following is an outline of the steps necessary to obtain these results.

II. Sampler Unit Preparation

A. Model 60 A: This basic Rotorod Sampler model, Figure 1, should be securely mounted to any convenient upright support at its sampling station before operation. An inexpensive support may be made from a four or five-foot length of 1/2" steel electrical conduit. The upper end of the conduit can be slotted 3 to 4 inches deep and a hole drilled clear through about 2 inches from the end and at right angles to the slot. Inserting a #8 or #10 machine screw through the hole and attaching a wing-nut allows pressure to be placed on the slot. The clamp thus formed securely holds the sampler when one side of its case is placed in the slot and the wing-nut tightened. The conduit should be firmly placed in the ground before attaching the sampler. See Figure 2.

An alternate method is to attach the sampler with 2 to 3 wraps of glass filament tape such as is used for package wrapping. The stake should not extend above the sampler case to avoid interference with the spinning collector rods. See Figure 3.

B. Model 60 A-T: This tripod-mount Sampler (included in the Rotorod Sampler Kits) is provided with a special tripod adapter in its base having a standard 1/4-20 thread. All that is required to prepare for operation is to screw the threaded mounting bolt on the tripod into the adapter and extend the legs of the tripod to the desired height for sampling. See Figure 4.

Fig. 2--Field Mounted Rotorod Sampler - Conduit. An inexpensive field mount made of light-weight ½" electrical conduit slotted to form a clamp. See Section II A, page 4.

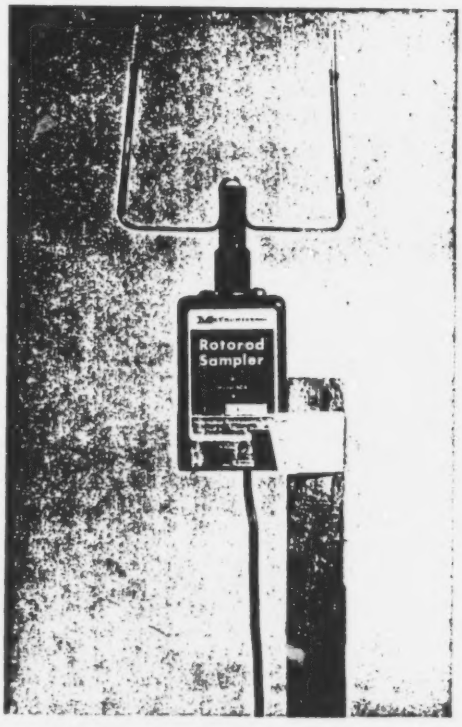

Fig. 3--Field Mounted Rotorod Sampler - Taped. The Rotorod Sampler can be temporarily fastened with glass filament tape to any convenient stake or post, See Section II A, page 4. The Fixed Collector Sampling Head shown utilizes a pair of 64mm clear acrylic plastic Type "I" rods as the collecting surface. See Sections II A, page 4; V A2, page 13; VI A, page 16.

Fig. 4--Tripod Mounted Rotorod Sampler. The Model 60A-T Rotorod unit may be mounted on a light-weight photographic tripod for temporary portable use. The NEDA No. 926 standard lantern battery will provide 50 hours of continuous operation. (Shown with the "H" rod.) See Section II B, page 4.

C. Model 60 A-B: This balloon-mount Rotorod Sampler is supplied with a light-weight suspension fixture which allows the sampler to be securely attached to a balloon tethering line. If the Rotorods are to be individually powered (i.e. not all operated from one power source on the ground) batteries are attached to the angled portion of the suspension bracket at the end opposite the sampler. For each Rotorod, connect two 6-volt dry cells (Burgess Z 4 or equivalent) in series by use of a short wire soldered from the positive terminal of one battery to the negative terminal of the other. One male snap connector (e.g. Cinch-Jones #5-M) should then be soldered to each of the two remaining battery terminals. Using vinyl electrical tape such as Scotchbrand #33 or #88, fasten the two batteries together, side-by-side, and then tape this assembly securely to the angled portion of the suspension bracket. See Figure 5. Shorten the sampler lead wires to about one foot and solder one female snap connector (e.g. Cinch-Jones #5-F) to each of the two lead ends. Attach each of the two eye-looped ends of the suspension bracket to the balloon tethering line by means of a clove-hitch, allowing minimum slack in the line. No cutting or permanent knotting of the tethering line is necessary or recommended. See Figure 6. Caution: To keep the dead-weight of mounting hardware as low as possible, the Rotorod balloon suspension brackets are fabricated from light gage aluminum and therefore are fragile and must be handled with care. The main vertical stem must not be excessively bent or flexed at the junction weld of the vertical and horizontal sections.

III. Sampler Unit Operation

A. Models 60 A and 60 A T: The Rotorod Sampler collector rods will be rotated at a nominal 2400 RPM $\pm$ 2% as long as the voltage applied to the motor is between 9 and 16 volts. Normal portable operation of the Rotorod utilizes a standard 12-volt lantern battery (Burgess TW 2 or equivalent). This type of battery is standard equipment in the Rotorod Sampler Kit and provides a minimum of 50 hours continuous operation or 70 hours intermittent operation. If a 12-volt auto battery is used, up to 1000 hours of intermittent operation is available. To operate the sampler, merely connect the leads to the battery terminals. The red insulated spade lug is attached to the positive terminal and the black insulated lug to the negative terminal for clockwise collector rod rotation. For counter-clockwise rotation the two connections are reversed.

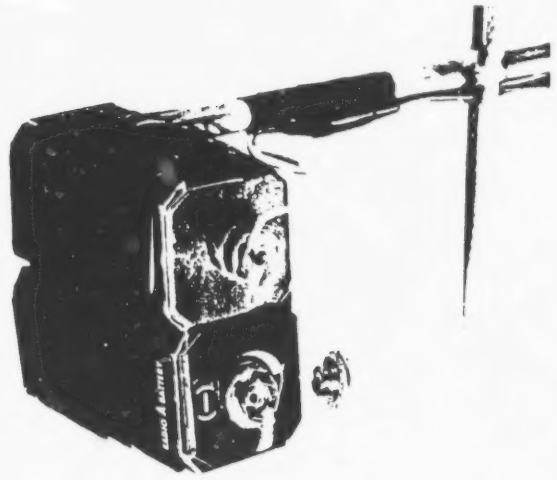

Fig. 5--Detailed View of Dry Cells Mounted on the Model 60A-B Sampler. The two 6V dry cells are electrically connected in series. The two cells are fastened together and then secured to the suspension bracket with electrical tape. See Section II C, page 6.

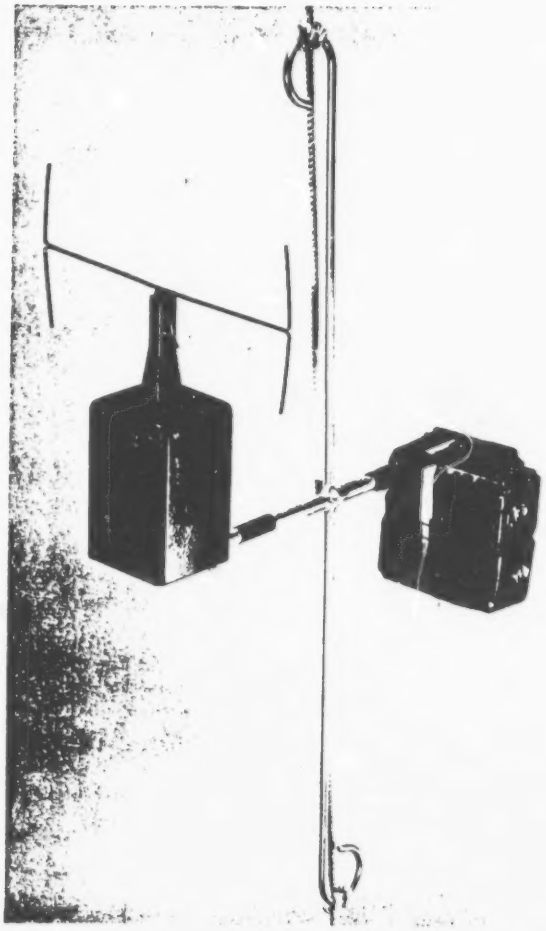

Fig. 6--Model 60A-B Balloon Mounted Rotorod Sampler. This model is secured to the tether of an aerial balloon with a lightweight suspension bracket. With the addition of two 6V dry cells (4 hours operation) the total weight of the equipment is less than 12 oz. Model 60A-B can be powered by parallel connections to a DC source on the ground. (Shown with H-Rod collector). See Section II C, page 6.

B. Model 60 A-B: Operation of the sampler is accomplished by fastening the two sampler snap connectors described above to the two battery connectors. Reversing these connections reverses collector rod rotation and it is suggested that the snap connector which gives clockwise rotation when connected to the positive battery terminal be marked with red paint for reference. (NOTE: Operation of the Rotorod Samplers from the ground is also possible by parallel connection of the samplers with a 12-volt battery on the ground.)

IV. Collector Rod Handling

All collector rods (see Figure 7 for Types-H, U and I) are mounted on a sampler by sliding the center clip portion of the rod into the slotted hub of the sampler. The best procedure is to grasp the hub with the fingers of one hand, with the sampler body held in that hand, and engage the collector rod clip in a pair of hub-slots with the forefinger and thumb of the other hand. See Figure 10.

Frequently small serial numbered tags are placed at the center of each H, U or U-CP rod as shown in Figure 8. They are printed on adhesive backed vinyl cloth and folded over the clip with the adhesive surfaces together. At this position they offer negligible interference with the sampler operation and provide an easy and error-free system of rod identification. The tags, however, are not physically strong enough to be used as handles for removing rods from the hubs and removal should begin by working the rod loose with the finger nails or a small screw driver blade if they are too tight. Removal is completed with the thumb and forefinger using care not to touch the collecting surfaces with the other fingers. (NOTE: When not being rotated the free ends of the normally upward or downward projecting arms of the collector rod are bent inward toward each other a few degrees; when the rod is rotated at the nominal motor speed of 2400 RPM these free ends move outward by centrifugal force until the collector arms become parallel to axis of rotation, i.e. vertically oriented and thus sweep-out a cylindrical annulus.)

V. Collector Rod Coating

A. Coating Materials and Procedures

To ensure the complete retention of all aerosol particles which

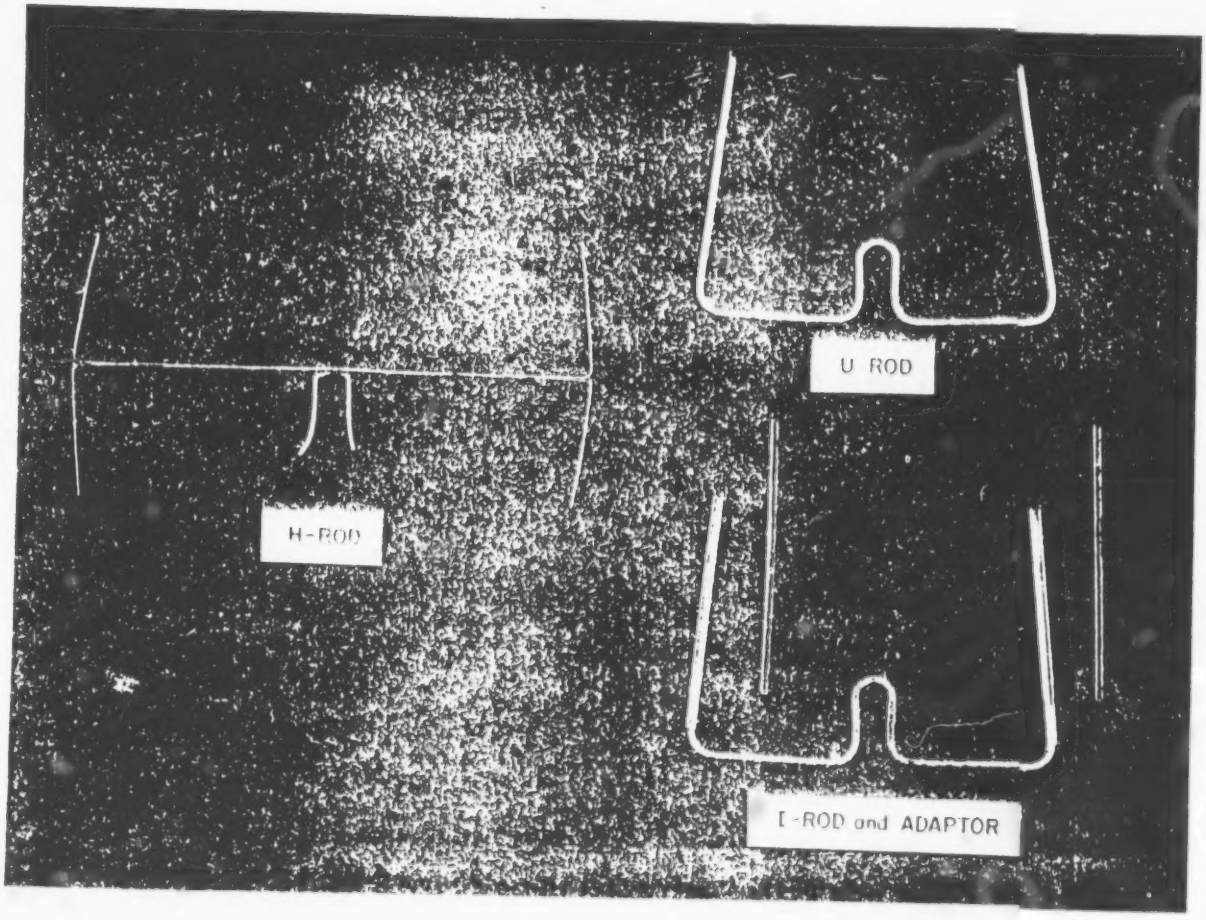

Fig. 7--Types of Collector Rods used with the Rotorod Sampler. The H-rod is optimized for particle collection in the size range 1-10μ and operates at a flow-rate of 52 liters per minute. The U-rod operates at a flow-rate of 120 liters per minute and collects particles most efficiently in the 10-100μ size range. The transparent acrylic plastic "I" rods have the same operating characteristics as the metal U-rod but are intended for the collection of particles requiring assessment by transmitted light. The H-rod and the U-rod can be operated both clockwise and counter-clockwise for collecting two separate samples. The nature of the "I" rod adapter, the Fixed Collector Sampling Head, however, limits its use to clockwise (CW) operation. See Section IV, page 8.

are impacted on the whirling collector arms of a Rotorod Sampler, it is essential that the intended collection surfaces be coated with a tacky or adhesive material.

The materials found to be most satisfactory for coating collector rods are rubber cement, silicone grease and a special blackened silicone adhesive. All three are available from Metronics Associates. In addition to the particle retention qualities, ease of application, and ready availability of various coating materials, consideration must also be given to the effect that a given coating material may have on the preservation and analysis of the specific type of particles to be collected and examined.

1. Rubber Cement

A satisfactory coating of rubber cement is applied by dipping each arm of the collector rod into a container of properly thinned rubber cement, Figure 9. A minimum of two dips is required to build up a suitable smooth and tacky collection surface - and when properly done two dips are sufficient for obtaining high collection and retention efficiency.

The rubber cement as supplied by the manufacturer is too viscous and hence must be thinned with a suitable solvent. Proper consistency is obtained when two to five drops of the thinned cement fall from the end of a collector rod after it is withdrawn from the liquid. The recommended materials for this procedure are "Best-Test White Rubber Paper Cement" and "Bestine Solvent and Thinner" both manufactured by Union Rubber & Asbestos Company, Trenton, New Jersey. These materials are usually available at stationery and art supply stores. A formulation consisting of equal proportions of cement and thinner usually give the desired consistency.

The thinned cement is available from Metronics in wide-mouth 8 oz. cans with screw-top caps. If two cans are placed at the proper distance apart, both arms of a collector rod can be immersed at the same time.

The following step-wise procedure applies literally only to the 2-arm Type-U or U-CP collector rods of 1.59 mm wide impaction surface, designed for 10-100 micron particles. Modification of this procedure for coating the 4 arms of the Type-H chromel collector rod of 0.48 mm wide impaction surface, used for 1-10 micron particles is obvious.

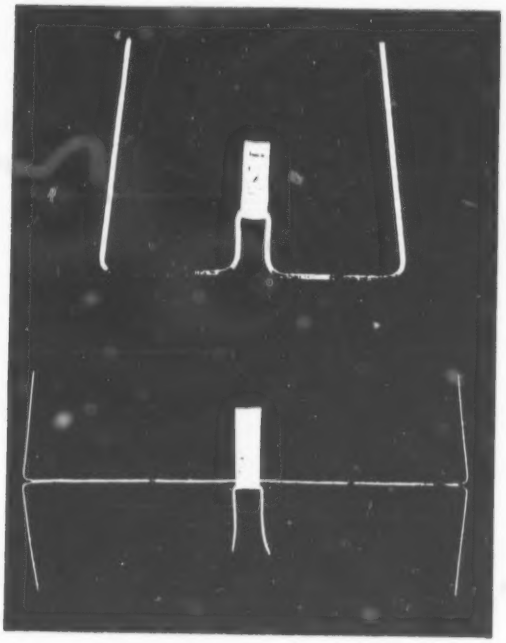

Fig. 8--Collector Rod Tag in place. Serially numbered vinyl cloth tags are folded over center clip portion of collector rods to provide easy sample identification. See Section IV, page 8.

Replace cap immediately after use
VOLATILE SOLUTION FLAMMABLE
Do not use near open flame
Metronics Associates, Inc.
Rubber Cement
Formulated for Rotorod Collector Coating

Fig. 9--Dipping Collector Rod in Rubber Cement. Technique used for dipping Type-U rod in specially formulated natural rubber cement. See Section V A1, page 10.

Fig. 10--Mounting Collector Rod on Rotorod Sampler Hub. Demonstrating the best method for mounting or removing a collector rod. The hub is held securely between the thumb and fore finger to avoid both turning and excess pressure being applied to motor shaft. See Section IV, page 8.

a. The rod arms are dipped into the cement slowly. This facilitates uniform wetting of the metal surfaces and prevents air bubbles from being carried into the liquid where they might become attached to the rod and disturb an otherwise smooth surface coating.

b. After both arms of the collector rod have been immersed to the desired depth, the rod is withdrawn slowly to allow the excess cement to drain off smoothly so that a uniform layer of cement will be retained on the rod.

c. On removal from the liquid the rod is kept suspended tip-end down to allow excess fluid cement to flow to the tip-end. The globule of liquid collecting at the tip-end should be removed by promptly touching the tip of the rod to the lip of the can.

d. After allowing at least one minute for the first dip to dry the second coating can be applied by repeating the above steps.

e. After the second coat has been applied the rods should be stored in a container, such as the Metronics Transit and Storage Case, Figure 11, which keeps the rods separated and dust free. Although extreme aging reduces the collection and retention efficiency of the rubber cement coating, collector rods which have been coated up to 90 hours prior to use have collection efficiencies equivalent to freshly coated rods.

2. Silicone Grease

Under certain environmental conditions such as very high or low temperatures or when the Rotorod Sampler is operated in rain or fog the rubber cement coating tends to lose some of its tackiness. Under such conditions, a thin coating of silicone grease provides a better surface for retention of impacted particles. Also for sampling very large particles, such as 50 micron glass beads, the silicone grease is superior to rubber cement. For this purpose General Electric G-697 Silicone Grease has been found to have superior retention properties and is thus included in the Rotorod Kits. Since this material tends to separate slightly in the tube, it is suggested that a small amount of the grease be transferred to a small wide-mouth jar so that the grease can be reblended with a stirring rod just prior to rod application to ensure a uniform coating.

Coating Type-H and U Rods

A coating of this grease may be applied to either the Type-H or Type-U collector rods in the following manner:

a. Lightly touch the surface of the grease in its container with the forefinger to pick up a small amount.

b. Spread this evenly and thinly on the fingers by smearing between the forefinger and thumb.

c. Hold the collector rod firmly at the center and grasp one end of the narrow impaction surfaces between the two greased fingers. Using gentle pressure, slide fingers along entire length of impaction surfaces, thus transferring a thin coating of grease to these metal surfaces.

At best a grease coating will not be as smooth as a rubber cement coating but if applied carefully, will be satisfactory and especially so for retention of particles 10 microns and larger. Since both impaction surfaces of each collection arm are coated with the silicone grease, the collector rod thus prepared can be rotated, first in one direction and then in the other to collect two separate samples.

Coating Type-I Rods

Although the procedure for coating Type-I rods is similar to Types-H and U, the mechanics is different. Namely, there is no center clip with which to grasp the rod and as collection may be done in only the clockwise direction, only one surface need be coated. The grease can be applied in any way best suited to the user, but by grasping a rod end with strong tweezers or needle-nose pliers, it can be securely held for finger-tip application. As rubber cement has a solvent which will craze the acrylic plastic, only silicone grease is recommended for coating the Type-I rods.

The coated rods can be placed either directly into the sampler head, Figure 3, or in the Transit and Storage Vial, Figure 12, available from Metronics. The vials will hold up to 6 pairs of Type-I rods and as the holes in the base are square to fit the rod, the rods will not turn and lose surface orientation either before or after exposure. The pairs of rod holes are numbered 1 through 6 for easy identification.

Since silicone grease, unlike the thinned rubber cement, does not easily flow and distribute itself uniformly over the metal surfaces, there is a tendency to use excessive amounts of grease and for some of this excess to overhang the narrow edges of the rod. Any such overhang increases the effective impaction width and thus decreases the collection efficiency. Such overhang can be avoided

Fig. 11--Collector Rod Transit and Storage Case (H and U). The plastic T & S Case carries up to 12 Type-H or 12 Type-U collector rods or any combination of the two. The rods are held securely and separated from each other in a dust free environment before and after exposure. See Section V A1e, page 12.

Fig. 12--Type-"I" Rods in Transit and Storage Vials. Both 32mm and 64mm Type-"I" collector rods are shown held in the appropriate length T & S vial. The collecting surfaces of the rods are protected both before and after exposure. See Section V A2, page 13.

by using smaller amounts of grease on the fingers when applying it to the rod. Excess grease overhanging the edges can be removed without disturbing the prepared impaction surfaces by running a sharp-edged tool along both sides of each collector arm.

The advantage of silicone grease as a collector rod coating is that it does not appear to lose any of its particle collection or retention effectiveness with age as does rubber cement. Thus silicone grease-coated rods may be safely prepared many days in advance of the time they are to be exposed. Prepared rods, coated with grease or any other tacky material, should of course be stored in a dust-free container, both before and after exposure.

3. Blackened Silicone Adhesive

Metronics has developed a new rod coating material specifically keyed to use with the fluorescent particle material often used to tag parcels of air in air pollution diffusion measurements. This coating material is properly tacky, as are other effective coatings, but its dull non-reflective black surface provides maximum contrast between the brightly fluorescent particles and the collecting substrate. These particles are assayed under illumination by ultra-violet light, which causes them to fluoresce, and as they are usually in the 1-5 micron range, all possible interference by background light must be eliminated. Particles in this size range are generally collected on the Type-H collector rods.

This coating is applied in a manner similar to that used for rubber cement dipping but has the advantage of having a very long shelf life and rods can be dipped many weeks prior to use.

B. Removal of Rod Coatings

If the exposed rods are to be re-used after assessment is complete, the coatings can be removed and the rods again coated. However, rods coated with silicone grease should only be re-coated with the grease, as the residue of the original coating will interfere with the wetting by rubber cement and an incomplete cement coating will result.

The rubber cement coating can be easily peeled off by starting at the fixed end of the collector arm and merely rolling it toward and off the tip-end. All particulate material will be enclosed within the tiny rubber ball and the rod can then be re-dipped in the thinned rubber cement without further cleaning treatment.

The silicone grease coating can be largely removed by wiping with an absorbent lint-free cloth. If necessary, further cleansing can be accomplished by immersion in one of several aromatic hydrocarbons such as xylene or toluene.

Although blackened silicone adhesive is not easily removed it is softened in xylene and can be wiped off after brief soaking. However, this procedure is not recommended as it is extremely messy.

VI. Aerobiology Sampling

The Metronics Rotorod Sampler is easily converted for use in sampling pollens, spores, or any other material which requires microscopic assessment using transmitted illumination by use of either a "Fixed Collector Sampling Head" or a "Retracting Collector Sampling Head."

A. Fixed Collector Sampling Head

This sampling head is a modified U-rod which performs as a carrier for two 1/16" square x 64 mm clear acrylic Type-I rods. See Figure 3. This Fixed Collector Sampling Head mounts on a Rotorod Sampler exactly like the Type-U brass rod and is used where sampling is to be done for a period of time without interruption and the collector rods picked up at the conclusion of the sampling period. Under these conditions the particles being sought will be collected as well as other background material. However, this type collector should not be turned off and left exposed as additional background material will continue to impact on the tacky surfaces due to normal movement of air past the collectors and tend to obscure the sought-after pollen or spore particles.

B. Retracting Collector Sampling Head

The Retracting Collector Sampling Head will avoid the above described unintentional collection in that the collecting surfaces are exposed only when the sampler is running. See Figure 13.

This rod carrier performs as a holder for two 1/2 length (32 mm long) Type-I rods, 1/16" square, and will retract these coated rods into a protective housing whenever the sampler is turned off. This carrier is used in situations where intermittent samples are taken throughout a day or week and operation is usually controlled by an automatic timer programmed to fit specific timing requirements. Such a device available from Metronics is called the

Fig. 13--Retracting Collector Sampling Head. In the left hand photograph the two collector rods are retracted into the protective housing as in the non-running or "off" period. As the sampler is turned on and begins to rotate the collectors snap out into the exposed position by centrifugal force, as shown on the right, and remain so during the "on" period. See Section VI B, page 16.

"Sequential Rotorod Timer" and is described fully in its Product Bulletin. Silicone grease coating procedures for Type-I rods are described under Section V above.

Because of the configuration of both of these Type-I rod carriers the Rotorod Sampler can be operated only in the clockwise (CW) direction.

After sampling, needle-nosed pliers or strong tweezers may be used to facilitate removal of the plastic collector rods from their holders without disturbing the samples.

The clear plastic collector rods may be mounted on a standard 1" x 3" microscope slide using a layer of coating material as a temporary adhesive or on a reusable microscope Stage Adapter, available from Metronics, having two milled slots that fit the 1/16" wide rods and hold them in alignment. If more permanent mounting of the rods is desired, clear silicone rubber such as General Electric RTV Sealer may be used. The slides with attached rods may then be stored in a standard microscope slide box.

VII. Evaluation of Samples

Two samples can be obtained on each Type-H, U or U-CP collector rod by rotating the rod clockwise for a period and then reversing the battery connections and rotating it in the counter-clockwise direction. (Both Type-I collector rods operate in the clockwise direction only.) It is important,however, to note the elapsed time of rotation in each direction and include this in the recorded test data. This will allow the total volume of air sampled to be determined in the following manner.

A. Air Sampling Rates for Type-H, U, U-CP and Fixed Type-I Rods

Find the air sampling rate for the Rotorod Sampler from Note 5 or 6 on Electro-mechanical Performance sheet provided with each Rotorod Sampler. See Figure 14. Depending on the type of rod used (U, U-CP and Fixed Type-I rods have the same dimensions and thus the same factor) the factor found in the footnote is multiplied by the 12-volt RPM for the particular sampler to give the air sampling rate in liters per minute for that direction of rotation.

Type-H example: If the 12 volt CW RPM is 2400, it is multiplied by the Type-H collector rod factor of 0.0218; thus the sampling rate would then be 2400 x .0218 or 52.3 liters per minute.

METRONICS ASSOCIATES, INC.

ELECTRO-MECHANICAL PERFORMANCE OF ROTOROD SAMPLER

Tests made using "H", "U" and "I" Type Collector Rods

Collector Type	Sampler Serial No.	12 VOLT OPERATION [1]				VOLTAGE RANGE FOR CONSTANT RPM [4]			
		Forward [2]		Reverse		Forward		Reverse	
		RPM	ma [3]	RPM	ma [3]	Low	High	Low	High
H	3477	2400	65	2380	65	8.5	20+	8.5	20+
U	3477	2390	70	2360	70	9.0	20+	8.5	20+
I	3477	2400	75	X	X	9.0	20+	X	X
H									
U									
I				X	X			X	X
H									
U									
I				X	X			X	X
H									
U									
I				X	X			X	X

Notes: 1. 12 Volts DC routinely used for field operation.

2. FORWARD - CLOCKWISE when viewed from above.

3. Milliamperes shown are for low wind speed; at a wind speed of 18 meters/sec (40 mph) the current drain is approximately twice that shown.

4. The 12 Volt test RPM remained constant when applied voltage was varied within the range shown.

5. Air sampling rate for 0.48mm collector (Type "H"); Rate (Liters/minute) = (0.0218)(RPM).

6. Air sampling rate for 1.59mm collector (Type "U"); Rate (Liters/minute) = (0.050)(RPM).

7. Air sampling rate for 1.59mm collector (Type "I"); Rate (Liters/minute) = (0.050)(RPM).

Date Tested 13 Nov. 1966

By DRL

MA 10

Fig. 14--Electro-Mechanical Performance Form. Typical performance data provided with each Rotorod Sampler to enable the user to determine the sampling rates for the three basic collector rod types, H, U, and I. The speeds are given in both CW and CCW direction, where applicable, and the low and high voltage range within which the RPM will remain constant ± 2% of the specified RPM value. See Section VII A, page 18. Although the motors used to power the Rotorod Samplers are precision made if they are subjected to driving rain or repeated blowing dust both the electrical elements and the bearings may become damaged rendering the calibration invalid. After extended use or long periods of inactivity the sampler speeds should be rechecked with an elctronic stroboscope* if available, or a vibrating reed tachometer**, to detect speed changes with normal brush and bearing wear.

*Strobotac Type 1531-A, General Radio Company, West Concord, Mass.

**Standco Tachometer, Model D-1, H. H. Sticht Co., Inc., New York, N. Y.

If the sampler is operated in the reverse direction, the counter-clockwise air sampling rate is obtained in like manner. For example, if the 12 volt sampler speed in the CCW direction was 2380 RPM, the sampling rate would be calculated by multiplying 2380 x .0218 or 51.8 liters per minute. (NOTE: Each sampler is individually speed (RPM) calibrated and data identified by the sampler serial number on the Electro-mechanical Performance Data Sheet).

Type-U, U-CP or Fixed Type-I example: If the 12 volt CW RPM is 2360, it is multiplied by the Type-U collector rod factor of 0.050; thus 2360 x 0.050 or 118.0 liters per minute.

Find the total volume of air sampled in each direction by multiplying the air sampling rate by the total elapsed sampling time. For a collector rod rotated in both directions, the air volumes sampled in each direction are added together to obtain the total volume of air sampled.

Example: If a Type-H collector was operated 24 minutes in the CW direction and 36 minutes in the CCW direction the total volume sampled becomes:

52.3 liters per minute x 24 minutes = 1255.2 liters, plus

51.8 liters per minute x 36 minutes = 1864.8 liters, for the total of 3120 liters sampled.

B. Air Sampling Rates for Retracting Type-I Collectors

It should be noted that the factor shown in Footnote No. 7 refers to the Fixed Collector Sampling Head using standard length, 64 mm Type-I rods of which 60 mm are exposed per arm, for a total length of 120 mm. For this rod the factor is 0.050 as shown. The Retracting Collector Sampling Head uses 32 mm long Type-I rods, of which only 23 mm is exposed per arm (46 mm total), the sampling rate being reduced in proportion. Thus the factor used for calculating Retracting Type-I rod sampling rates, although not shown on the form, is 0.019.

For example: For U, U-CP or Fixed Type-I rods: 2400 RPM x 0.050 = 120 liters per minute sampling rate while for the shorter Retracting Type-I rods operating at the same speed: 2400 RPM x 0.019 = 45.6 liters per minute.

The total volume of air sampled for each if they both ran for 30 minutes would be 120 liters per minute x 30 minutes or 3600 liters, and 45.6 liters per minute x 30 minutes or 1370 liters, respectively.

At the conclusion of the sampling period, each collector rod should be carefully removed and stored in a covered case until assessment. Care

must be taken to avoid contact with the coated, particulate-laden arms. To identify and count the number of particles on the collector rods, they are usually mounted on special microscope stage adapters; one design handles Types-H, U and U-CP rods and another the Type I rods, both available from Metronics. After the total number of particles collected has been determined, the concentration of these particles per unit volume in the atmosphere may be found by dividing the total number of particles observed by the total volume of air sampled as determined above.

For additional information contact Metronics Associates, Inc. 3201 Porter Drive, Palo Alto, California, Attention: Rotorod Sampler. Information about various accessories designed for application to your specific requirement may be obtained upon request.

VIII. Rotorod Sampler Specifications

A. General Specifications

Nominal Operating Voltage	12 volts DC
Current Drain (depending on wind speed)	60-100 milliamps
Nominal Speed of Rotation	2400 RPM
Usable Voltage Range for Constant Speed	9-16 volts
Dimensions, Basic Model 60 A (without Collector Rod)	1-1/2" x 1-1/2" x 4"
Weight, Basic Model 60 A	6 ozs.

B. Battery Specifications

	Intermittent Operation	Continuous Operation
Minature Radio Battery (2 ea Burgess Z4 or any NEDA #2 connected in series)	8 hrs.	4 hrs.
Standard Lantern Battery (1 ea Burgess TW 2 or any NEDA #926, 12 volts)	70 hrs.	50 hrs.
Automobile Storage Battery (12 V 40 ampere-hour auto battery)	500 hrs.	500 hrs.

C. Collector Rod Specifications

	Type-H	Type-U and I
Optimum Particle Size Collection Range	1-10μ	10μ and larger
Height of Impaction Face	2.36 in. (6.00 cm)	2.36 in. (6.00 cm)
Width of Impaction Face	0.0190 in. (0.0483 cm)	0.0625 in. (0.159 cm)
Total Area (All Forward Impaction Faces Included)	0.0898 $in.^2$ (0.579 cm^2)	0.295 $in.^2$ (1.91 cm^2)
Swing Diameter	4.72 in. (12.0 cm)	3.28 in. (8.33 cm)
Volume of Air Sampled per Revolution	1.33 $in.^3$ (21.8 cm^3)	3.04 $in.^3$ (49.9 cm^3)
Nominal Sampling Rate at 2400 RPM	1.85 CFM (52.4 ℓ/m)	4.23 CFM (120 ℓ/m)